A roadmap of Sedimentology in China until 2030

SEDIMENTOLOGY AT THE CROSSROAD OF NEW FRONTIERS

Illustration of the cover photo

The Photo shows the latest marine strata of Tingri area in the Tethys Himalayas of southern Tibet. The latest marine strata consist of greenish gray siliciclastic rocks (Enba Formation) and overlying red shales (Zhaguo Formation). The strata were dated by nannofossils and foraminifera as late early Lutetian to late Priabonian age (NP15–NP20, deposited ~ 47–34 Ma) (Wang et al., 2002). Detrital zircon U-Pb dating revealed that clastics sourced from Lhasa terrane and indicated that the Tethyan ocean was closed and the India had collided with the Asia before the depositional ages of the Enba-Zhaguo formations (Najman et al., 2010; Hu et al., 2012). The overlain is the Zongpu Fm. of Palaeocene-Early Eocene, which is composed mainly of thick bedded and nodular limestones deposited in a carbonate ramp of passive margin of Indian continent. Photo is provided by Prof. Xiumian Hu.

Hu, X. M., Sinclair, H. D., Wang, J. G., Jiang, H. H., Wu, F. Y., 2012. Late Cretaceous-Palaeogene stratigraphic and basin evolution in the Zhepure Mountain of southern Tibet: implications for the timing of India-Asia initial collision. Basin Research 24, 520-543.

Najman, Y., Appel, E., Boudagher-Fadel, M., Bown, P., Carter, A., Garzanti, E., Godin, L., Han, J., Liebke, U., Oliver, G., Parrish, R., Vezzoli, G., 2010. Timing of India-Asia collision: geological, biostratigraphic, and palaeomagnetic constraints. J. Geophys. Res. Solid Earth 115 (B12), B12416. http://dx.doi.org/10.1029/2010JB007673.

Wang C.S., Li, X. H., Hu, X. M., Jansa, L. F., 2002. Latest marine horizon north of Qomolangma (Mt Everest): implications for closure of Tethys seaway and collision tectonics. Terra Nova 14, 114-120.

Citation:

Wang, C. S., Immenhauser, A., Ogg, J., Mckenzie, J., de Boer, P., Hu, X. M., Chen, Z. Q., Liu, Z. F., Li, C., Shen, Y-A., Chen, X., eds. 2020. A roadmap of sedimentology in China until 2030: Sedimentology at the crossroad of new frontiers. 87pp. https://sedimentologists.org/#sed-in-china.

WRITING COMMITTEE CO-CHAIRS

(In alphabetical order by last name)

Poppe de Boer	Adrian Immenhauser	Judith McKenzie	Chengshan Wang

DOCUMENT CONTRIBUTORS AND REVIEWERS

(In alphabetical order by last name)

Xi Chen	Zhong-Qiang Chen	Poppe de Boer	Youfeng Gao
Yuan Gao	Zhong Han	Jun Hu	Xiumian Hu
Adrian Immenhauser	Wen Lai	Chao Li (Nanjing University)	Chao Li (China University of Geosciences, Wuhan)
Juan Li	Zhifei Liu	Genming Luo	Timothy W. Lyons
Pengfei Ma	Judith McKenzie	James Ogg	Cheng Quan
Yanan Shen	Chengshan Wang	Pujun Wang	Tiantian Wang
Shucheng Xie	Shouye Yang	Laiming Zhang	Shihong Zhang
Yulong Zhao	Chuanming Zhou		

ORGANIZING COMMITTEE

(In alphabetical order by last name)

Xi Chen ▪ Changsong Lin ▪ Xuelian You

WORKSHOP COMMITTEE

(In alphabetical order by last name)

Poppe de Boer ▪ Adrian Immenhauser ▪ Judith McKenzie ▪ Chengshan Wang ▪ Hongfu Yin

WORKSHOP PARTICIPANTS

(In alphabetical order by last name)

Marcos Aurell Cardona	Matthieu Cartigny	Daizhao Chen	Hongde Chen
Xi Chen	Poppe de Boer	Zhong-Qiang Chen	Shu Gao
Yuan Gao	Songzhu Gu	Ping Guan	Peter Homewood
Mingcai Hou	Jianfang Hu	Adrian Immenhauser	Xiumian Hu
Tao Jiang	Zaixing Jiang	Zhenkui Jin	Chao Li
Shunli Li	Yiqun Liu	Ping Luo	Timothy W. Lyons
Judith McKenzie	Nigel Mountney	James Ogg	Jianye Ren
Robert Riding	Longyi Shao	Chengshan Wang	Jian Wang
Pujun Wang	Tiantian Wang	Shucheng Xie	Xinong Xie
Jianghai Yang	Changmin Zhang	Laiming Zhang	Chuanming Zhou
Rukai Zhu	Jiaxin Yan	Xiaomin Zhu	Caineng Zou

Contents

Background and Rationale

Chengshan Wang[1], Adrian Immenhauser[2], Xi Chen1, Judith McKenzie[3]

[1] **China University of Geosciences (Beijing), Beijing 100083, China.**

[2] **Ruhr-University Bochum, 150 44801 Bochum, Germany**

[3]**ETH Zürich, 8092 CH-8092 Zurich, Switzerland**

About 75% of the Earth's surface is covered by unconsolidated sediments and their lithified products, sedimentary rocks. They record information of the Earth's history and the evolution of life, and provide natural resources for human survival and development. The discipline of "Sedimentology" focuses on the processes of formation of inorganic, organic, and organomineralogic sediments and their depositional environments, and of sedimentary rocks and their diagenetic pathways. Sedimentologists, in cooperation with stratigraphers and palaeontologists, investigate processes and products over a vast spatial and temporal range from the sub-micrometer scale and seconds to thousands of kilometres and astronomical time scales of thousands to many million years. As such, sedimentology forms a crucial element for other disciplines, such as ore geology, marine geology, palaeoceanography, and structural geology.

The first studies that qualify as "sedimentology" reach back more than a century. Sedimentology reached its first "golden age" during the 1960s to 1970s (Miall, 1995), when fundamental concepts, theories, and research methods of sedimentology were developed rapidly, including the turbidity current theory (e.g. Kuenen and Miglhiorini, 1950; Meiburg and Kneller, 2010), the study of sedimentary processes in modern depositional environments, the study of diagenesis of sediments in subsurface hydrocarbon reservoirs and outcrops (e.g. Swart, 2015), and the emergence of seismic stratigraphy (Vail and Mitchum, 1977) evolving into modern concepts of sequence stratigraphy (Catuneanu et al., 2009). At this stage, next to curiosity-driven fundamental research, the demand for oil and gas was the intrinsic motivation and led to a significant advance of sedimentology. International geoscience research programs, such as the ocean drilling (DSDP, ODP, IODP) and continental drilling (ICDP) programs have opened new views on the sediments depositied on the ocean floor and on the continents.

In the early 21stcentury, mankind is confronted with new challenges. In addition to the demand for energy, resources, and a sustainable development, mitigation of global climate change and the wish to live on a habitable planet are obviously in the focus of decision makers and the scientific community. These factors demand the input of sedimentologists and stratigraphers. As laid out in the National Research Council Report (NRC, 2011) of the US National Science Foundation, the study of sedimentary records in deep time has important implications for understanding, predicting, and mitigating future global change. A number of major geoscience research programs in Europe and the United States have been initiated and are coordinated by sedimentologists. These include the "DREAM" programme, the "MARGINS" programme, deep-time research, the study of sediments and sedimentary rocks on our neighbouring planets, such as Mars, etc.

For historical reasons, China did not fully benefit from the "golden age" of international sedimentology. The connection of Chinese sedimentologists with the international sedimentological community only began in the late 1970s. At that time, the Sedimentary Geology Committee of the Geological Society of China and the Sedimentology Committee of the Chinese Society for Mineralogy, Petrology and Geochemistry were established. As a result, the Chinese sedimentological community began to increasingly participate in various international conferences on Sedimentology, and the International Association of Sedimentologists (IAS) registered its first Chinese members. Subsequently, the field of sedimentology in China has developed by leaps and bounds. Domestic academic exchange was officially started and since then has witnessed a rapid development. Since 1979, six National Sedimentological Congresses have been held in China, representing a nationally important event that is now organized every four years. In addition, biennial sedimentological conferences are organized, the last one in Wuhan in 2015. With the rapidly increasing visibility of Chinese researchers and the vast geological heritage found in China, much collaboration is now taking place between Chinese and international sedimentologists. Examples of the unique geological archive of China include long Cretaceous lacustrine records (Wang et al., 2013a, 2013b), the unique terrestrial biotas in Jehol and Chengjiang (e.g., Zhou et al., 2003), the Precambrian sedimentary records that are widely distributed in southern and northern China (Zhao and Cawood, 2012), and the Cenozoic loess deposits (An, 2000; Guo et al., 2002). Moreover, investigations of marine and continental petroliferous basins provide a solid basis for the sustainable development of oil and gas resources in China.

The rationale and mission of this report is to evaluate how to take full advantage of the unique sedimentary records in China through to the year 2030. This effort must lead to a sustainable use of energy, including non-traditional energy resources. Moreover, it should help to mitigate the effects of global change, and help to maintain a habitable planet Earth. This mission is not solely that of Chinese sedimentologists, but it is a common challenge for all sedimentologists around the world. Clearly, extensive international cooperation is needed.

The Chinese Academy of Sciences and the National Science Foundation of China (NSFC) jointly launched the "Strategy of the Development of Sedimentology in China". Under the leadership of two respected academic authorities, Prof. Chengshan Wang and Prof. Pingan Peng, a team of 40 scientists from various sub-disciplines of the Chinese sedimentology community contributed to this report and roadmap. In September 2016, co-organized by Prof. Chengshan Wang (CAS) and Prof. Adrian Immenhauser (IAS), an international workshop on the future of sedimentology in China was held in Beijing. In total, 37 Chinese and 11 invited international sedimentologists participated in this workshop resulting in intense discussions on various key themes for the next decade of sedimentological research in China. Embracing the new opportunities and challenges in the field of sedimentology, the development of new technologies, and the vast geological heritage of China, four key themes for sedimentology in China were defined:

(1) **Earth's greenhouse states** including paleoclimate modes and drivers and the related hydrological cycle on various tectonic and orbital scales. This theme includes tectogeomorphologic topics, palaeoclimate and palaeogeographic reconstructions, and research on paleo-drainage basins.

(2) **Sedimentary and geochemical processes and products during critical transition periods.** These themes include periods with significant evolutionary steps of microbiota and metazoans, Paleozoic mass extinction events, Mesozoic oceanic anoxic events (OAEs) and interaction between oceans and continents.

(3) **Source-to-sink systems.** This theme studies the transport of sediments from orogenic belts to marginal ocean basins. Topics include the uplift of the Tibetan Plateau and its reflection in sedimentation patterns, the evolution of the major rivers of Asia, the South China Sea sedimentary system, and the Chinese loess deposits.

(4) **The Precambrian sedimentary record.** This theme includes long-term geochemical cycles and bio-sedimentary processes. Topics include microbialite formation and evolution,and the advent of early life in relation to geochemical cycles, or the sedimentological archive of snowball Earth events.

The present **White Paper** provides an overview and rationale for these topics. In order to enable the NSFC to provide more funding to the development of sedimentology, the Chinese sedimentological community documents evidence of past successes combined with prospects for the future. This document is, thus, both (i) a summary of the *achievements of Chinese* sedimentology and *China's sedimentological* heritage in recent years and (ii) *a roadmap for research in Sedimentology* during the next 10 years. A Chinese proverb states that being good at using the existing conditions is a prerequisite to succeed in the future. With the rapid development of social economy, Chinese research institutes have now been equipped with advanced state-of-the-art research facilities. This infrastructure provides a solid foundation for conducting research in sedimentology and acts as a guideline for further investments. This White Paper is a joint product of the *Chinese academic sedimentology community* and the *International Association of Sedimentologist (IAS).*

References

An, Z., 2000. The history and variability of the East Asian paleomonsoon climate. Quaternary Science Reviews 19, 171-187.

Catuneanu, O., Abreu, V., Bhattacharya, J.P., Blum, M.D., Dalrymple, R.W., Eriksson, P.G., Fielding, C.R., Fisher, W.L., Galloway, W.E., Gibling, M.R. and Giles, K.A., 2009. Towards the standardization of sequence stratigraphy. Earth-Science Reviews 92, 1-33.

Guo, Z.T., Ruddiman, W.F., Hao, Q.Z., Wu, H.B., Qiao, Y.S., Zhu, R.X., Peng, S.Z., Wei, J.J., Yuan, B.Y. and Liu, T.S., 2002. Onset of Asian desertification by 22 Myr ago inferred from loess deposits in China. Nature 416, 159.

Hou, X.G., Siveter, D.J., Siveter, D.J., Aldridge, R.J., Cong, P.Y., Gabbott, S.E., Ma, X.Y., Purnell, M.A. and Williams, M., 2017. The Cambrian Fossils of Chengjiang, China: The Flowering of Early Animal Life. John Wiley & Sons, 315pp.

Kuenen, P.H. and Migliorini, C. I., 1950. Turbidity currents as a cause of graded bedding. The Journal of Geology, 58: 91-127.

Meiburg, E. and Kneller, B., 2010. Turbidity currents and their deposits. Annual Review of Fluid Mechanics 42, 135-156.

Miall, A.D., 1995. Whither stratigraphy? Sedimentary Geology 100, 5-20.

NRC (National Research Council of the National Academies), 2011. Understanding Earth's Deep Past: Lessons for Our Climate Future. The National Academies Press, Washington, D.C., pp. 1-212.

Swart, P.K., 2015, The geochemistry of carbonate diagenesis: The past, present and future. Sedimentology, 62, 1233-1304.

Vail, P. R and Mitchum, R.M., 1977. Seismic stratigraphy and global changes in sea level, part 1: overview. In: Payton, C.E., Seismic Stratigraphy-Applications to Hydrocarbon Exploration. AAPG Memoir. Tulsa: AAPG: 51-212.

Wang, C., Feng, Z., Zhang, L., Huang, Y., Cao, K., Wang, P., Zhao, B., 2013a. Cretaceous paleogeography and paleoclimate and the setting of SKI borehole sites in Songliao Basin, northeast China. Palaeogeography, Palaeoclimatology, Palaeoecology 385, 17-30.

Wang, C., Scott, R.W., Wan, X., Graham, S.A., Huang, Y., Wang, P., Wu, H., Dean, W.E., Zhang, L., 2013b. Late Cretaceous climate changes recorded in Eastern Asian lacustrine deposits and North American epeiric sea strata. Earth-Science Reviews 126, 275-299.

Zhao, G. and Cawood, P.A., 2012. Precambrian geology of China. Precambrian Research 222, 13-54.

Zhou, Z., Barrett, P.M. and Hilton, J., 2003. An exceptionally preserved Lower Cretaceous ecosystem. Nature 421(6925), 807.

Chapter 1.

Earth's environments during greenhouse episodes of the Mesozoic-Paleogene: paleoclimate modes and drivers

Xiumian Hu[1], Zhong Han[2], Adrian Immenhauser[3], Yuan Gao[4], Laiming Zhang[4], Wen Lai1, Chao Li1, Juan Li1, Xi Chen[4], James Ogg[5]

[1] Nanjing University, Nanjing 210023, China

[2] Chengdu University of Technology, Chengdu 610059, China [3] Ruhr-University Bochum, 150 44801 Bochum, Germany

[4] China University of Geosciences (Beijing), Beijing 100083, China

[5] Purdue University, West Lafayette, IN 47907, USA

1. Overview

1.1 The importance of deep-time greenhouse climate research for our future

The current rapid climate warming trend of our planet is partly caused by an enhanced greenhouse effect, as the modern atmospheric CO_2 level surpasses the highest levels of the past 400,000 years and possibly is approaching the maximum level ever recorded during the past 30 Myr. What will be our future world, especially the environments within China, as global climate shifts from one state with polar ice sheets to one without permanent polar ice (cf. *Hay, 2011*)?

Chinese civilization has a long history of conquering droughts and floods, but we are now entering a new, uncertain climate pattern without historical parallels. What will happen to the monsoonal summer rain distribution, which regions will become drier and which ones wetter, what will be the frequency and intensity of major coastal typhoons, and what will be the rates of soil erosion? Some answers to these and other vital questions can be provided by examining ice-free episodes in the Earth's past, including those when tropical temperatures may have attained levels that were lethal to some larger land animals (*Sun et al., 2012; Wignall, 2015*).

Earth's climate has alternated between greenhouse and icehouse conditions during the Phanerozoic (Fig. 1-1), and the past 250 million years (Triassic through Paleogene) were predominantly characterized by a greenhouse climate punctuated by some extreme hyperthermal events. This Mesozoic-Paleogene interval has been intensely studied using marine sedimentary archives (e.g., *Zachos et al., 2001; Sun et al., 2012;*

Wang, et al., 2014, 2015). Peaks in atmospheric CO_2 often correlate with periods in which abundant organic matter was stored in marine sediments ("Oceanic Anoxic Events", or OAEs) (e.g. *Hönisch et al., 2012*).

If we learn to understand how the world, especially East Asia and Southeast Asia, responded to past rapid climate warming and sustained ice-free conditions in "Deep Time", then we can arguably make more reliable models for our future (e.g. *Sun and Wang, 2009*). This aim will be a major goal of sedimentological research in the coming decades.

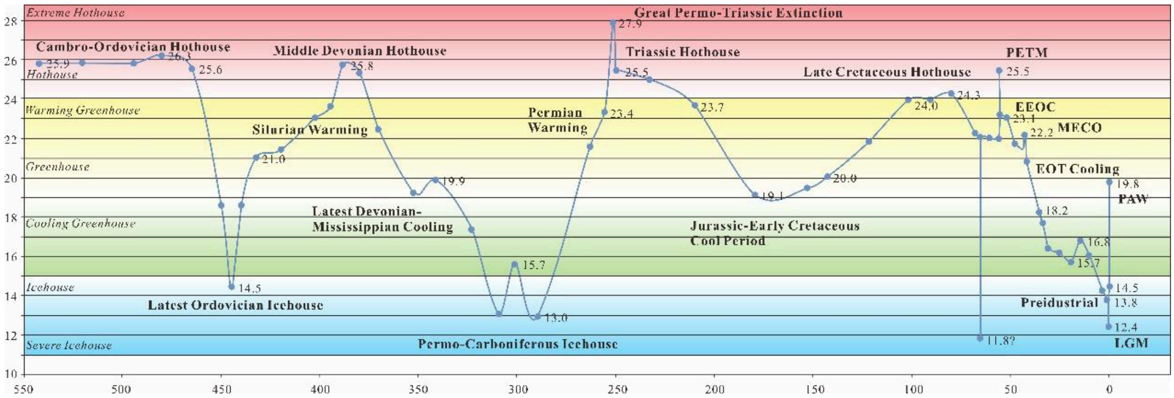

Fig. 1-1 ▲

Greenhouse conditions have dominated most of the Phanerozoic, with only a few extended periods of cool conditions (blue intervals) including "icehouse" intervals for which there is evidence of continental ice sheets at one or both poles. Source: Scotese, 2015.

1.2. Rich terrestrial records for deciphering and modelling paleoclimate in China

China is blessed by having rich sedimentary records in many terrestrial basins that collectively span nearly the entire Mesozoic up to the present day (Figs. 1-2, 1-3). Some of those basins were occupied by long-lived lakes (e.g., Songliao Basin), which provide an unparalleled detailed record of past climate conditions and the response of vegetation and land erosion to climate change. These basins include diverse sedimentary environments, such as deserts, lakes, rivers, and paleosols, as well as deltaic to shallow-marine deposits, with a continuous sedimentary record. Altogether, these deposits provide a superb inventory for paleoclimate studies. Some of the organic-rich lake deposits are the sources of China's main oil and gas fields (e.g. Songliao Basin, Bohai Bay Basin; Fig. 1-2). Other basins record the contrasts between humid and arid conditions and changing land biota.

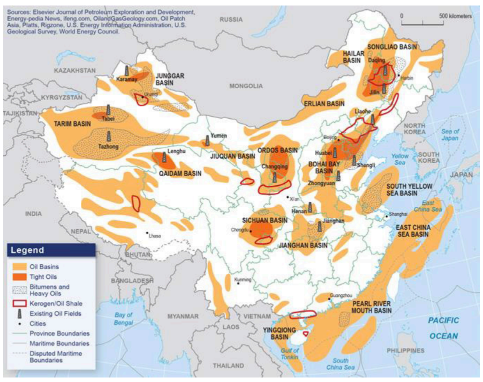

Fig. 1-2. ▲

Major terrestrial basins of China, which also host major oil fields. The majority of the source rocks are lacustrine deposits in closed basins, and the majority of the oil reservoirs are sand-rich intervals in those basin fills. These basins and others provide an unparalleled record of the response of terrestrial environments and ecosystems to Mesozoic through Recent climate change. Sources: http://carnegieendowment.org/2014/05/06/china-s-oil-future/h93y

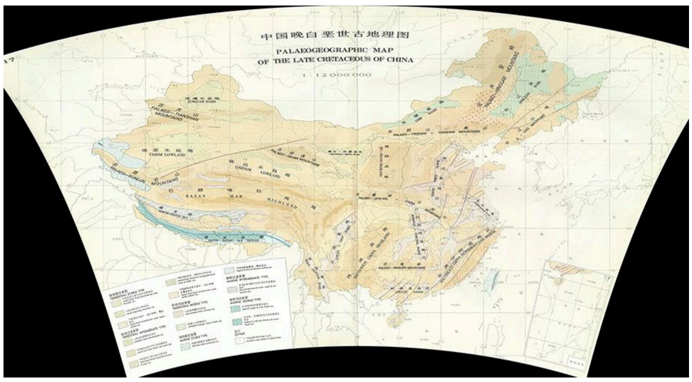

Fig. 1-3.▲

Late Cretaceous paleogeography of China in present-day coordinates (not adjusted for Cretaceous plate positions) showing the typical predominance of terrestrial deposits during the Mesozoic through Paleogene. Source: Wang (1985).

These sedimentary records can be placed in a temporal context by applying a combination of radiometric dating, magnetic polarity stratigraphy, cyclo-stratigraphy, regional paleontology and isotope stratigraphy to establish a reasonably detailed timescale. This approach to integrated stratigraphy was applied to the on-going deep-drilling of the terrestrial deposits in the Songliao Basin (e.g., *Wang et al., 2013, 2016*). The International Continental Scientific Drilling Project of the Cretaceous Songliao Basin (SK-1 and -2 wells), and on-going continuation into deeper deposits has currently obtained over 5000 meters of continuous lacustrine sedimentary records spanning the Cretaceous, thereby providing unique research material for the study of the terrestrial climate of this region.

The paleogeographic record of past terrestrial environments can be projected onto paleo-plate reconstructions (*Hou et al., 2018*), thereby enabling modelling of past wind patterns (Fig. 1-4). Tectonics and topography play an important role in atmospheric circulation and in the terrestrial climate system. Consequently, the restoration of paleotopography is one of the prerequisites for terrestrial paleoclimate research. For example, the rise of the Tibetan Plateau, caused by collision of the Indian-Asian continents, is an important factor in controlling the evolution and intensity of the Asian monsoon system and the Intertropical Convergence Zone. (e.g., *Wu et al., 2012*). Some have proposed that the rise of the Himalayas has led to increased chemical weathering to such extent that the lowered pCO_2 would have triggered global cooling and the onset of the Pleistocene Ice Age (*Raymo and Ruddiman, 1992*).

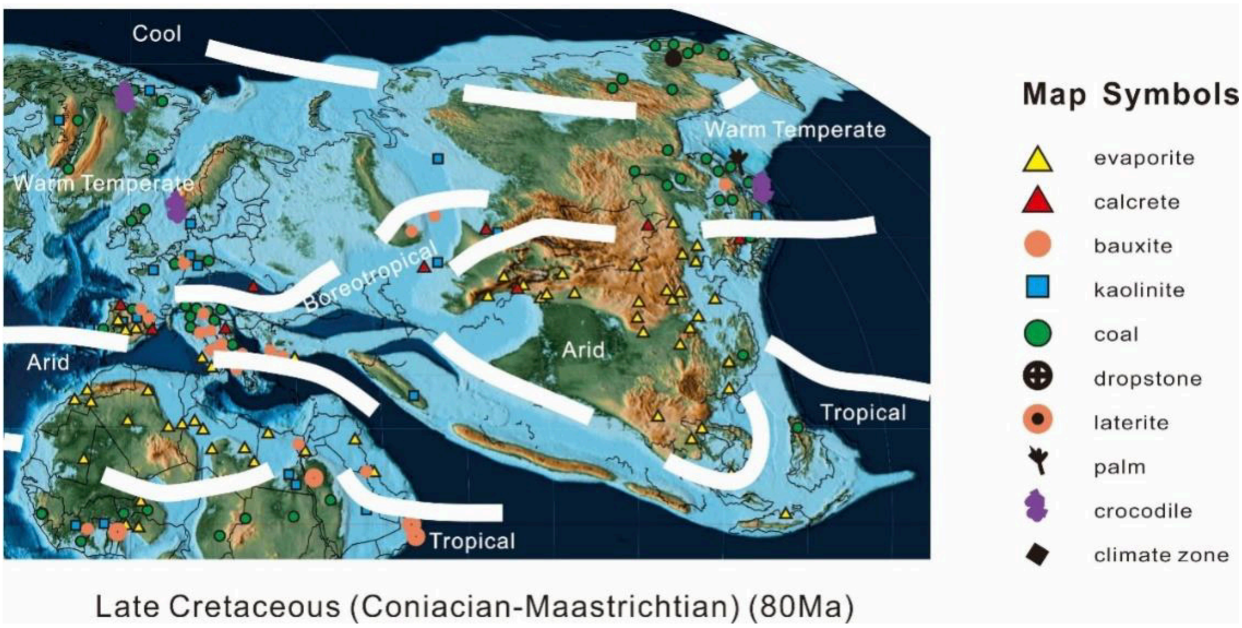

Fig. 1-4. ▲
Upper Cretaceous (Coniacian-Maastrichtian) basins in China placed into a global paleogeographic context with plate reconstructions (Source: Scotese, 2014) with positions of paleoclimate-related sediments and possible wind patterns. Source: Boucot et al. (2013).

1.3. Advances in technology and methods allow the reconstruction of deep-time terrestrial climate and paleogeography

Sedimentological observations and paleontological data provide the main sources for the interpretation of paleoenvironments from the record of sedimentary basins. The main challenge in terrestrial climate research is the precise reconstruction of climate parameters, such as paleotemperature, pCO_2, paleoprecipitation, evaporation, aridity and humidity (Fig 1-5). Quantitative high-resolution studies of the terrestrial greenhouse climate parameters and their coupling to oceanic records are an important direction in future paleoclimate research (e.g., *Tabor and Meyers, 2015*).

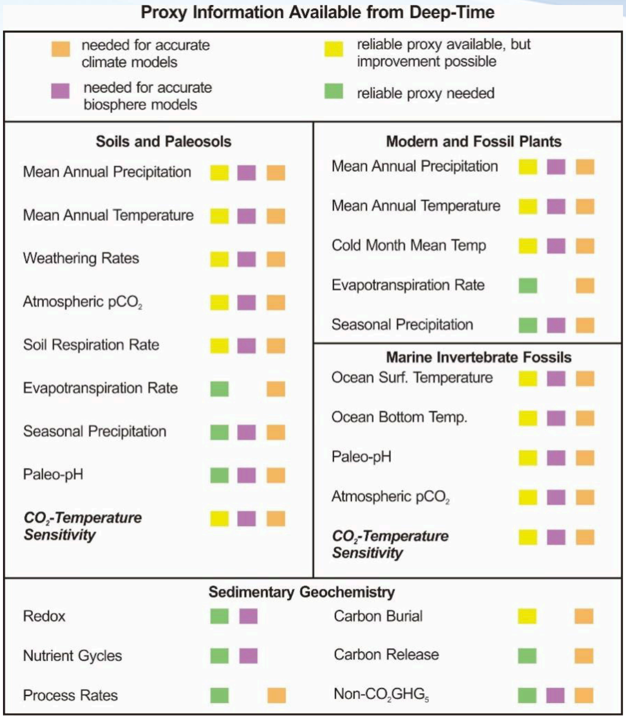

Fig. 1-5. ▲

Summary of paleoclimate proxies in fossil terrestrial and marine settings needed for developing and testing of models on future climate change. Source: Erwin and Whiteside (2012).

Terrestrial deposits have an obvious advantage over marine records for reconstructing the paleo-atmospheric pCO_2 as they provide proxies of stomatal indices and the stomatal density of higher land vascular plants (*Wu et al., 2016*), types of paleosols, and paleosol carbonates. By using such methods, preliminary estimates of paleo-atmospheric pCO_2 have been obtained through the Mesozoic-Cenozoic greenhouse (e.g., *Pagani et al, 1999; Retallack, 2001; Wang et al., 2014*). Some researchers applied records of paleosol and plant fossil assemblages to quantitatively reconstruct paleo-precipitation (e.g., *Retallack, 2005; Sheldon and Tabor, 2009*) and humidity (*Quan et al., 2013*).

The rapid development and increasing maturity of climate proxies, paleo-plate reconstructions, provenance analysis, source-to-sink systems, structural geomorphology, low-temperature thermochronology, techniques for recognizing depositional systems, and numerical modelling all allow improved interpretations and reconstructions of paleo-geomorphology, paleo-topography and paleo-climate.

1.4. Main research goals

With the development of analytical techniques in multiple disciplines and on-going concerns about future climate and geomorphology, greenhouse paleoclimate and paleo-geomorphology studies should receive more attention. The National Research Council of USA (2011) compiled six HIGH-PRIORITY goals for a deep-time scientific research agenda to address critically important scientific issues over the next decade:

- How sensitive are climates to increased atmospheric pCO_2?
- How is heat transported around the globe, and what are the controls on pole-to-equator thermal gradients?
- How will sea level and ice sheets behave in a warming world?
- How will water cycles operate in a warming world?
- Do abrupt transitions across tipping points occur in a warming world?
- What are the ecosystem thresholds and their resilience in a warming world?

We propose seven major research themes that can be addressed by sedimentologic research in China's terrestrial basins, and we will explore aspects of some of these in the following sections:

(1) The effective ways to extract terrestrial paleoclimate proxies (e.g. seasonal temperature, CO_2 concentration, precipitation/evaporation, humidity/aridity, etc.) from the geological record.

(2) The controlling factors and operating mechanisms of greenhouse and icehouse climates on different time scales, and the interactions between continents and oceans.

(3) The relationships and controlling factors between rapid climate warming events and the carbon and

terrestrial hydrological cycles. What are the coupling mechanisms between the terrestrial hydrological cycle and oceanographic processes?

(4) The responses, characteristics and consequences of rapid climate events on the continents, especially their influence on terrestrial life?

(5) The mechanisms, controlling factors, and rates of sea-level change during the transition to an ice-free greenhouse world?

(6) Quantitative and accurate reconstructions of terrestrial paleo-elevations of plateaus and mountains through geological history, as these have a major influence on climate.

(7) Establish reliable methods to identify the characteristics and evolution of monsoons under greenhouse conditions and reconstruct and interpret the monsoon evolution through different climate cycles.

2. Research frontiers

2.1. Quantitative reconstructions of terrestrial paleoclimate parameters

Terrestrial paleoclimate reconstructions are based on proxies for a broad range of surface and atmospheric conditions (paleotemperatures, pCO_2, pO_2, contents of other greenhouse gases (e.g. CH_4, N_2O), paleoprecipitation, seasonality, humidity). Higher precision and accuracy of these proxies can be achieved through the combination of proxy refinement, proxy development, and multiproxy studies (*Zhang et al., 2016*).

(1) Reconstruction of paleo-atmospheric pCO_2: Currently paleo-atmospheric pCO_2 estimates in deep time mainly come from geochemical carbon models, fossil organic and mineral matter proxies (*Royer et al., 2001*). Fossil marine and terrestrial flora provide the highest-precision paleoatmospheric pCO_2 proxies, including the alkenone paleobarometer derived from haptophyte algae in marine sediments (Pagani et al., 1999), and the stomatal-index method based on fossil leaf stomata (McElwain and Chaloner, 1995). Other, fossil soil carbonate and goethite pCO_2 proxies have been widely developed in the Mesozoic and Paleozoic paleoclimate studies (*Tabor and Yapp, 2005; Breecker et al., 2009*).

(2) Reconstruction of continental paleotemperatures: Numerous proxies have been developed for estimating continental paleotemperatures from lacustrine, coastal, and terrestrial deposits. One major proxy (stomata index?) is based on fossil plant leaves and pollen (Royer et al., 2001). Mineral-based isotopic paleothermometry offers another independent set of proxies. For example, the $\delta^{18}O$ values of pedogenic carbonates and $\delta^{18}O$ and δD values of hydroxylated clay minerals (kaolinite and smectite) and iron oxides (goethite and hematite) from paleosols are paleotemperature recorders back to the Late Paleozoic (*Tabor and Montañez, 2005*). The carbonate clumped isotope thermometer has been successfully applied to paleosol carbonates in fossil records (*Passey et al., 2010*). Conventional $\delta^{18}O$ and clumped isotope analysis of vertebrate bioapatites have been used to reconstruct paleotemperature for warm periods (*Fricke and Wing, 2004*). The presence of picoplankton members of the Archaea in ancient lake deposits opens the possibility of using the relative abundances of their membrane lipids (TEX86) as a paleothermometer of surface water (*Eglinton and Eglinton, 2008*).

(3) Reconstruction of paleo-precipitation on land: Reconstructing regional patterns in relative humidity and precipitation in deep time is very challenging. Quantitative proxies for estimating mean annual precipitation have been developed by using the iron content in pedogenic Fe-Mn nodules, by measuring the depth to the pedogenic carbonate horizon, and by measuring chemical ratios within paleosol horizons (*Sheldon and Tabor, 2009*). The measured $\delta^{18}O$

compositions of ancient soil minerals (phyllosilicates, carbonates, iron oxides, and sphaerosiderites) have been shown to be reliable proxies of soil-water $\delta^{18}O$ and, in turn, $\delta^{18}O$ of precipitation at a given paleolatitude (*Tabor and Montañez, 2005*). The hydrogen isotope ratios (δD) of individual lipids in fossil plant tissues show a great potential for reconstructing continental hydrological cycles (*Sachse et al., 2012*). The Köppen aridity index, expressed as mean annual precipitation divided by the mean annual temperature plus a constant, has proved useful to quantify aridity/humidity conditions in the past (*Quan et al., 2013*).

Future research challenges for sedimentary geochemists and paleontologists are to develop proxies for other important weather factors that govern life on land, to apply these to basin records, and to use the results for predicting future developments.

2.2. Rapid short-term climate events and the carbon cycle

In less than 100 years, industrial activity has increased greenhouse gases by over 30% and it is likely that they will exceed pre-industrial levels by over 50% before international efforts to stabilize them may become successful. A number of rapid climate-change events on different time scales (millennial to tectonic scale) have been recorded in geological history (e.g., *Jenkyns, 2010*). They offer the opportunity to uncover the mechanisms of climate change at different time scales and to assess their consequences on physical, chemical and biological processes, thereby providing a reference for impacts of climate change and for human climate-adjustment strategies in the future. Beyond stabilizing greenhouse gas emissions, an important question is how does natural carbon sequestration occur and how long it would take to reduce the amount of carbon dioxide that has built up in our atmosphere.

Past global rapid warming events during the Jurassic and Cretaceous and during the Paleocene-Eocene Thermal Maximum appear to coincide with a number of features: oceanic anoxic conditions and acidification, accelerated hydrological cycle, consequently increased continental weathering, enhanced nutrient discharge to oceans and lakes, an increase of organic productivity, and, in extreme cases, mass extinction in certain ecosystems (see recent overview paper of *Hu et al., 2020*). Studies to evaluate the amount and rate of carbon released, and the time required by nature to sequester that carbon and return to a more "normal" climate, have utilized the magnitude and rates of carbon isotope excursions (e.g., *Bauer et al. 2017; Them et al., 2017*) to better understand possible initial triggering mechanisms and feedbacks within the carbon cycle. For example, the Early Jurassic (Toarcian) OAE, which has been associated with a rapid and massive injection of 13C-depleted carbon, had an estimated duration of several hundred kyr (Boulila et al., 2014). This OAE caused significant climatic and paleoecological changes in the global ocean-atmosphere system (*Han et al., 2018*) (Fig. 1-6). The triggering mechanism and feedbacks of this major Toarcian carbon-isotope excursion are still unclear, but were probably a combination of volcanic CO_2, and thermogenic methane release caused by the eruption of the Karoo-Ferrar LIP and methane hydrate destabilization and/or decomposition of terrestrial organic matter (*Hesselbo et al., 2000; McElwain et al., 2005; Them et al., 2017*).

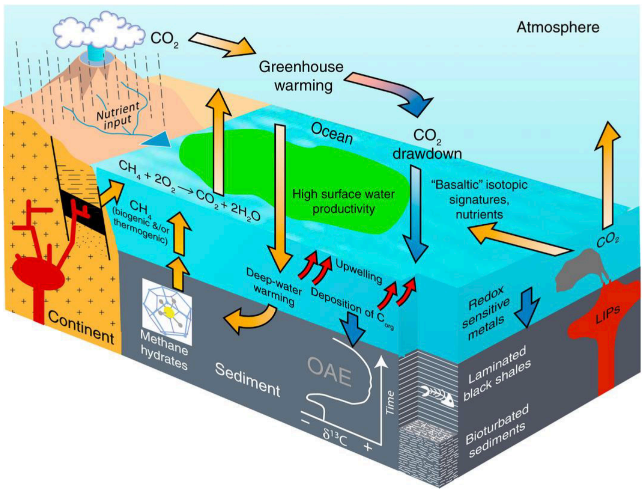

Fig. 1-6. ▲
Cartoon illustrating major positive and negative feedbacks that led to the onset and eventual termination of CO2 increase and OAEs. LIPs = large igneous provinces. Source: Robinson et al. (2017). Published with the agreement of IAS.

2.3. Short-term sea-level change and the hydrological cycle

Geological evidence indicates that sea level changed quickly during the warm Cretaceous from tens to over a hundred meters over time spans of tens of thousands to millions of years (e.g., *Maurer et al. 2013*), while this period is generally considered to have been free of low altitude ice caps. The scientific community is having a fierce debate on whether or not short-term ice sheets were controlling sea-level change during the Cretaceous greenhouse period (*Hay, 2017*). Another mechanism may be a significant redistribution between underground water storage (aquifers), lakes and the ocean (e.g., *Sames et al., 2016*). A novel concept is that high temperatures would lead to an accelerated hydrological cycle and an increase of continental aquifer water storage, and therefore a drawdown of sea level (Fig. 1-7). Records of global sea-level oscillations and possible groundwater storage during greenhouse conditions need to be investigated further in the margins and interior basins of China plates. Answers to questions about future sea-level rise (or fall) are urgently needed for societal planning and preparation. Cretaceous epicontinental seas on stable cratons, such as Tarim, Lhasa and in northeastern China, provide excellent opportunities to study and model the mechanisms of short-term sea-level change.

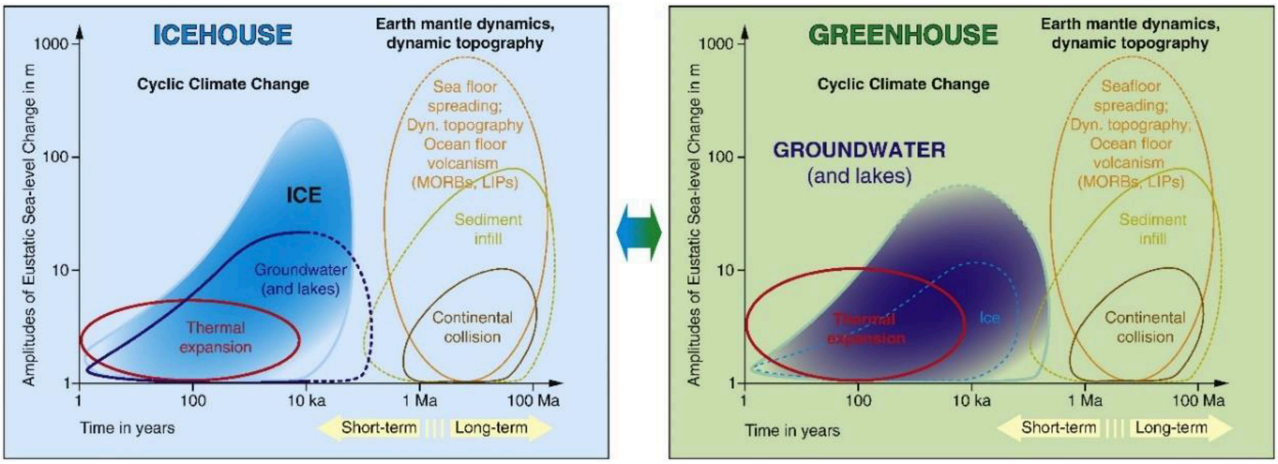

Fig. 1-7. ▲

Comparative log-scale diagrams of the timing and amplitudes of major geologic mechanisms for driving eustatic sea-level change during icehouse (left) and greenhouse (right) climate modes. Dashed lines give dimensions of efficacy that are of lesser relevance in the warm Cretaceous. The dominant processes proposed by Sames et al. (2016) for short-term eustatic sea-level change are glacio-eustasy during icehouse phases and aquifer-eustasy during warm greenhouse phases. Source: Sames et al. (2016).

2.4. Reconstructing continental paleo-drainage

Paleo-drainage, the amount of water and sediment being carried down by river systems, is the most direct representation of paleo-sedimentary and source-to-sink sediment transport. It is closely related to the regional-scale to global-scale controls of paleogeographic, paleoclimatic and plate-tectonic evolution. Reconstructions of paleo-drainage can be used to constrain the paleo-geomorphology in three dimensions and against the background of geological events, climate change and tectonic evolution in time and space (e.g., studies of North American and European paleo-drainage during the Mesozoic-Cenozoic by *Dickinson and Gehrels, 2008; Hoorn et al., 2010; Garzanti et al., 2011; Blum and Pecha, 2014).*

With the development of experiment techniques for terrestrial sedimentary processes and the broad applications of provenance studies of detrital minerals, breakthroughs in the precise

evolution mechanisms of paleo-drainage and their dependence on climatic and tectonic trends are to be expected.

2.5. Reconstruction of paleo-elevation

The uplift history of Chinese plateaus and mountains did not only constrain the development, distribution and direction of drainage systems, but also affected regional climate (e.g., the monsoon) and had significant impacts on biological evolution and ecosystem distribution. Weathering and erosion of uplands changed the downstream sedimentation and the chemical composition and nutrient levels of sea water, thereby further affecting global oceanic and terrestrial environments (e.g., *Bishop, 2007*).

The uplift history of the Tibetan Plateau, an important factor in the regional paleoclimate and the Asian monsoon, is complex (e.g., *Wang et al., 2014; Ding et al., 2014; Liu et al., 2017a, b*). Was there a proto-Tibetan Plateau in the Late Mesozoic? How did the uplift of coastal mountain ranges in East China affect climate? What were their scale, height, and impacts? The answers to these questions will deepen our understanding of the continental climate and environment. Developing a quantitative reconstruction of the paleo-elevation in different regions through time is one of the great challenges for sedimentologists.

In the past two decades, the available tools have been augmented by analyses of hydrogen and oxygen isotopes, 'clumped' CO_2 isotopes ($\Delta 47$), and Climate-Leaf Analysis Multivariate Program (CLAMP). For example, a study using 'clumped' isotopes in the Jiaolai Basin indicates that coastal mountains with paleo-elevations of at least 2-3 km might have had a significant influence on the East-Asian paleoclimate during the Late Cretaceous (*Zhang et al., 2016*) (Fig. 1-8).

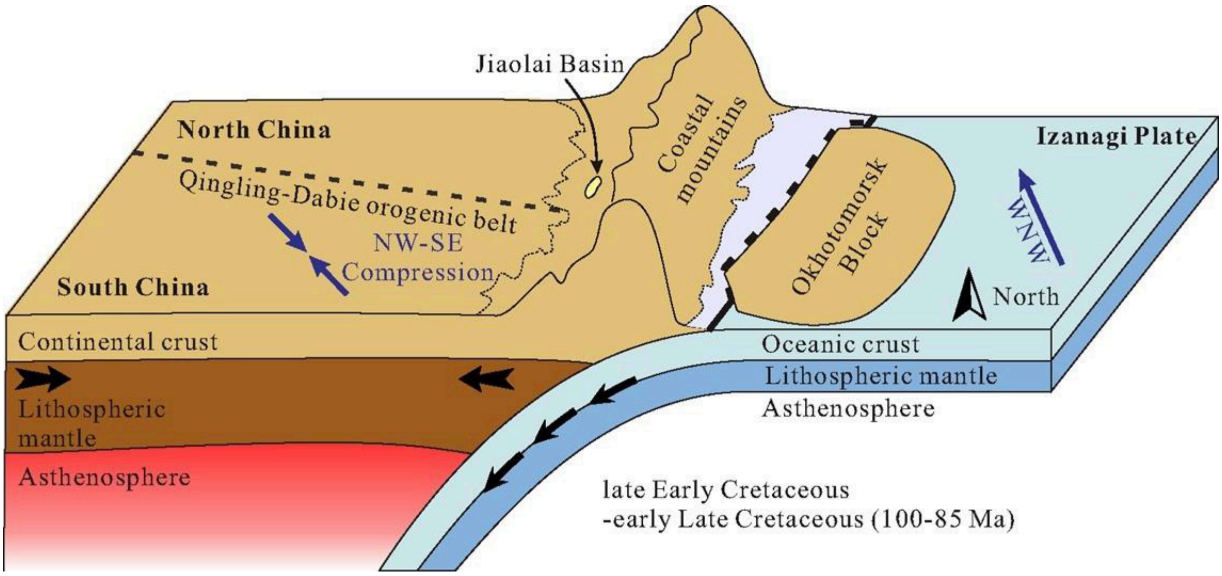

Fig. 1-8. ▲
Simplified cartoon showing the Cretaceous tectonic evolution of East China during late Early Cretaceous–early Late Cretaceous (100–85 Ma). Source: Zhang et al. (2016).

2.6. Global wind patterns, monsoons, and the hydrological cycle

Our understanding of the response of continental and oceanic wind systems, especially changes in the intensity of the monsoon systems, to increasing greenhouse conditions is very limited. The planetary wind system during a greenhouse climate might have been completely different from that during icehouse conditions due to the relatively small pole-to-equator temperature difference (Hay, 2011). Determining the paleowind fields based on precise reconstructions of paleogeography and plate orientations is the main target for many researchers (e.g., *Jiang and Pan, 2005; Liu et al., 2017a, b*).

The monsoon system plays a major role in the hydrological cycle of terrestrial environments. The Cenozoic convergence of the Indian and Asian subcontinents led to the southern Asian monsoon (*Liu et al., 2017a, b*), and the initiation of the eastern Asian monsoon in the early Miocene was closely related to the uplift of the Tibetan Plateau (*Guo et al., 2002*). Up to now, the driving mechanisms of the monsoon system remain unclear, on both long-term geological (tectonic and orbital) and short-term centennial time scales.

3. Requirements for making progress

(a) Quantitative reconstructions of the terrestrial paleoclimate requires a focus on: 1) major scientific continental drilling programs (such as the Scientific Continental Drilling Project of the Cretaceous Songliao Basin, the Colorado Plateau Coring Project on Triassic-Jurassic terrestrial strata, and the Bighorn Basin Coring Project (penetrating the PETM interval) and 2) high-precision geochronology and quantitative chronostratigraphy methods for precisely determining the ages and sequences in deep-time.

(b) Studies of rapid short-term climate events and the effects of major surges of greenhouse gasses in terrestrial settings to decipher their impacts on continental temperature, the carbon cycle, the water cycle and biological changes.

(c) Reconstruction of high-resolution sea-level changes from sedimentary records on relatively stable continental margins and making stratigraphic correlations between different regions and continents.

(d) Studies of the rate, frequency and scale of paleo-drainage evolution in different climate modes, i.e., icehouse and greenhouse, to clarify the effect of climate change on the frequency of floods.

(e) A quantitative reconstruction of paleo-elevation in different regions through time to better understand the effect of (changing) climate and topography on global oceanic and terrestrial environments.

(f) Extracting monsoon information from the terrestrial and marine records has been and will be an important research topic for terrestrial climate studies and for testing computer models of climate change.

4. China's opportunity and future strategy

To date, the understanding of paleoclimate and paleoenvironment during the Mesozoic through Cenozoic has been mainly derived from marine sections. East Asia, especially China, has extensive terrestrial deposits throughout this period, and they represent a wide diversity of paleo-environments. China in particular has many Mesozoic lacustrine basins from which we can obtain continuous records of terrestrial climate change, such as paleotemperature, pCO_2, precipitation and aridity. The terrestrial basins contain unparalleled records of the evolution of terrestrial vertebrates and the origin of birds, such as the deposits that yielded the famous Jehol and Yanliao biota. China has an obvious advantage in the study of these terrestrial basins to understand the relationships between the evolution of biota and paleoclimate change, the role of greenhouse conditions in sequestering carbon in lacustrine sediments (the source rocks for some of our modern continental oil and gas), the effect of uplifting plateaus on monsoon intensity, the change in frequency and intensity of floodings and droughts during greenhouse conditions in different settings, and many other aspects of paleoclimate history on continental landmasses. Few other continents have such an extensive and continuous terrestrial record spanning 200 million years from the Mesozoic through Paleogene. Therefore, applying current and future tools to unravel China’s terrestrial climate record will enable a much better prediction of future climate effects on other continental habitats.

References

Barrett, P., 1999. Antarctic climate history over the last 100 million years. Terra Antarctica Reports 3, 53-72.

Barrett, 1999 is not cited in text

Bauer, K.W., Zeebe, R.E., Wortmann, U.G., 2017. Quantifying the volcanic emissions which triggered Oceanic Anoxic Event 1a and their effect on ocean acidification: Sedimentology 64, 204-214.

Bishop, P., 2007. Long-term landscape evolution: linking tectonics and surface processes. Earth Surface Processes and Landforms 32, 329-365.

Blum, M., and Pecha, M., 2014. Mid-Cretaceous to Paleocene North American drainage reorganization from detrital zircons. Geology 42, 607-610.

Boucot, A.J., Chen X., Scotese, C.R., 2013. Phanerozoic Paleoclimate: An Atlas of Lithologic Indicators of Climate. SEPM Concepts in Sedimentology and Paleontology, (Print-on-Demand Version) 11, 478. Society for Sedimentary Geology, Tulsa, OK.

Boulila, S., Galbrun, B., Huret E., Hinnov, L. A., Rouget I., Gardin, S., Bartolini A., 2014. Astronomical calibration of the Toarcian Stage: implications for sequence stratigraphy and duration of the early Toarcian OAE. Earth and Planetary Science Letters 386, 98-111.

Breecker, D., Sharp, Z., McFadden, L. D., 2009. Seasonal bias in the formation and stable isotopic composition of pedogenic carbonate in modern soils from central New Mexico, USA. Geological Society of America Bulletin 121, 630-640.

Dickinson, W.R., Gehrels, G.E. 2008. U-Pb ages of detrital zircons in relation to paleogeography: Triassic paleodrainage networks and sediment dispersal across southwest Laurentia. Journal of Sedimentary Research 78, 745-764.

Ding, L., Xu, Q., Yue, Y., Wang, H., Cai, F., Li, S., 2014. The Andean-type Gangdese Mountains: Paleoelevation record from the Paleocene–Eocene Linzhou Basin. Earth and Planetary Science Letters 392, 250-264.

Eglinton, T., and Eglinton, G. 2008. Molecular proxies for paleoclimatology. Earth and Planetary Science Letters 275, 1-16.

Erwin, D., and Whiteside, J., 2012. Transitions: The Changing Earth-Life System-Critical Information for Society from the Deep Past 1-61.

Fricke, H., and Wing, S, 2004. Oxygen isotope and paleobotanical estimates of temperature and $\delta^{18}O$–latitude gradients over North America during the early Eocene. American Journal of Science 304, 612-635.

Garzanti, E., Vezzoli, G., Andò, S., 2011. Paleogeographic and paleodrainage changes during Pleistocene glaciations (Po Plain, northern Italy). Earth-Science Reviews 105, 25-48.

Guo, Z., Ruddiman, W.F., Hao, Q., Wu, H., Qiao, Y., Zhu, R.X., Peng, S., Wei, J., Yuan, B., Liu, T., 2002. Onset of Asian desertification by 22 Myr ago inferred from loess deposits in China. Nature 416, 159-163.

Hay, W. W., 2011. Can humans force a return to a 'Cretaceous' climate?. Sedimentary Geology 235(1-2), 5-26.

Hay, W.W., 2017, Toward understanding Cretaceous climate—An updated review: Science China Earth Sciences 60(1), 5-19.

Hesselbo, S.P., Gröcke D.R., Jenkyns H.C., Bjerrum C.J., Farrimond, P., Bell, H.S.M., Green, O.R., 2000. Massive dissociation of gas hydrate during a Jurassic oceanic anoxic event. Nature 406, 392-395.

Hönisch, B., Ridgwell, A., Schmidt, D.N., Thomas, E., Gibbs, S.J., Sluijs, A., Zeebe, R., Kump, L., Martindale, R.C., Greene, S.E., Kiessling, W., Ries, J., Zachos, J.C., Royer, D.L., Barker, S., Marchitto, T.M., Moyer, R., Pelejero, C., Ziveri, P., Foster, G.L., Williams, B., 2012. The geological record of ocean acidification. Science 335, 1058-1063.

Hoorn C., Wesselingh F.P., ter Steege H., Bermudez, M.A., Mora, A., Sevink, J., Sanmartin, I., Sanchez-Meseguer A., Anderson, C.L., Figueiredo, J.P., Jaramillo, C., Riff, D. Negri, F.R., Hooghiemstra,H., Lundberg, J., Stadler, T., Särkinen, T., Antonelli, A., 2010. Amazonia through time: Andean uplift, climate change, landscape evolution, and biodiversity. Science 330(6006), 927-31.

Hou, M.C., Chen, A.Q., Ogg, J.G., Ogg, G., Huang, K.K., Xin, F.C., Chen, H.D., Jin, Z.K., Liu, Y.Q., Shi, Z.Q., Zhen, H.R., Hu, Z.Q., Huang, H., Liu, X.C., 2019. China paleogeography: Current status and challenges. Earth-Science Reviews 189, 177-193. https://doi.org/10.1016/j.earscirev.2018.04.004.

Hu, X., Li, J., Han, Z., Li, Y., 2020. Two types of hyperthermal events in the Mesozoic-Cenozoic: Environmental impacts, biotic effects, and driving mechanisms. Science China Earth Sciences 63, 1041-1058.

Jenkyns, H.C., 2010, Geochemistry of oceanic anoxic events. Geochemistry, Geophysics, Geosystems, 11(3), 427-428.

Jiang, X.S., and Pang, Z.X, 2005. Cretaceous Deserts in China and Palaeoclimate. Geological publishing house in Beijing. (in Chinese with English abstract).

Liu, X.H., Xu, Q., Ding L., 2017a. Differential surface uplift: Cenozoic palaeoelevation history of the Tibetan Plateau. Science China Earth Sciences 59, 2105–2120 (in Chinese with English abstract).

Liu, X.D., Dong, B.W., Yin, Z.Y., Smith, R.S., Guo, Q.C., 2017b. Continental drift and plateau uplift control origination and evolution of Asian and Australian monsoons. Scientific Reports 7, 40344.

Maurer, F., van Buchem, F.S.P., Eberli, G.P., Pierson B.J., Raven, M.J., Larsen, P.H., Al-Husseini, M.I., Vincent, B., 2013. Late Aptian long-lived glacio-eustatic lowstand recorded on the Arabian Plate. Terra Nova 25, 87-94.

McElwain, J.C., and Chaloner, W.G., 1995. Stomatal density and index of fossil plants track atmospheric carbon dioxide in the Paleozoic. Annals of Botany 76, 389-395.

McElwain, J.C., Wade-Murphy, J., Hesselbo, S.P., 2005. Changes in carbon dioxide during an oceanic anoxic event linked to intrusion into Gondwana coals. Nature 435, 479-482.

National Research Council (NRC), 2011. Understanding Earth's Deep Past: Lessons for Our Climate Future, The National Academies Press (Washington, D.C.), 208 pp.

Pagani, M., Freeman, K.H., Arthur, M.A., 1999. Late Miocene atmospheric CO_2 concentrations and the expansion of C4 grasses. Science 285, 876-879.

Passey, B.H., Levin, N.E., Cerling, T.E., Brown, F.H., Eiler, J.M, 2010. High-temperature environments of human evolution in East Africa based on bond ordering in paleosol carbonates: Proceedings of the National Academy of Sciences of the United States of America 107, 11245-11249.

Quan, C., Han, S., Utescher, T., Zhang, C., Liu, Y.S., 2013. Validation of temperature–precipitation based aridity index: Paleoclimatic implications. Palaeogeography, Palaeoclimatology, Palaeoecology 386, 86-95.

Raymo, M.E., Ruddiman, W.F. 1992. Tectonic forcing of late Cenozoic climate change. Nature 359, 117–122.

Retallack, G.J., 2001. A 300-million-year record of atmospheric carbon dioxide from fossil plant cuticles. Nature 411, 287-290.

Retallack, G.J., 2005. Pedogenic carbonate proxies for amount and seasonality of precipitation in paleosols. Geology 33, 333-336.

Robinson, S.A., Heimhofer, U., Hesselbo, S.P., Petrizzo, M.R., 2017. Mesozoic climates and oceans–a tribute to Hugh Jenkyns and Helmut Weissert. Sedimentology 64, 1-15.

Royer, D.L., Wing, S.L., Beerling, D.J., Jolley, D.W., Koch, P.L., Hickey, L.J.R., Berner, A., 2001. Paleobotanical evidence for near present-day levels of atmospheric CO_2 during part of the Tertiary. Science 292, 2310-2313.

Sachse, D., Billault, I., Bowen, G.J., Chikaraishi, Y., Dawson, T.E., Feakins, S.J., Freeman, K.H., Magill, C.R., McInerney, F.A., Van der Meer, M.T., 2012. Molecular Paleohydrology: interpreting the hydrogen-isotopic composition of lipid biomarkers from photosynthesizing organisms. Annual Review of Earth and Planetary Sciences 40, 221-249.

Sames, B., Wagreich, M., Wendler, J., Haq, B., Conrad, C., Melinte-Dobrinescu, M., Hu, X., Wendler, I., Wolfgring, E., Yilmaz, I., 2016. Review: Short-term sea-level changes in a greenhouse world—A view from the Cretaceous. Palaeogeography, Palaeoclimatology, Palaeoecology 441, 393-411.

Scotese, C., 2014. Atlas of Late Cretaceous paleogeographic maps, PALEOMAP atlas for ArcGIS, volume 2, The Cretaceous, Maps 16–22, Mollweide Projection.

Scotese, C.R., 2015. Phanerozoic Temperature Curve, PALEOMAP Project, Evanston, IL.

Sheldon, N.D., Tabor, N.J., 2009. Quantitative paleoenvironmental and paleoclimatic reconstruction using palaeosols. Earth-Science Reviews 95, 1-52.

Sun, S., Wang, C.S., 2009. Deep Time and sedimentology. Acta Sedimentologica Sinica 27, 792-810 (in Chinese with English abstract).

Sun, Y., Joachimski, M.M., Wignall, P.B., Yan, C., Chen, Y., Jiang, H., Wang, L., Lai, X., 2012. Lethally hot temperatures during the Early Triassic greenhouse. Science 338, 366-370.

Tabor, N.J., Montañez, I.P., 2005. Oxygen and hydrogen isotope compositions of Permian pedogenic phyllosilicates: Development of modern surface domain arrays and implications for paleotemperature reconstructions. Palaeogeography, Palaeoclimatology, Palaeoecology 223, 127-146.

Tabor, N.J., Myers, T.S., 2015. Paleosols as indicators of paleoenvironment and paleoclimate. Annual Review of Earth and Planetary Sciences 43, 333-361.

Tabor, N.J., Yapp, C.J., 2005. Coexisting goethite and gibbsite from a high-paleolatitude (55 N) Late Paleocene laterite: concentration and 13 C/12 C ratios of occluded CO_2 and associated organic matter. Geochimica et Cosmochimica Acta 69, 5495-5510.

Them, T., Gill, B., Caruthers, A., Gröcke, D., Tulsky, E., Martindale, R., Poulton, T., Smith, P., 2017. High-resolution carbon isotope records of the Toarcian Oceanic Anoxic Event (Early Jurassic) from North America and implications for the global drivers of the Toarcian carbon cycle. Earth and Planetary Science Letters 459, 118-126.

Wang, C., Dai, J., Zhao, X., Li, Y., Graham, S.A., He, D., Ran, B., Meng, J., 2014. Outward-growth of the Tibetan Plateau during the Cenozoic: A review. Tectonophysics 621, 1-43.

Wang, C.S., Scott, R.W., Wan, X.Q., Graham, S.A., Huang, Y.J., Wang, P. J., Wu, H.C., Dean, W.E., Zhang, L.M., 2013. Late Cretaceous climate changes recorded in Eastern Asian lacustrine deposits and North American epieric sea strata. Earth-Science Reviews 126, 275–299.

Wang, H.Z., 1985. Atlas of the Palaeogeography of China. Cartographic Publishing House: Beijing, 170 pp.

Wang, T., Ramezani, J., Wang, C., Wu, H., He, H., Bowring, S. A., 2016. High-precision U–Pb geochronologic constraints on the Late Cretaceous terrestrial cyclostratigraphy and geomagnetic polarity from the Songliao Basin, Northeast China. Earth and Planetary Science Letters 446, 37-44.

Wang, Y., Huang, C., Sun, B., Quan, C., Wu, J., Lin, Z., 2014. Paleo-CO_2 variation trends and the Cretaceous greenhouse climate. Earth-Science Reviews 129, 136–147.

Wang, Y.D., Sun, B., Huang, C., Quan, C., 2015. Variation of palaeo-CO_2 and greenhouse climate in the geological history: A case study from the Cretaceous of the Mesozoic. Chinese Journal of Nature 37, 108-114 (in Chinese with English abstract).

Wignall, P.B., 2015. The Worst of Times: How Life on Earth Survived Eighty Million Years of Extinctions. Princeton University Press, 224 pp.

Wu, G., Liu, Y., Bian, H., Bao, Q., Duan, A., Jin, F.F., 2012. Thermal controls on the Asian Summer Monsoon. Scientific Reports 2, 404.

Wu, H.C., Wang, C.S., Zhang, S.H., Yang, T.S., and Wan, X.J., 2011. EARTHTIME Project: Dating precision and temporal resolution in the “Deep Time” record. Geoscience 25, 419-428 (in Chinese with English abstract).

Wu, J.Y., Ding, S.T., Li, Q.J., Sun, B.N., Wang, Y.D., 2016. Reconstructing paleoatmospheric CO_2 levels based on fossil Ginkgoites from the Upper Triassic and Middle Jurassic in Northwest China. PalZ 90, 377-387.

Zachos, J., Pagani, M., Sloan, L., 2001. Trends, rhythms, and aberrations in global climate 65 Ma to present. Science 292, 686-693.

Zhang, L., Wang, C., Cao, K., Wang, Q., Tan, J., Gao, Y., 2016. High elevation of Jiaolai Basin during the Late Cretaceous: Implication for the coastal mountains along the East Asian margin. Earth and Planetary Science Letters 456, 112-123.

Chapter 2.

Sedimentation, biological and geochemical processes over major Microbe-Metazoan Transitions (MMTs) in the geologic past

Zhong Qiang Chen [1] , Chuanming Zhou [2] , Chenyi Tu [1] , Yu Pei [1] , Yuheng Fang [1] ,

[1]- State Key Laboratory of Biogeology and Environmental Geology, Chi na University of Geosciences (Wuhan), Wuhan 430074 , China

[2]- Nanjing Institute of Geology and Palaeontology, Chinese Academy of Sciences, Nanjing 210008, China

1. Overview

Growing evidence shows that biotic activities are involved in most, if not all, sedimentation processes from the ancient geological past to the present day. As reflected by presentations at recent major international conferences (i.e., ISC, GSA meetings, etc.), organism-induced sedimentation (also termed "biosedimentology") has attracted increasing interest from global paleontologists and sedimentologists. The theme of this chapter in the Roadmap of Sedimentology in China to 2030 is organism, including microbes. involvement in sedimentation throughout Earth's history from the Proterozoic to the present-day, with an emphasis on well-preserved examples from China. Highlighted, in particular, are organism-environment interactions during critical periods for the evolution of life on Earth.

Biosedimentary records show that sedimentary systems and ecosystems have undergone at least five major microbe-metazoan transitions (MMTs) from the Precambrian to the Present (*Chen et al., 2017*). The first MMT witnessed the rise of complex multicellar organisms in the microbial mat-dominated ecosystems in the late Ediacaran, the last period of the Precambrian. Microbial participation was crucial for the establishment of metazoan-dominated ecosystems and for the preservation of late Ediacaran animal embryos (*Xiao et al., 1998*). Since the early Cambrian explosion, the sea floors of shallow seas changed from matgrounds to highly bioturbated substrates through the early to middle stages of the Cambrian. Microbial and metazoan reefs are exceptional, and their alternate occurrences, as well as their co-occurrence, characterize the Cambrian MMT. The remaining three MMTs are linked to three intervals of major biotic extinction and environmental stress, i.e., in the aftermaths of the Ordovician–Silurian (O–S), Frasnian–Famennian (F–F), and Permian–Triassic (P–Tr) mass extinctions. These MMTs seem to have been more profound than younger ones. In contrast, both the Triassic–Jurassic and Cretaceous–Paleogene (C–Pg) mass extinctions did not result in typical MMT deposits in their aftermaths. In addition, distinct geochemical signatures characterize depositional systems during several major life and environmental turning points, such as the O–S boundary, F–F boundary, Guadalupian–Lopingian (G–L, Middle and Late Permian) boundary, and the mid-Jurassic and late Cretaceous AOEs, which are well recorded in China (Fig. 2-1).

The overall goal of this chapter is to provide a brief overview of biological processes in physical sedimentation from the Ediacaran to the present day, together with their possible consequences and controls. It emphasizes three aspects: (1) microbially mediated and microbially induced sediments (i.e., microbial mats, microbialites, oolites, oncolites), (2) metazoan build-ups (i.e., reefs, bioherms, and carbonate platforms), and (3) (bio)geochemical signals of extreme environmental and climatic change during these critical transitions. How rapidly ecosystems can adjust to abrupt environmental extremes and climate change are fundamental questions accompanying present-day global warming and environmental stress. An important tool to address this question is to document and understand the outcome of equivalent 'natural experiments' in the deep-time geological record, in particular where the magnitude and/or rates of change in the global environment/climate system were sufficiently large to threaten biodiversity, leading at times to mass extinctions. Thus, the rock and fossil records of large-scale ecosystem collapse should provide insight into the potential response of present-day ecosystems to environmental and climate change. This also links into current global concerns and issues such as 'sustainable use of biodiversity', 'biodiversity response to global warming' and 'keeping our planet environmentally sustainable'.

Global biosedimentary records provide important materials for evaluating the nature and importance of organismal involvement in sedimentation through geological time. The emphasis on multidisciplinary studies in these Chinese examples is also timely because Biosedimentology is a field of intense research in the geosciences worldwide. Thus, this chapter will address the relationships between organisms and sedimentation throughout the geological past, based on exceptionally well-preserved materials from China.

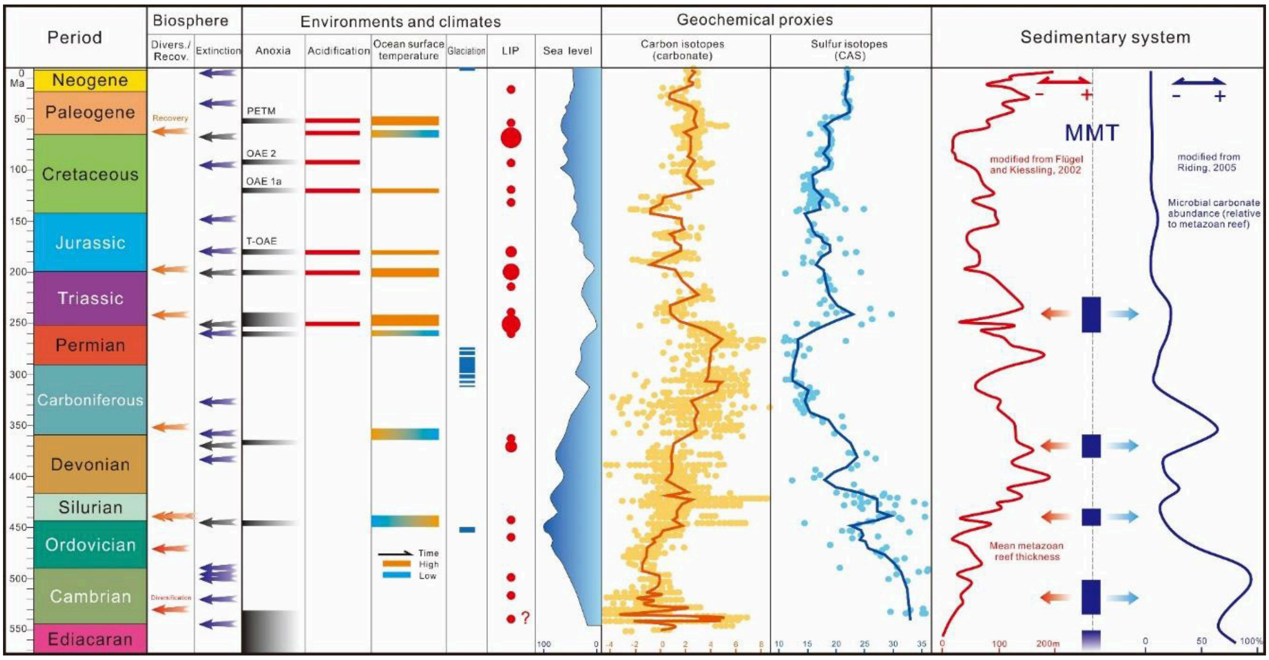

Fig. 2-1.▲

Environmental, climatic and biotic extremes, and biosedimentary processes, through the late Neoproterozoic to the present day (modified from Chen et al., 2019). Abbreviations: PETM = Paleocene-Eocene Thermal Maximum, OAE 1a = Early Aptian Oceanic Anoxic Event, OAE 2 = Cenomanian-Turonian Oceanic Anoxic Event, T-OAE = Early Toarcian Oceanic Anoxic Event, LIP = Large Igneous Province, MMT = microbe-metazoan transition, Pt3 = Neoproterozoic, Pre-C = Precambrian. The geological timescale follows Ogg et al. (2016). Data for biotic diversification, recovery and mass extinctions are after Chen et al. (2014a). Data for LIP, anoxia, acidification, glaciation, and sulfur isotopes follow Bond and Grasby (2017); carbon-isotope data follow Rong and Huang (2014). Data for cumulative thickness of metazoan carbonate and microbial carbonate abundance are from Flügel and Kiessling (2002) and Riding and Liang (2005), respectively.

Of the deep-time biosedimentary records, both metazoan-induced carbonates and microbial carbonates are the most important proxies revealing oceanic geochemical conditions and biological process during sedimentation. They are among the most common sedimentary rocks in the geological record and alternately dominate deep-time sedimentary successions. These two types of sedimentary rocks, therefore, are important target materials to investigate the relationships among organism, environment and climate regimes. Accordingly, four major scientific questions linked with Biosedimentology need to be addressed:

(1) What are the sedimentary patterns of critical microbe-metazoan transitions in actual stratigraphical sections?

(2) How many MMTs are recognizable from the late Neoproterozoic to present day?

(3) What are the carbonate production mechanisms for both metazoan and microbial carbonates?

(4) What are the environmental, climatic and biotic responses to the major changes in carbonate factory mechanisms during the geological past?

Ultimately, we hope that these biosedimentological records will advance global knowledge of biotic involvement in sedimentation during critical life and environmental transforming transitions, and provide strategies to help manage current global extreme events and subsequent restoration of marine ecosystems. In particular, switching between metazoan carbonate and microbial carbonate depositional systems typically corresponds to major environmental, climatic and biotic changes linked with major mass extinctions during geological history.

2. Examples of research frontiers

2.1. Microbe-Metazoan Transitions from the Ediacaran to Cenozoic

Global data show major accumulative thickness peaks of metazoan reef development in the early Late Devonian and Middle Permian. The former is characterized by abundant coral and stromatoporoid reefs (*Copper, 2002*), while the Middle Permian reef peak is mainly attributed to thriving sponge build-ups worldwide (*Flügel and Kiessling, 2002*). Several secondary peaks also occurred in the Middle Ordovician, Middle Triassic and Late Jurassic to Early Cretaceous (Fig. 2-1). In contrast, major Phanerozoic microbial carbonate abundance peaks occur in the Cambrian and Late Devonian, with two shorter peaks in the Early Silurian and Early-Middle Triassic (*Riding and Liang, 2005*). Overall, accumulative thickness peaks of metazoan reefs correspond to the lower values of microbial carbonate abundance, and their lower values point to the abundance peaks of microbial carbonates through the Phanerozoic (Fig. 2-1). Five major MMTs have been recognized in the Ediacaran, Cambrian, Early Silurian, Late Devonian to Early Carboniferous, and Early-Middle Triassic, respectively, and are briefly summarized below.

2.1.1. Ediacaran

Prior to the Snowball Earth interval, microbial communities dominated marine Earth's ecosystems for more than 2.5 billion years. Stromatolite reefs first appeared in the Archean, proliferated in Paleoproterozoic-Mesoproterozoic times, and eventually declined in the late Neoproterozoic (*Riding, 2006*). In contrast, metazoan reefs first appeared after the late Neoproterozoic glaciations. For example, Cloudina represents early animal skeletons, which formed skeletal reef buildups often in association with microbial reefs (thrombolites and stromatolites) in the Ediacaran Nama Group of Namibia (*Penny et al., 2014*). Many Ediacaran-type multicellar animals occur with microbial mats in the Flinders Range, South Australia, and at Mistaken Point, Newfoundland (*Gehling, 1999; Liu et al., 2015*). In South China, early Neoproterozoic microbial reefs are widely distributed at the margins of the North China Craton, particularly in Shandong and eastern Liaoning, and in northern areas of Jiangsu and Anhui (*Cao and Yuan, 2003; Xiao et al., 2014*), while metazoans (i.e., Cloudina and other metazoans) are abundantly associated with thrombolites following the Snowball Earth event in Hubei-Shaanxi border areas. In addition, one of the most remarkable discoveries of early life in China are exceptionally well-preserved animal embryos from the late Ediacaran Doushantou Formation in Guizhou Province (*Xiao et al., 1998*). These tiny eggs demonstrate reproductive patterns and processes of animal cells, marking the emergence of the first animals on Earth. Microbes were intimately involved in the preservation of these animal embryos (Xiao et al., 1998). Another important find bearing on the origin of early animal life is the early Ediacaran Lantian biota from Anhui Province (Fig. 2-1), which probably represents the earliest known assemblage of macroscopic and morphologically differentiated eukaryotes, comprising diverse algal, including microbes, and putative animal fossils (*Yuan et al., 2011*). Thus, the coexistence of both microbes and metazoans seems to have set the agenda for full-scale metazoan biodiversification in the late Ediacaran.

2.1.2. Early Paleozoic

The earliest Paleozoic, marking the beginning of the Phanerozoic, witnessed the well-known Cambrian Explosion or Cambrian radiation (*Zhuravlev and Riding, 2000*), marked by emergence of many new metazoan groups. As multiple fossil groups evolved, shallow-marine substrates were fundamentally altered, ranging from Neoproterozoic microbially sealed seafloors to bioturbated niches in the Cambrian. This has been called the 'Cambrian substrate revolution' (Bottjer et al., 2000). During the Cambrian, substrates sealed by microbial mats were gradually converted to highly bioturbated seafloors. In carbonate settings, metazoan reefs, composed mainly of archaeocyath and lithistid sponges, co-existed with microbialites, mainly stromatolites and thrombolites (*Yan et al., 2017; Lee and Riding, 2018*). The thrombolites are primarily constructed by various forms of Epiphyton and are interbedded with metazoan-dominated carbonate build-ups. In the field, the most common examples are microbialites, which are often interbedded with highly bioturbated carbonate units or metazoan fossil-bearing carbonates. Such alternations are commonly present throughout the Cambrian Series 2 to Furongian strata in North China (*Fig. 2-2; Qi et al., 2014, 2017*). Therein, alternations of digitate stromatolite layers and Skolithos-bearing bioturbated limestone layers are exposed within the Zhangxia Formation of the Lushan-Dengfeng areas, Henan Province, North China (Fig. 2-2). This association of microbe- and metazoan-bearing horizons represents the first major MMT period of the Phanerozoic (Fig. 2-1).

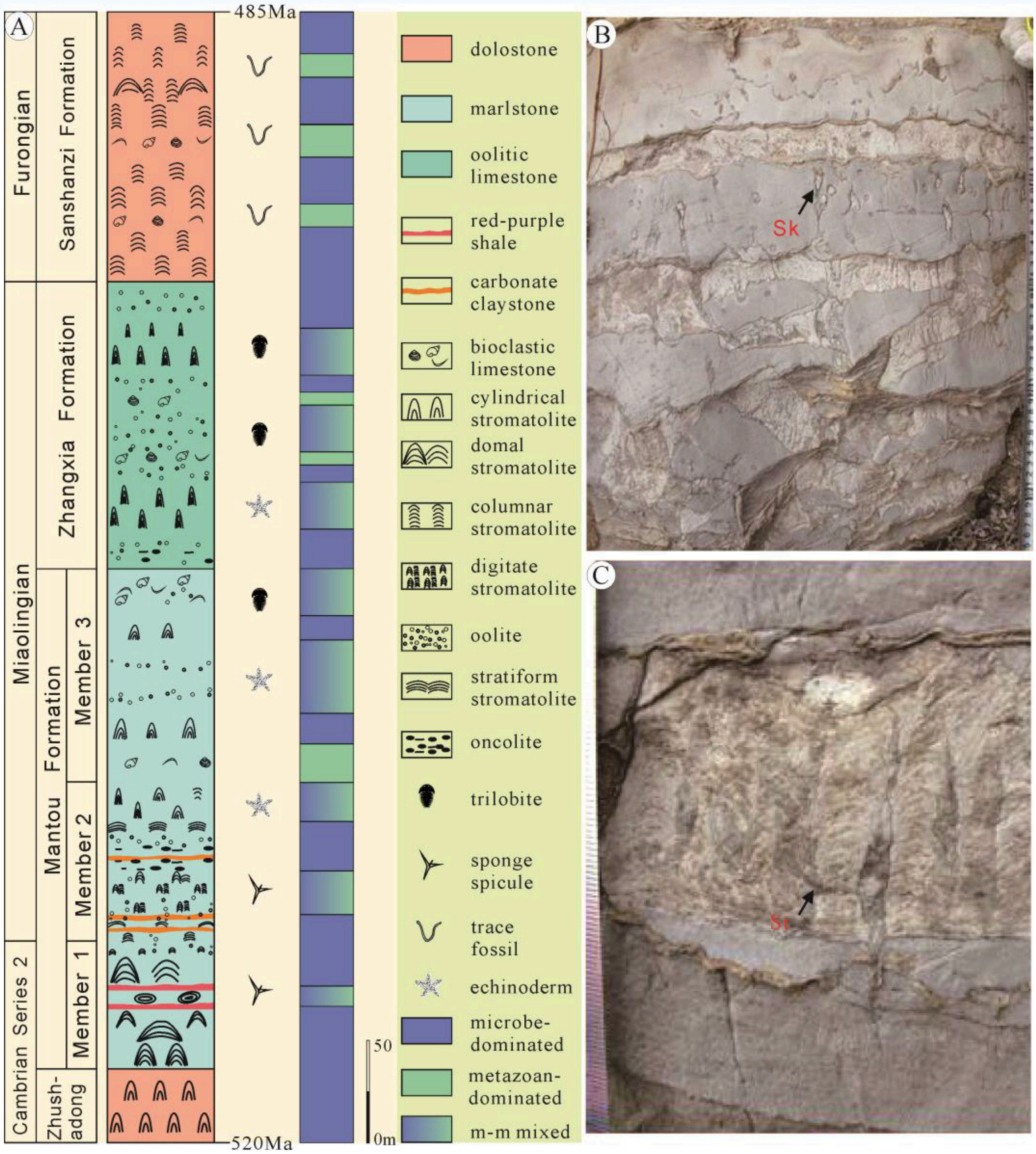

Fig. 2-2. ▲

(A) Schematic composite stratigraphical columnar of Cambrian Series 2 to Furongian carbonate successions; MMT stacking patterns of microbe-dominated, of metazoan-dominated, and of microbe-metazoan mixed units; and stratigraphical distributions of trilobites, sponge spicules, echinoderms, and ichnofossils in the Lushan and Dengfeng areas, Henan Province, North China (Qi et al., 2014, 2017). (B) Alternations of stromatolite and highly bioturbated (Skolithos sp.) limestone (or carbonate pipe rock) outcropping in the field, Cambrian Series 3 Mantou Formation of Lushan, Henan Province, North China. Sk = Skolithos (C.) Close-up of digitate stromatolite and limestone layers. St = Stromatolites. Cambrian age model is after Ogg et al. (2016). Source: Chen et al., 2019

The Great Ordovician Biodiversification Event (GOBE, *Harper, 2006; Servais and Harper, 2018*) marks the first proliferation of metazoan reefs following the Cambrian MMT. Calathium reefs proliferated globally during the Early Ordovician, and Calathium-microbial reefs are common in China. Towards the Late Ordovician, metazoan-dominated reefs declined, and microbial-dominated build-ups again proliferated locally in carbonate settings.

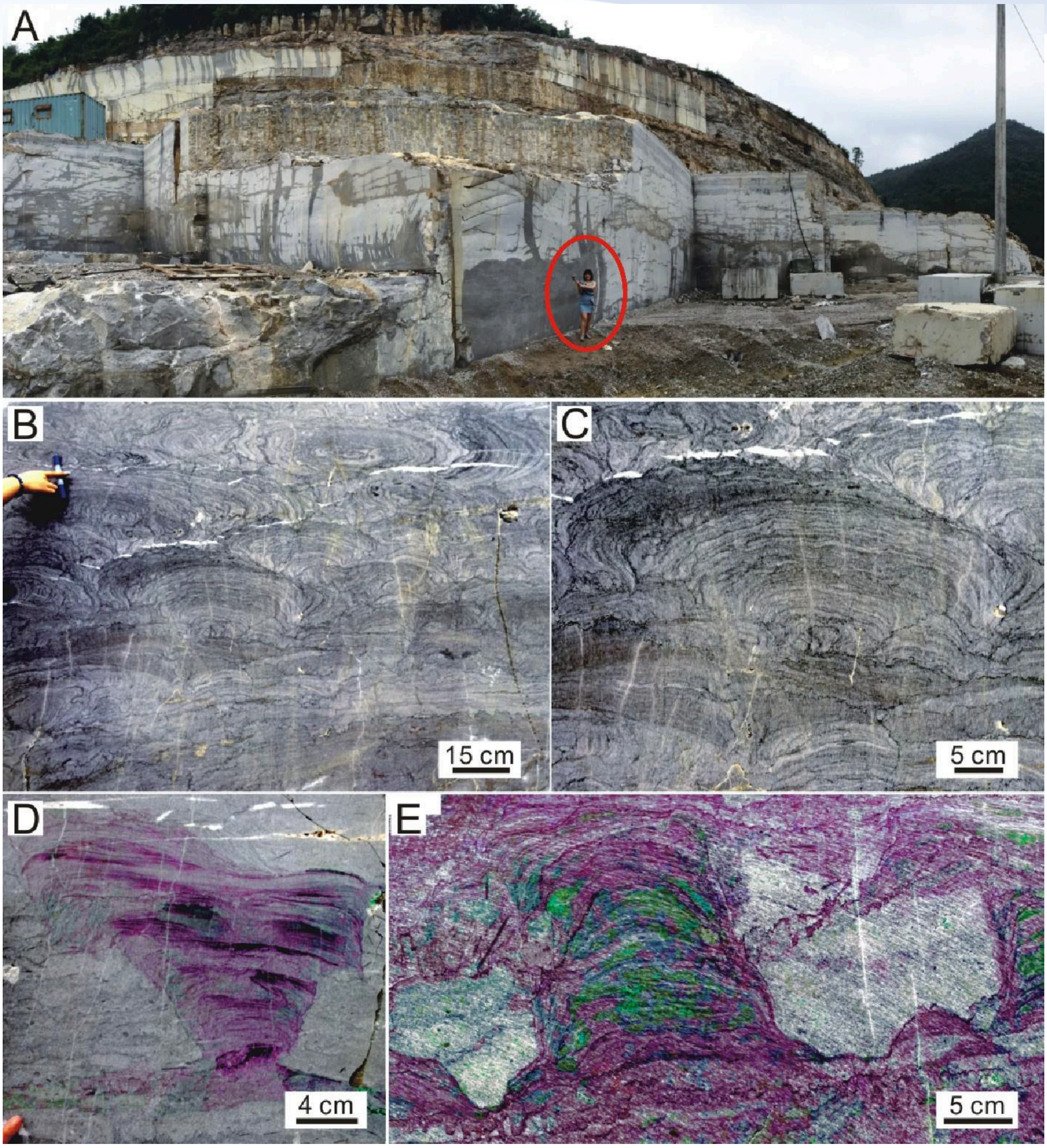

Fig. 2-3. ▲

The giant stromatolites from the upper Daye Formation (early Smithian) of the Lichuan section, western Hubei Province, South China (Fang et al., 2017). (A) Outcrop showing the thick stromatolite, up to 16 m in thickness, the person is 1.6 m high. (B−E) Various morphologies of stromatolites revealed on the quarry wall. Source: Fang et al., 2017.

Microbes increased again after the end-Ordovician mass extinction, and both microbial and metazoan reefs are commonly present in the Early Silurian (i.e., upper Aeronian, Llandovery) in China. Stromatolite reefs formed in the nearshore zone, whereas coral reefs, which represent biotic recovery following the end-Ordovician extinction, grew on the outer-shelf ramp. Co-existence of microbial and metazoan reefs in the upper Aeronian characterizes the Early Silurian MMT (Fig. 2-1). Lower Silurian metazoan communities, therefore, represent initial recovery following the end-Ordovician crisis.

2.1.3. Late Paleozoic

Another surge in microbially dominated sedimentation occurred in the Late Devonian, in association with the Frasnian–Famennian (F–F) mass extinction. However, these microbialite deposits are not confined to the aftermath of the F–F extinction but are, also, common during the Frasnian. In China, lower Frasnian reefs are typically built by stromatoporoids and corals, and upper Frasnian reefs reflect the final Devonian proliferation of global metazoan reefs (*Copper, 2002*). Famennian limestones contain stromatolites and thrombolites. These are well-represented by the microbial reefs that are widely developed in Guangxi and Hunan provinces, South China (*Shen et al., 1997, 2017; Chen et al., 2001, 2002*) and represent a microbial 'bloom' following the F–F mass extinction. The Late Devonian MMT, therefore, is much more extended than those of other ages.

2.1.4. Paleozoic–Mesozoic transition

The Paleozoic–Mesozoic (Permian–Triassic: P–Tr) transition witnessed the greatest crisis for life on Earth during the Phanerozoic, which devastated marine ecosystems (*Chen and Benton, 2012*). In the aftermath of the P–Tr mass extinction, unusual biosedimentary facies are widely preserved in Lower Triassic successions, including microbialites, oncoids, giant ooids, and vermicular limestones. These suggest a very high precipitation rate, indicative of calcium carbonate supersaturation within shallow watermasses, which may have resulted from the upwelling of alkaline, anoxic deep water, accompanied by high rates of evaporation due to elevated temperatures at that time (*Woods, 2014*). Microbialites are widely recognized from P–Tr boundary beds throughout the tropical Paleo-Tethyan region (*Kershaw et al., 2012*). They are also commonly present in the Early Triassic and, locally, in the early Anisian (early Middle Triassic) (*Baud et al., 2007; Luo et al., 2014*). It thus appears that microbes proliferated rapidly immediately after the mass extinction, throughout the Early Triassic and into the early Anisian (Luo et al., 2014). Post-extinction proliferation of microbes is also indicated by widespread microbially induced sedimentary structures (MISSs) in siliciclastic shallow-marine and terrestrial settings (*Chu et al., 2015; Tu et al., 2016; Xu et al., 2017*), suggesting that P–Tr mass extinction provided favourable habitats for MISS development in terrestrial ecosystems. For example, increases in MISS appear to coincide with die-back of terrestrial vegetation, disappearance of coal beds, extinction of pareiasaur tetrapods, and decrease in lacustrine bioturbation.

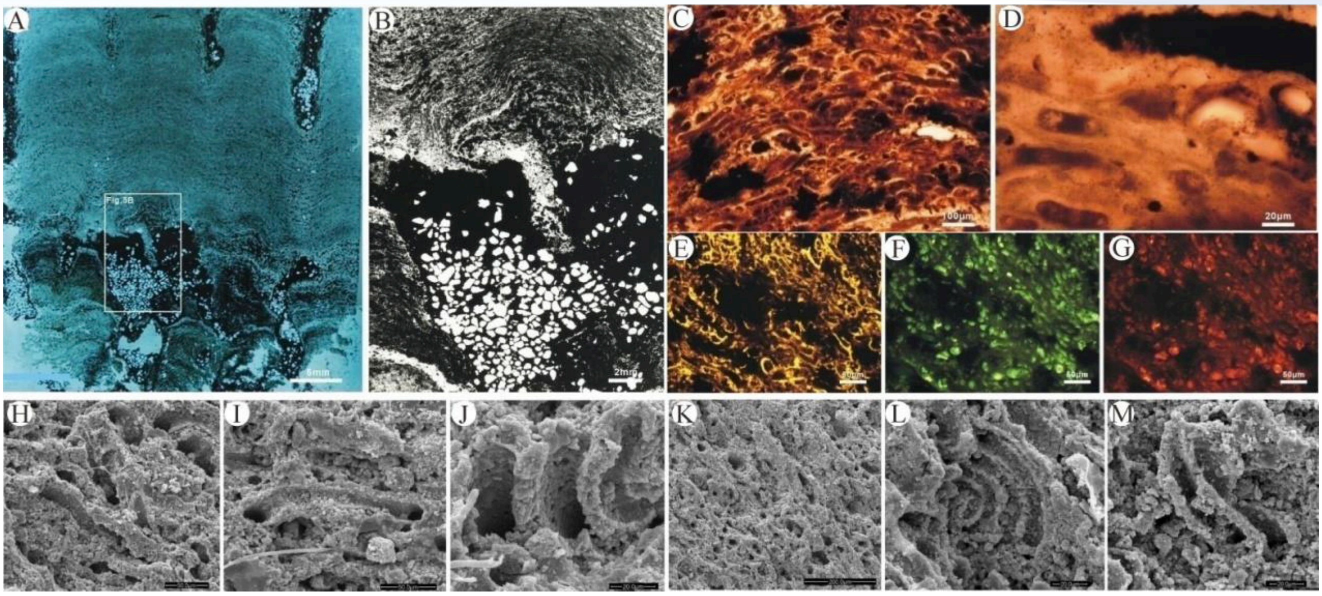

Fig. 2-4. ▲

Smithian stromatolites from the Northampton area of the northern Perth Basin, Western Australia yielding abundant filament sheaths that are superficially analogous to their modern cyanobacteria counterparts and, thus, were interpreted as putative filamentous cyanobacteria (Chen et al., 2014b).

(A–B) Photomicrographs showing stromatolite columns and laminae. Note cavities are usually filled with well-sorted quartz grains (white dots).

(C–D) Polarized photomicrographs showing densely arranged, layered filaments forming stromatolite laminae.

(E–G) Transmited light images showing filament sheaths forming laminae.

(H–M) SEM images of filament sheaths from the dark stromatolite laminae. Note that cyanobacteria were dissolved and only their sheaths remain. Source: Chen et al., 2014b.

When compared with the best studied the P–Tr boundary microbialites, the slightly younger Lower Triassic unusual biosedimentary facies have attracted much less attentions from sedimentologists. These microbe-mediated deposits or sedimentary structures include microbialites, oncoids, giant ooids, microbial mats, sand veins, wrinkle structures, vermicular limestones, flat pebble conglomerates, sea-floor fans (precipitates), and limestone nodules in mudstone. They are preserved throughout the entire Lower Triassic successions worldwide and are vaguely grouped into a broad 'anachronistic facies' (*e.g., Baud et al., 2007*). Interestingly, most of these unusual sedimentary features also occurred within the Cambrian carbonate successions, and their resurgences in Lower Triassic hints at a temporary return to a more primitive ocean ecosystem (*Baud et al., 2007*). These 'anachronistic facies' are widely distributed in the Early Triassic in China. Here, we briefly examine some of the sedimentary characteristics of several distinct examples.

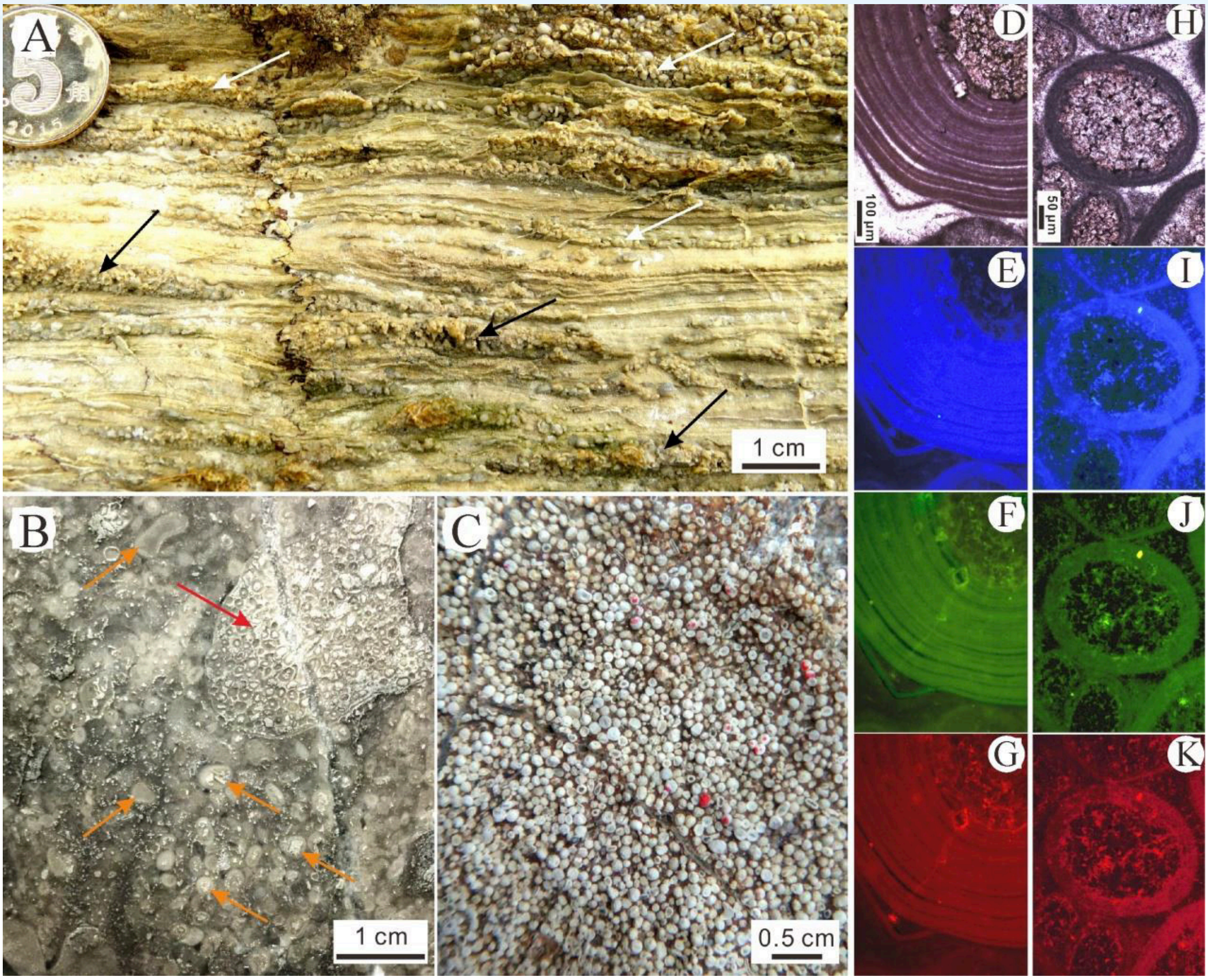

Fig. 2-5. ▲

Giant ooid bank from the upper Daye Formation (early Smithian) in the Lichuan area, western Hubei Province, South China (Fang et al., 2017).

(A) Surfaces of one sample showing ooids are arranged along the laminated layers to form distinct 'ooid laminae' (white arrows) or 'oolitic lenses' (black arrows). Giant ooids form laminae (arrows) on the outcrop.

(B) Two different sizes of ooids; an oolitic grainstone is composed of giant ooids with local oolite intraclasts (arrow).

(C) Weathered surface of oolitic grainstone showing aggregation of giant ooids.

(D–K) Photomicrographs of ooids in plane-polarized transmitted light

(D, H) and different wavelengths of fluorescent light under various exciting light wavelengths

(E–G, I–K) (Fang et al., 2017). Note that dark laminae in ooid samples are all actively responding to exciting light wavelengths, reflecting a considerably high content of organic matter. Source: Fang et al., 2017.

The P–Tr boundary microbialites usually have three types: (i) stromatolites, (ii) thrombolites, and (iii) dendrolites. The microbialites occurring at relatively higher horizons of the Early Triassic are dominated by stromatolites. These build-ups can be much thicker than the P–Tr boundary stromatolites. The thickest Lower Triassic stromatolite, up to 16 m in thickness, has been reported from the Smithian (lower Olenekian) successions in Lichuan, western Hubei Province, South China (Fig. 2-3), and it is notably constructed by cyanobacteria (*Fang et al., 2017*). Many upper Lower Triassic stromatolites also yield abundant well-preserved, putative fossilized filamentous cyanobacteria (Fig. 2-4), suggesting that they are the builders of these biosedimentary build-ups (*Chen et al., 2014b*).

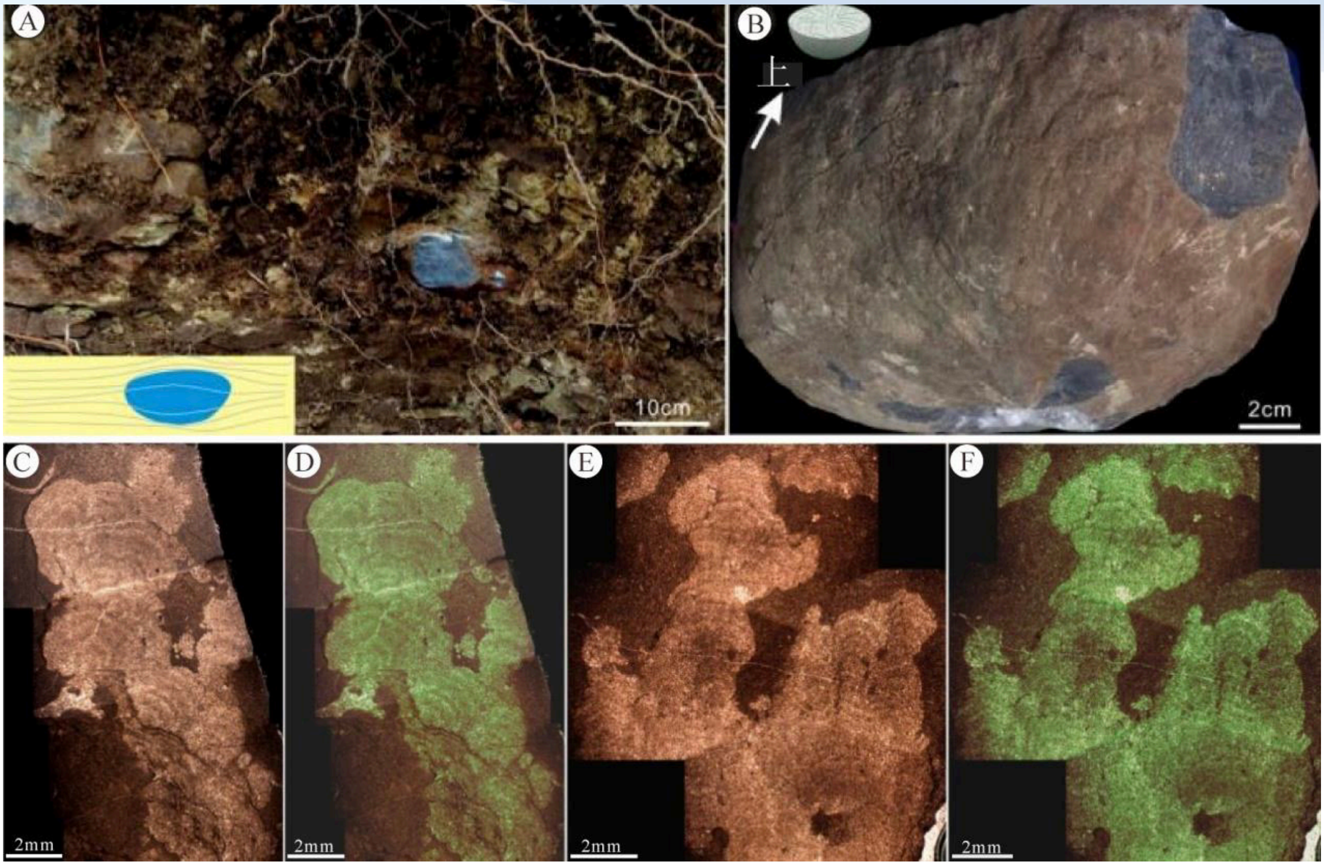

Fig. 2-6. ▲

(A) Limestone nodules embedded within mudstones slightly above the P–Tr boundary in the Tieshikou section, Xinfeng County, southern Jiangxi Province, South China (Yang et al., 2019).

(B) Single nodule showing bowl-shaped outline;

(C–F) Stromatolite-like and carbonate cement structures within limestone nodule. Source: Yang et al., 2019.

Similar to microbialites, giant oolites are also widely distributed worldwide in Lower Triassic carbonates (Fig. 2-5; *Li et al., 2015*). The ooid banks are also observable in P-Tr boundary intervals worldwide and have been recorded from at least 38 sections around the world, of which more than half are associated with the P-Tr boundary microbialites (*Li et al., 2015*). Growing evidence shows that ancient ooids record imprints of primitive nano-scale extracellular polymetric substances (EPS) and have similar REE compositions and distributions as those formed in modern-day seawaters (*Li et al., 2017*). This suggests that microbes mayhave been involved in the formation of these ancient ooids, particularly the giant ooids (*Li et al., 2017*). In addition to carbonates, the Lower Triassic successions are also characterized by widely distributed mudstones, in which calcareous nodules are commonly present. These limestone nodules embedded within mudstone facies are another possible microbe-mediated carbonate cement deposit (Fig. 2-6). *Yang et al. (2019)* found stromatolite-like structures and sea-floor cement fans in limestone nodules within mudstone strata from the lowest Triassic succession in the Tieshikou section, southern Jiangxi Province, South China (Fig. 2-6). Abundant nano-scaled organic grains and EPS are detected in those stromatolite-like structures, demonstrating that microbes may have participated in the formation of these limestone nodules interbedded in the mudstone strata (*Yang et al., 2019*).

In carbonate settings, although microbial reefs dominated Upper Triassic carbonate build-ups, sponge-microbial patch reefs occurred in Olenekian (Smithian) (*Brayard et al., 2011*), and metazoan reefs (i.e., Tubiphytes, sponges) started to proliferate in the early Middle Triassic (*Payne et al., 2006*). At the same time, stromatolites were common in the Early Triassic and early Anisian (*Luo et al., 2014*). Thus, both microbial and metazoan reefs co-occurred in the early Middle Triassic, prior to the full recovery of marine ecosystems in the late Pelsonian or middle-late Anisian, i.e., the Luoping biota and Qingyan faunas (*Chen and Benton, 2012*). Accordingly, the Early and Middle Triassic MMT (Fig. 2-1) represents a characteristic post-extinction ecosystem that lasted for ~7–8 Myr following the P–Tr mass extinction (*Chen and Benton, 2012*).

Both the Triassic−Jurassic boundary and Cretaceous−Paleogene mass extinctions also seriously impacted biodiversity and ecosystems, but metazoans relatively quickly recovered from these biotic crises. No microbial communities and sediments are known to widely represent post-extinction ecosystems at these times, although some microbially induced sediments are locally present, e.g., in the lowest Jurassic of England. The post-extinction successions are, in most cases, characterized by bioclastic limestone, indicating metazoan involvement in Early Jurassic biosedimentation. Although a secondary peak of microbial carbonate abundance occurs in the Middle Jurassic, probably due to the early Toarcian Oceanic Anoxic Event (T−OAE), contemporaneous metazoan build-ups are also quite abundant (Fig. 2-1). Hence, no MMT can be recognized from this time interval, and no microbial sediments have been observed in the aftermath of the Cretaceous-Paleogene extinction.

2.2. Geochemical signatures of major biotic and environmental extremes during the Phanerozoic

During the Phanerozoic, life on Earth experienced the "Big Five" mass extinctions, at the end-Ordovician, end-Frasnian, end-Permian, end-Triassic, and end-Cretaceous (*Sepkoski et al., 1981*), combined with up to 15 additional lesser extinction events (*Chen et al., 2014b*). Geochemical proxies reflect several of these major biotic extinction and environmental events (Fig. 2-1).

The end-Ordovician (Hirnantian) biocrisis was the first of the five severe extinctions, and has been ranked the second largest biocrisis by most authors (*Rong and Huang, 2014; Fig. 2-1*). Earth life suffered two discrete pulses of mass extinction associated with the climatic and oceanographic effects of ice sheet advance and demise in Gondwana during the Late Ordovician (*Harper et al., 2014*). Each of these phases of biocrisis coincided with an intense but short-lived glaciation at the South Pole. The first extinction resulted in a large loss of nektonic and planktonic species, as well as those living on shallow shelf and deeper water environments during the middle Ashgillian substage (*Sheehan, 2001*). The second pulse is less well defined, but it is associated with the end of a positive $\delta^{13}C$ excursion and includes the demise of the presumably cool-adapted Hirnantia fauna, which only appeared after the initial phases of the first pulse of extinction. Several effects, such as glacially induced cooling, falling sea level and geochemical patterns in the oceans, have been proposed as killing mechanisms for this first extinction event. The second phase is more clearly linked to near-global anoxia during a distinct transgression in the late Hirnantian (*Rong and Huang, 2014*). Widespread euxinia, together with habitat destruction due to global tectonic activity, may also have promoted the biocrisis at the end of the Ordovician. *Harper et al. (2014)* concluded that these effects took place contemporaneously and together resulted in the end-Ordovician catastrophe.

Two anoxic events, the lower Kellwasser and upper Kellwasser, occurred in the latest Frasnian, and are well defined by two distinctive positive carbonate carbon isotope excursions. Of these, the upper Kellwasser event, just below the Frasnian−Famennian (F−F) boundary, is marked by a positive shift followed by a pronounced negative shift in carbonate carbon isotope values (Fig. 2-1). The same pattern is also reflected in organic carbon and sulfur isotopic excursions (*Xu et al., 2012*). The upper Kellwasser event is, therefore, usually considered to be coincident with the F−F mass extinction. The major kill-factor of the F−F extinction is widely considered to have been oceanic anoxia, which may have resulted from increases in sea level, seawater temperature, and physical and chemical weathering (*Bond and Grasby, 2017*). The ultimate trigger could have been the eruption of a large igneous province (LIP) in the Siberia region (*Bond and Grasby, 2017*). The Famennian ecosystem was subsequently further impacted by the Hangenberg anoxic event, which occurred just prior to the Devonian–Carboniferous boundary. The Hangenberg event is marked by a distinct negative carbonate carbon isotope excursion in Europe and South China (*Bond and Grasby, 2017*).

Two lesser extinctions occurred in the mid-Capitanian and end-Capitanian (the last stage of the Middle Permian) (*Bond and Grasby, 2017*). Both extinction events are marked by pronounced negative shifts in carbon isotope values. Recently, a distinctive negative shift in sulfur isotopes has also been recognized from the end-Capitanian extinction horizon, suggesting deep euxinic seawater incursion into shallow habitats due to upwelling. The Emeishan LIP volcanism is considered to have triggered the end-Capitanian extinction.

In contrast to the extremely cold Ordovician–Silurian transition, the P–Tr interval represents a highly heated Earth. A rapid 8oC increase in seawater temperature was associated with the P–Tr boundary biocrisis (*Joachimski et al., 2012; Sun et al., 2012*). Several factors, including increase in carbon dioxide concentration, oceanic anoxia, hypercapnia (CO_2 poisoning), Siberian basalt eruption, and rapid global warming have been proposed to explain the P–Tr biotic extinction (*Knoll et al., 2007; Chen and Benton, 2012*). There is increasing evidence that shallow incursion of euxinic waters may have been an important killing agent in the P–Tr mass extinction. This is interpreted as evidence of a combination of upward and oceanward expansion of photic-zone euxinia, possibly fuelled by elevated riverine nutrient fluxes from land due to climatic warming, terrestrial ecosystem destruction, and enhanced erosion (*Algeo et al., 2011*). Euxinic watermasses at intermediate depths could have formed an oxygen minimum zone (OMZ) (*Algeo et al., 2011; Winguth and Winguth, 2012*), which may have established a long-term reservoir feeding episodic incursions of H_2S-bearing waters into shallow-marine habitats, delaying biotic recovery throughout the Early Triassic (*Bottjer et al., 2008*).

The P–Tr global warming also seriously impacted continental habitats and terrestrial life during this critical period. Apart from the loss of >70% of life on land, the P–Tr crisis resulted in the removal of forests, and their prolonged absence from the Earth's surface for up to 10 Myr created a pronounced coal gap in the Early Triassic (*Benton and Newell, 2014*). Thus, the terrestrial effects could have been substantial, with elevated chemical weathering following stripping of vegetation and massive volcanism associated with long-term aridification and episodes of warming and acid rain. These physical crises on land impinged on the oceans, leading to tight interlocking of terrestrial and marine crises (*Algeo et al., 2011*).

The Triassic–Jurassic (T–J) mass extinction is also marked by a pronounced negative carbon isotope excursion, probably linked to the LIP volcanism. The latter may also have caused widespread oceanic anoxia, global warming and elevated chemical and physical weathering on land, effects that could also have occurred during the P–Tr, F–F and end-Capitanian mass extinctions (Fig. 2-1).

Three oceanic anoxic events (OAEs) also caused Mesozoic ecological crises, in the Early Jurassic and Middle–Late Cretaceous. The bulk of the late Pliensbachian–early Toarcian (Early Jurassic) extinction may have occurred in the earliest Toarcian (*Harries and Little, 1999*), associated with a major negative carbon isotope excursion (CIE), OAE, marine transgression, and global warming, all of which may have been triggered by flood basalt magmatism (*McElwain et al., 2005*). However, the chronology of these physical events and associated biocrisis require greater precision to clarify their possible linkage and mechanisms.

The OAEs in the early Aptian (Middle Cretaceous) and at the Cenomanian–Turonian (C–T) transition (early Late Cretaceous) (Fig. 2-1) are marked by positive carbon isotope excursions and associated with lesser biotic marine extinctions (*Bambach, 2006*). Various geochemical proxies (i.e., biomarkers) reveal repeated anoxic/euxinic events that coincided with climatic warming and biotic extinctions within intermediate to surface waters during these critical periods (*Kaiho et al., 2014*).

Cenozoic climatic extremes have been relatively well studied, and the Paleocene−Eocene Thermal Maximum (PETM) is thought to potentially parallel events that might occur in the near future. This abrupt greenhouse gas-induced global warming began at ~55 Ma. It has been variously linked to large and rapid releases of 'fossil' carbon and to LIP volcanism that caused major disruption of the carbon cycle. Global warming was accompanied by extreme changes in hydroclimate and accelerated weathering, deep-ocean acidification, and possible widespread oceanic anoxia (*Barnosky et al., 2004*).

3. Requirements for making progress

The goal of Biosedimentology is to observe biological and geochemical processes during sedimentation from Precambrian to the Recent. The observation of present-day biosedimentary processes is essential for understanding the biotic involvement in modern and deep-time sedimentary processes and geochemical responses. These modern-day biosedimentary processes and mechanisms are also the key for us to understand how early life was involved in the sedimentary processes on our Earth during Precambrian times. Study of present-day biosedimentary processes, therefore, requires: (1) direct long-term observations at field stations of microbe growth patterns and participation in mineral precipitation in various extreme environments, such as microbe-reef systems in modern oceans, microbial build-ups in high-slainity lakes near oceans or in high-evaporitic inland areas (e.g., Qinghai and Inner Mongolia, western and northern China); and (2) laboratory experimental studies of how some crucial microbial assemblages grow and participate in mineral precipitation under selected extreme conditions, e.g., culturing various algae and cyanobacteria can provide direct observation of accretion and precipitation processes mediated or influenced by microbes under various oxygen and chemical conditions in the laboratory.

The study of biosedimentary processes during critical microbe-metazoan transitions (MMT) during the Phanerozoic requires that (1) precise chronostratigraphical frameworks for these important MMTs are reconstructed cyclostratigraphical, magnetostratigraphical and radiometric dating studies, (2) detailed sedimentological analysis based on petrological and sequence stratigraphical approaches are used to reconstruct sedimentary processes during these critical periods, and (3) multiple geochemical analyses (i.e., isotopic and elemental geochemistry) are conducted to enable the application of various proxies to reconstruct extreme environmental and climatic signals. All of these studies require cutting-edge geochemical laboratories equipped with world-class instruments.

4. China's opportunity and future strategy

The recent new findings in the evolving field of Biosedimentology identify three priority areas for future research directions in Biosedimentology: (1) observations of present-day biosedimentary processes, (2) studies of sedimentary processes during critical microbe-metazoan transitions (MMT) during the Phanerozoic, and (3) recognition of biosedimentary processes in the Precambrian based on modern analogues. Present-day biosedimentary processes can be observed in experimental studies and can also be evauated by conducting long-term observations at field stations. These modern-day biosedimentary processes and mechanisms offer analogues to better understand biological processes involved in physical sedimentation in the geological past. The Phanerozoic records of critical MMTs provide examples of organism-environment interactions and their underlying mechanisms.

In this context, understanding biosedimentary processes is crucial for an understanding of the evolution of early life. The application of modern analogues can, therefore, be important to improve our understanding of the Precambrian record of life.

There are many opportunities to pursue research in these three priority areas. Firstly, well-developed modern-day coral reefs and microbial carbonate analogues exist in the South China Sea. Abundant salt lakes and hot springs in western China also provide natural laboratories for geobiological and biosedimentological studies in contrasting environmental settings. Secondly, exceptional records of the Ediacaran–Devonian metazoan and microbial carbonates in both North China and South China, as well as excellent complete Permian–Triassic microbe-metazoan successions in South China, provide unique opportunities to study the patterns and formation mechanisms of MMTs and their responses to major global events. Thirdly, stratigraphical and paleontological records of well-preserved Mesoproterozoic and Neoproterozoic successions in China provide an outstanding basis for examining environment-organism interactions in the Precambrian world (See Chapter 4 for an elaboration of this tpoic). Finally, ambitious deep drilling programs will provide new sample material and upgraded instrumentation (e.g., nano-SIMS) will provide essential new analytical approaches for future biosedimentological research.

Acknowledgements

The present report is derived from multiple discussions at the Xiangshan Sedimentology Workshop held in Beijing in September of 2016. We are grateful to Judith McKenzie, Hongfu Yin, Robert Riding, Chuanming Zhou, Yu Pei, Shucheng Xie, Chao Li, and Ping Luo for the input of their ideas and constructive suggestions at the XiangshanWorkshop.

References

Algeo, T.J., Chen, Z.Q., Fraiser, M.L., Twitchett, R.J., 2011. Terrestrial-marine teleconnections in the collapse and rebuilding of Early Triassic marine ecosystems. Palaeogeography, Palaeoclimatology, Palaeoecology 308, 1-11.

Bambach, R.K., 2006. Phanerozoic biodiversity mass extinctions. Annual Review of Earth and Planetary Sciences 34, 127-155.

Barnosky, A.D., Koch, P.L., Feranec, R.S., Wing, S.L., Shabel, A.B., 2004. Assessing the causes of Late Pleistocene extinctions on the continents. Science 306, 70-75.

Baud, A., Richoz, S., Pruss, S., 2007. The lower Triassic anachronistic carbonate facies in space and time. Global and Planetary Change 55, 81-89.

Benton, M.J., Newell, A.J., 2014. Impacts of global warming on Permo-Triassic terrestrial ecosystems. Gondwana Research 25, 1308-1337.

Bond, D.P.G., Grasby, S.E., 2017. On the causes of mass extinctions. Palaeogeography, Palaeoclimatology, Palaeoecology 478, 3-29.

Bottjer, D.J., Clapham, M.E., Fraiser, M.L., Powers, C.M., 2008. Understanding mechanisms for the end-Permian mass extinction and the protracted Early Triassic aftermath and recovery. GSA Today 18, 4-10.

Bottjer, D.J., Hagadorn, J.W., Dornbos, S.Q., 2000. The Cambrian substrate revolution. GSA Today 10, 1-7.

Brayard, A., Vennin, E., Olivier, N., Bylund, K.G., Jenks, J., Stephen, D.A., Bucher, H., Hofmann, R., Goudemand, N., Escarguel, G., 2011. Transient metazoan reefs in the aftermath of the end-Permian mass extinction. Nature Geoscience 4, 693-697. Cao, R.J., Yuan, S.L., 2003. Current advances of stromatolite studies in China. Acta Micropaleontologica Sinica 20, 5-14.

Chen, D.Z., Tucker, M.E., Jiang, M.S., Zhu, J.Q., 2001. Long-distance correlation between tectonic-controlled, isolated carbonate platforms by cyclostratigraphy and sequence stratigraphy in the Devonian of South China. Sedimentology 48, 57-78.

Chen, D.Z., Tucker, M.E., Zhu, J.Q., Jiang, M.S., 2002. Carbonate platform evolution: from a bioconstructed platform margin to a sand-shoal system (Devonian, Guilin, South China). Sedimentology 49, 737-764.

Chen, Z.Q., Benton, M.J., 2012. The timing and pattern of biotic recovery following the end-Permian mass extinction. Nature Geoscience 5, 375-383.

Chen, Z.Q., Joachimski, M., Montañez, I., Isbell, J., 2014a. Deep time climatic and environment extremes and ecosystem response: an introduction. Gondwana Research 25, 1289-1293.

Chen, Z.Q., Wang, Y., Kershaw, S., Luo, M., Yang, H., Zhao, L., Feng, Y., Chen, J., Yang, L., Zhang, L., 2014b. Early Triassic stromatolites in a siliciclastic nearshore setting in northern Perth Basin, Western Australia: Geobiologic features and implications for post-extinction microbial proliferation. Global and Planetary Change 121, 89-100.

Chen, Z.Q., Zhou, C., Stanley, G.J., 2017. Biosedimentary records of China from the Precambrian to present. Palaeogeography, Palaeoclimatology, Palaeoecology 474, 1-6.

Chen, Z.Q., Tu, C.Y., Pei, Y., Ogg, J., Fang, Y.H., Wu, S.Q., Feng, X.Q., Huang, Y.G., Guo, Z., Yang, H., 2019. Biosedimentological features of major microbe-metazoan transitions (MMTs) from Precambrian to Cenozoic. Earth-Science Reviews 189, 21-50.

Chu, D., Tong, J., Song, H., Benton, M.J., Bottjer, D.J., Song, H., Tian, L., 2015. Early Triassic wrinkle structures on land: stressed environments and oases for life. Scientific Reports 5, 10109e.

Copper, P., 2002. Reef development at the Frasnian/Famennian mass extinction boundary. Palaeogeography, Palaeoclimatology, Palaeoecology 181, 27-65.

Fang, Y., Chen, Z.Q., Kershaw, S., Li, Y., Luo, M., 2017. An Early Triassic (Smithian) stromatolite associated with giant ooid banks from Lichuan (Hubei Province), South China: Environment and controls on its formation. Palaeogeography, Palaeoclimatology, Palaeoecology 486, 108-122. Flügel, E., Kiessling, W., 2002. Patterns of Phanerozoic reef crises. In: Kiessling W, Flügel E, Golonka J. (eds), Phanerozoic Reef Pattern. SEPM Special Publications 72, 691-733.

Gehling, J.G., 1999. Microbial Mats in Terminal Proterozoic Siliciclastics: Ediacaran Death Masks. Palaios 14, 40-57.

Harper, D.A.T., 2006. The Ordovician biodiversification: Setting an agenda for marine life. Palaeogeography, Palaeoclimatology, Palaeoecology 232, 148-166.

Harper, D.A.T., Hammarlund, E.U., Rasmussen, C.M.Ø., 2014. End Ordovician extinctions: A coincidence of causes. Gondwana Research 25, 1294-1307. Harries, P.J., Little, C.T., 1999. The early Toarcian (Early Jurassic) and the Cenomanian–Turonian (Late Cretaceous) mass extinctions: similarities and contrasts. Palaeogeography, Palaeoclimatology, Palaeoecology 154, 39-66. Joachimski, M.M., Lai, X.L., Shen, S.Z., Jiang, H.S., Luo, G.M., Chen, B., Sun, Y.D., 2012. Climate warming in the latest Permian and the Permian–Triassic mass extinction. Geology 40, 195-198. Kaiho, K., Katabuchi, M., Oba, M., Lamolda, M., 2014. Repeated anoxia–extinction episodes progressing from slope to shelf during the latest Cenomanian. Gondwana Research 25, 1357-1368. Kershaw, S., Crasquin, S., Li, Y., Collin, P.Y., Forel, M.B., Mu, X., Guo, L., 2012. Microbialites and global environmental change across the Permian–Triassic boundary: a synthesis. Geobiology 10, 25-47. Knoll, A.H., Bambach, R.K., Payne, J.L., Pruss, S., Fischer, W.W., 2007. Paleophysiology and end-Permian mass extinction. Earth and Planetary Science Letters 256, 295-313.

Lee, J.H., Riding, R., 2018. Marine oxygenation, lithistid sponges, and early history of Paleozoic skeletal reefs. Earth-Science Reviews, 181, 98-121.

Li, F., Yan, J., Chen, Z.Q., Ogg, J.G., Tian, L., Korngreen, D., Liu, K., Ma, Z.L., Woods, A.D., 2015. Global oolite deposits across the Permian–Triassic boundary: a synthesis and implications for palaeoceanography immediately after the end-Permian biocrisis. Earth-Science Reviews 149, 163-180

Li, F., Yan, J.X., Burne, R.V., Chen, Z.Q., Algeo, T.J., Zhang, W., Tian, L., Gan, Y.L., Liu, K., Xie, S.C., 2017. Paleo-seawater REE compositions and microbial signatures preserved in laminae of Lower Triassic ooids. Palaeogeography, Palaeoclimatology, Palaeoecology 486, 96-107. Liu, A.G., Matthews, J.J., Menon, L.R., McIlroy, D., Brasier, M.D., 2015. The arrangement of possible muscle fibres in the Ediacaran taxon Haootia quadriformis. Proceedings of the Royal Society of London B: Biological Sciences 282, 20142949e

Luo, M., Chen, Z.Q., Zhao, L., Kershaw, S., Huang, J., Wu, L., Yang, H., Fang, Y., Huang, Y., Zhang, Q., 2014. Early Middle Triassic stromatolites from the Luoping area, Yunnan Province, Southwest China: Geobiologic features and environmental implications. Palaeogeography, Palaeoclimatology, Palaeoecology 412, 124-140.

McElwain, J.C., Wademurphy, J., Hesselbo, S.P., 2005. Changes in carbon dioxide during an oceanic anoxic event linked to intrusion into Gondwana coals. Nature 435, 479-482.

Ogg, J., Ogg, G., Gradstein, F.M., 2016. A Concise Geologic TimeScale: 2016. Amsterdam: Elsevier. Payne, J.L., Lehrmann, D.J., Christensen, S., Wei, J., Knoll, A.H., 2006. Environmental and biological controls on the initiation and growth of a Middle Triassic (Anisian) reef complex on the Great Bank of Guizhou, Guizhou Province, China. Palaios, 21, 325-343.

Penny, A.M., Wood, R., Curtis, A., Bowyer, F., Tostevin, R., Hoffman, K.H., 2014. Ediacaran metazoan reefs from the Nama Group, Namibia. Science 344, 1504-1506.

Qi, Y.A., Wang, Y.P., Dai, M.Y., 2014. Thrombolites from Cambrian Series 3 Zhangxia Formation of western Henan and their controlling factors. Micropaleontologia Acta 31, 243-255.

Qi, Y.A., Sun, X.F., Dai, M.Y., Zhang, X.Y., 2017. Microbialite cycles and evolutions from Cambrian Mentou Formation of Lushan area, western Henan. Micropaleontologia Acta 34, 170–178. Riding, R., 2006. Microbial carbonate abundance compared with fluctuations in metazoan diversity over geological time. Sedimentary Geology 185, 229-238.

Riding, R., Liang, L., 2005. Geobiology of microbial carbonates: metazoan and seawater saturation state influences on secular trends during the Phanerozoic. Palaeogeography, Palaeoclimatology, Palaeoecology 219, 101-115. Rong, J.Y., Huang, B., 2014. Three-decade studies on mass extinction. Science in China, Earth Science 44, 377-404.

Sepkoski, J.J., Bambach, R.K., Raup, D.M., Valentine, J.W., 1981. Phanerozoic marine diversity and the fossil record. Nature 293, 435-437. Servais, T., Harper, D.A.T., 2018. The Great Ordovician Biodiversification Event (GOBE): definition, concept and duration. Lethaia 51, 151-164. Sheehan, P.M., 2001. History of marine biodiversity. Geological Journal 36, 231-249. Shen, J.W., Yu, C.M., Bao, H.M., 1997. A Late Devonian (Famennian) Renalcis-Epiphyton reef at Zhaijiang, Guilin, South China. Facies 37, 195-209.

Shen, J.W., Zhao, N., Mao, Y.J., Wang, Y., Jin, Y., 2017. Late Devonian reefs and microbialite in Maoying, Ziyun County of southern Guizhou, South China—implications for changes in paleoenvironment. Palaeogeography, Palaeoclimatology, Palaeoecology 474, 98-112.

Sun, Y., Joachimski, M.M., Wignall, P.B., Yan, C., Chen, Y., Jiang, H., Wang, L., Lai, X., 2012. Lethally hot temperatures during the Early Triassic greenhouse. Science 338, 366-370. Tu, C.Y., Chen, Z.Q., Retallack, G.J., Huang, Y.G., Fang, Y.H., 2016. Proliferation of MISS-related microbial mats following the end-Permian mass extinction in terrestrial ecosystems: evidence from the Lower Triassic of the Yiyang area, Henan Province, North China. Sedimentary Geology 333, 50-69.

Winguth, C., Winguth, A.M.E., 2015. Simulating Permian-Triassic oceanic anoxia distribution: Implications for species extinction and recovery. Geology 40, 127-130.

Woods, A.D., 2014. Assessing Early Triassic paleoceanographic conditions via unusual sedimentary fabrics and features. Earth-Science Reviews 137, 6-18.

Xiao, S., Shen, B., Tang, Q., Kaufman, A.J., Yuan, X., Li, J., Qian, M., 2014. Biostratigraphic and chemostratigraphic constraints on the age of early Neoproterozoic carbonate successions in North China. Precambrian Research 246, 208-225.

Xiao, S., Zhang, Y., Knoll, A.H., 1998. Three-dimensional preservation of algae and animal embryos in a Neoproterozoic phosphorite. Nature 391, 553-558. Xu, B., Gu, Z., Wang, C., Hao, Q., Han, J.T., Liu, Q., Wan, L., Lu, Y.W., 2012. Carbon isotopic evidence for the associations of decreasing atmospheric CO2 level with the Frasnian-Famennian mass extinction. Journal of Geophysical Research-Biogeosciences 117, 1–12. Xu, Y.L., Chen, Z.Q., Feng, X.Q., Wu, S.Q., Shi, G.R., Tu, C.Y., 2017. Proliferation of MISS-related microbial mats following the end-Permian mass extinction in the northern Paleo-Tethys: Evidence from southern Qilianshan region, western China. Palaeogeography, Palaeoclimatology, Palaeoecology 474, 198-213. Yan, Z., Liu, J., Ezaki, Y., Adachi, N., Du, S., 2017. Stacking patterns and growth models of multiscopic structures within Cambrian Series 3 thrombolites at the Jiulongshan section, Shandong Province, northern China. Palaeogeography, Palaeoclimatology, Palaeoecology 474, 45-57.

Yang, H., Chen, Z.Q., Kershaw, S., Liao, W., Lü, E.L., Huang, Y.G., 2019. Small microbialites from the basal Triassic mudstone (Tieshikou, Jiangxi, South China): geobiologic features, biogenicity, and paleoenvironmental implications. Palaeogeography, Palaeoclimatology, Palaeoecology 519, 221-235. Yuan, X.L., Chen, Z., Xiao, S.H., et al. 2011. An early Ediacaran assemblage of macroscopic and morphologically differentiated eukaryotes. Nature 470, 390-393.

Zhuravlev, A., Riding, R., 2000. The Ecology of the Cambrian Radiation. New York: Columbia University Press.

Chapter 3.

Source-to-sink systems: from orogenic belts to marginal sea basins

Zhifei Liu[1], Shouye Yang [1], Yulong Zhao [1], Pengfei Ma [1], Poppe de Boer [2]

[1]- State Key Laboratory of Marine Geology, Tongji University, Shanghai 200092 China

[2]- Department of Earth Sciences, Utrecht University, 3584 CS Utrecht, The Netherlands

1. Introduction

Earth-surface processes operate across erosion-dominated landscapes and deliver sediment to depositional systems that can be preserved in the stratigraphic record. Source-to-sink systems comprise production, transport, and deposition of sediments and solutes (Fig. 3-1). Sediment production and transport from orogenic source areas to terrestrial and marine depocentres is driven and influenced by tectonics, climate and sea level (change). For predicting and mitigating the changes and threats, which global warming and sea-level rise may impose on the Earth and on our society in the next decades and centuries, the understanding of Chinese source-to-sink systems and their future evolution is crucial.

Various source-to-sink systems have been extensively investigated, such as the small Eel River system (STRATAFORM program, 1994–2000; *Nittrouer et al., 2007*), the large Ganges–Brahmaputra–Bengal system fed by tectonically active mountains (*Romans et al., 2016*), and the Po and Rhone sediment dispersal systems (EUROSTRATAFORM program, 2002–2005; *Durrieu de Madron et al., 2008*). The Fly River (Papua New Guinea) and Waipaoa River (New Zealand) dispersal systems have become the most remarkable sediment routing system studies at the observational, laboratory, and theoretical level (*MARGINS, 2004; Kuehl et al., 2016*). Over the last decade significant progress has been made in exploring the complicated behavior of individual sedimentary system (*Walsh et al., 2016* and references therein). Most previous studies emphasized transport and deposition on the continental margin, and studied sediment dispersal systems are relatively small in time and space, such as the Fly and Waipaoa source-to-sink systems of the MARAGINS program. Investigations of large source-to-sink systems with a long history and a complicated interaction between tectonics and climate are scarce, especially along the East Asian margin.

Three key scientific issues in source-to-sink studies merit attention: (1) the question how tectonics, climate, and sea-level fluctuations regulate the production, transfer, and storage of sediments and solutes; (2) the question which processes affect erosion and sediment transfer, and; (3) the question how sedimentary processes and fluxes built the stratigraphic record, reflecting the history of global change? Only when the behaviour of past systems is understood, can estimates be made about their future behaviour and adequate measures be taken to safeguard our populations in the future.

In China, the uplift of the Tibetan Plateau and the opening of East Asian marginal seas following the India-Asia collision, a principle event in the last 100 Myr (*Wang et al., 2014*), have created unique sediment source-to-sink systems, from orogenic belts to marginal marine basins (Fig. 3-2). During the Cenozoic, the sediment routing systems dramatically evolved from a generally west-tilting topography towards the Tethyan Ocean in the west, followed by the present east-tilting relief with the Tibetan Plateau in the west and the marginal seas in the east (*Wang, 2004*). The large drainage systems, the Yellow, Yangtze, Pearl, Red, and Mekong rivers, were initiated or reconfigured along with this topographic reversal. The uplift of the Tibetan Plateau and chemical weathering have been proposed to have been the major triggers for the significant Cenozoic climate change, including global cooling and Asian monsoon development (*Raymo and Ruddiman, 1992; An et al., 2015*). Obviously, the Tibetan Plateau–East Asian marginal sea source-to-sink systems are critical for answering key scientific questions about the past and future earth-surface evolution.

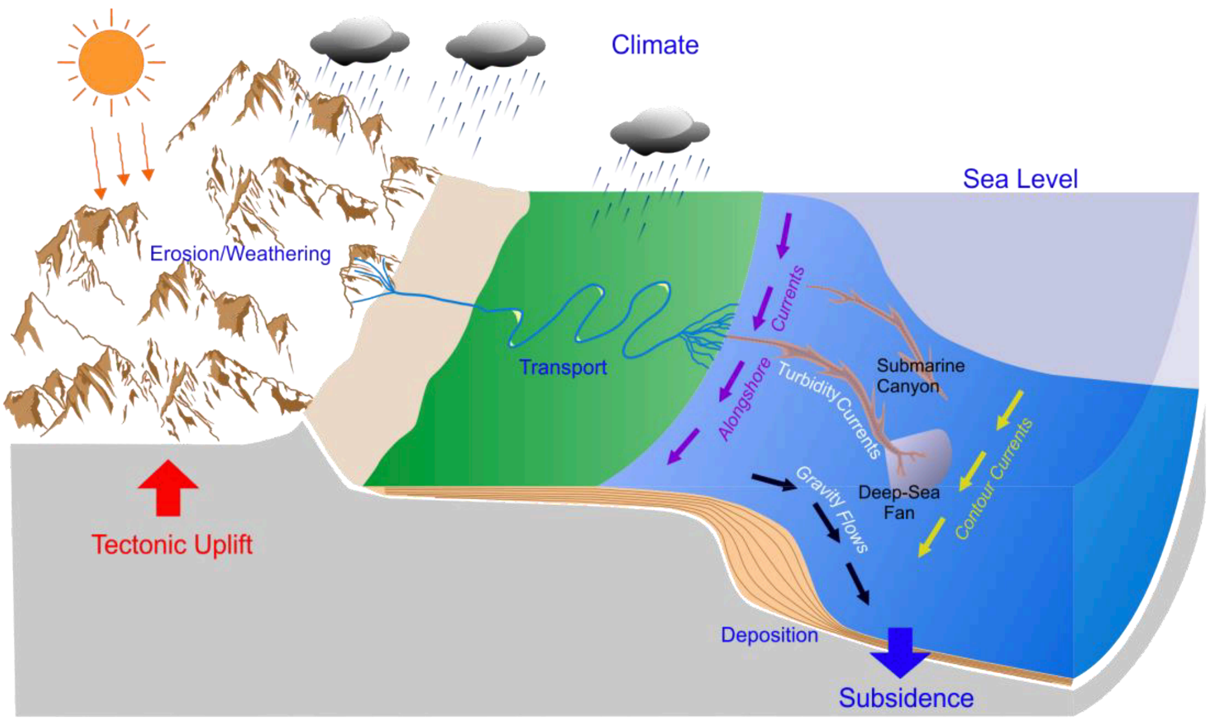

Fig. 3-1. ▲

Cartoon of source-to-sink systems with production, transport, and deposition of sediments and solutes, and the controls of tectonics, climate, and sea level change.

2. Research questions and challenges

Four key research questions are formulated:

1: To which degree are erosion/weathering, transport, and deposition of sediments and solutes linked? This question requires a good qualitative and quantitative understanding of surface processes, from the Tibetan Plateau to the East Asian marginal seas.

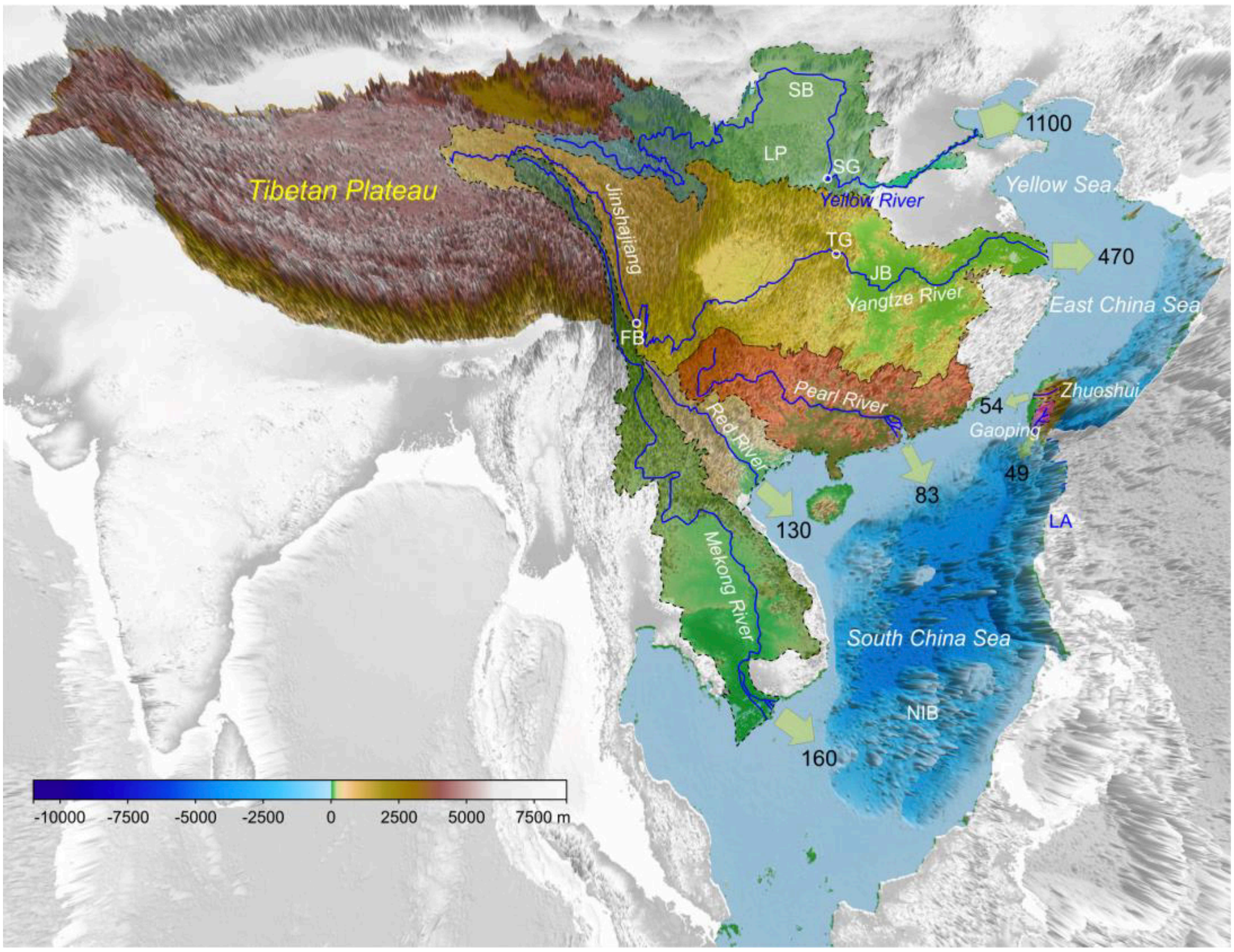

Fig. 3-2. ▲
Sediment routing systems with topography and drainage areas of the Yellow, Yangtze, Pearl, Red, and Mekong rivers and the bathymetry of shelf and deep basins of the Yellow Sea, the East China Sea, and the South China Sea. The Zhuoshui and Gaoping drainage systems in Taiwan are also displayed. Green arrows with numbers indicate observed suspended sediment discharge (in million tons annually; data from Milliman and Syvitski, 1992; Dadson et al., 2003; Milliman and Farnsworth, 2011). Abbreviations: FB = First Bend; TG = Three Gorges; JB = Jianghan Basin; LP = Loess Pleateau; SB = Square Bend; SG= Sanmen Gorge; NIB = Nansha Islands Block; LA = Luzon Arc.

Four key research questions are formulated:

2: How did sediment source-to-sink processes and their responses to climate change and tectonic activity vary since the late Miocene, when the modern topography of East Asia had more or less formed? Were the monsoon climate and sea-level change the only factors affecting the sedimentary processes?

3: How did the uplift of the Tibetan Plateau, the opening of East Asian marginal seas, and the initiation and/or reconfiguration of large eastward-flowing fluvial systems develop during the Cenozoic, and how did these processes interact?

4: Which was (and is) the relation between tectonic uplift and climate change, and how did (and does) the Tibetan Plateau uplift and related chemical weathering affect the global climate?

3. Requirements for making progress

Requirements to make progress include:

(1) Sediment production by physical and chemical weathering in uplifting mountains and stable flood plains. The Tibetan Plateau and Taiwan are two excellent examples of uplifted high-relief areas. The middle-lower reaches of the Yellow, Yangtze, and Pearl rivers provide contrasting cases, with different geological and climatic setting, for addressing sediment transfer in source-to-sink systems.

(2) Transport processes and residence time of sediments in various drainage systems. The Yellow, Yangtze, Pearl, Red, and Mekong river systems represent case examples of long-distance transport from the Tibetan Plateau to marginal seas. In contrast, small mountain rivers such as the Zhuoshui and Gaoping rivers in Taiwan drain over very short distances from high–relief areas to the Taiwan Strait and the South China Sea.

(3) Transport and deposition of sediments and solutes in the East Asian marginal seas. The Yellow Sea and the East China Sea consist mostly of continental shelf with strong hydrodynamics. The South China Sea is a semi-enclosed deep-sea transport and deposition system. In addition, the two contrasting sediment routing systems of the Yangtze and Taiwan rivers interact on the southern East China Sea shelf.

(4) The topographic reversal of East Asia and the contrasting sediment dispersal patterns for which the Tibetan uplift and opening of the East Asian marginal seas are key examples. Results from the International Ocean Discovery Program (IODP) drilling in the South China Sea (Expeditions 349, 367, 368 and 368X) will further clarify the rifting and opening history of the South China Sea.

4. China's opportunity and future strategy

4.1 Uplift history of the Tibetan Plateau

The uplift and expansion of the Tibetan Plateau has created the most extensive high terrain globally. Tremendous amounts of clastic sediment have been yielded through physical and chemical weathering in response to orogenic uplift and climate (change). Sediments were and are transported to interior lacustrine and marginal marine basins through a variety of source-to-sink drainage systems draining a large part of East and South Asia (Fig. 3-2). Paleoclimate was influenced by the Tibetan uplift, i.e. by the drawdown of atmospheric CO_2 and consequent global cooling (*Garzione, 2008*), the development of a monsoon climate and inland aridification (*Ding et al., 2017*), and regional climate change and drainage reorganization of the plateau interior (*Ma et al., 2017*).

History of the uplift of the Tibetan Plateau

The timing of the India-Asia collision has been debated for decades but remains controversial (e.g. *Wang et al., 2014* and references therein). New results from reconstructions of local drainage systems, based on detrital zircon geochronology and micropaleontology in southern Tibet, give an age of 59±1 Ma (*Hu et al., 2015*), whereas, based on detrital zircon provenance in northern Pakistan, an age of ca. 56 Ma was found for the early collision (*Ding et al., 2016*). The initiation of deposition in interior lacustrine basins like the Hoh Xil Basin and in marginal marine basins such as the Arabian Sea (*Liu et al., 2003; Clift, 2006*) are probably far field effects of the collision event. Although the sediment accumulation rates in these basins were relatively low initially, the start of coarse-clastic deposition reflects the development of drainage systems.

Different viewpoints about the Tibetan Plateau's uplift history include diachronous uplift from the east to the west since the Eocene, synchronous uplift in the Late Miocene, northeastward oblique stepwise rise since the Eocene, and uplift starting in the central and extending to the peripheral areas (*Chung et al., 1998; Tapponnier et al., 2001; Wang et al., 2008)*. Although models that consider a diachronous, complex rise of the plateau, rather than as a rigid block, are commonly accepted, the exact uplift history of the Tibetan Plateau remains debated. *Chung et al. (1998)* compiled the age distribution of potassic lavas and concluded that the plateau was uplifted diachronously from east to west. This model, however, does not constrain the source region of the melt (*Harris, 2006*). Based on Cenozoic deformation, magmatism, and seismics, *Tapponnier et al. (2001)* concluded that the plateau has grown in the south during the Eocene, in the center during the Oligocene–Miocene, and finally further to the northeast during the Pliocene–Pleistocene. Low-temperature thermochronology and reconstruction of the paleoaltimetry, however, indicate that the central plateau had undergone rapid exhumation and reached a relatively high elevation already during the Eocene *(Wang et al., 2014)*. *Wang et al. (2008)* proposed a "proto-Tibetan Plateau model" with the highland between the Gangdese Mountains and the Tanggula Range having reached an elevation similar to today already 40 Myr ago. Since then, this proto-Tibetan Plateau gradually grew outward and formed the present plateau topography with the final rise of the peripheral orogens in the Miocene (Fig. 3-3). This scenario is in accordance with the exhumation history of the central plateau and changes in paleoaltimetry estimated on the basis of carbonate oxygen isotopes in the Eocene–Oligocene interior drainage systems (e.g., *Ding et al., 2017*). In contrast, the above scenario is in contradiction with the Oligocene-Miocene paleoaltimetric evolution of the central plateau constrained by $\delta^{13}C$ and δD of C29 n-alkane (*Deng and Ding, 2015*).

Global climate response to the Tibetan Plateau uplift

Response and feedback of the regional and global climate are important for evaluating the uplift history of the Tibetan Plateau. It is argued that continental weathering consumes atmospheric CO_2 and, thus, causes global cooling (*Raymo and Ruddiman, 1992; Garzione, 2008*). This global climate change can be succinctly registered in sediments accumulated in and around the plateau. Based on sedimentology, paleoclimate studies, magnetostratigraphy, and cyclostratigraphy in the Xining Basin, *Dupont-Nivet et al. (2008)* show that the plateau uplift took place at 38 Ma and that regional aridification started around the Eocene–Oligocene transition (34 Ma). The rise of the Tibetan Plateau and Himalayas significantly intensified the Asian summer monsoon and the interior aridification since the late Paleocene–early Eocene. This paleoclimate effect was synchronously recorded in small drainage basins in the Himalaya orogen and in eolian deposits in the Asian interior (*An et al., 2015; Ding et al., 2017*). The surface uplift also led to a drainage reorganization and perturbation of the depositional system in the interior plateau (*Ma et al., 2017*). Thermochronometry studies and numerical simulations indicate that the fast uplift of the Himalayas resulted in a sudden decrease of erosion in southern Tibet by blocking precipitation at ~10 Ma (*Tremblay et al., 2015*). A careful analysis of the plateau uplift and reconstruction of the high-resolution temporal framework of the sedimentary history are prerequisites for unraveling the interplay between plateau uplift and climate change.

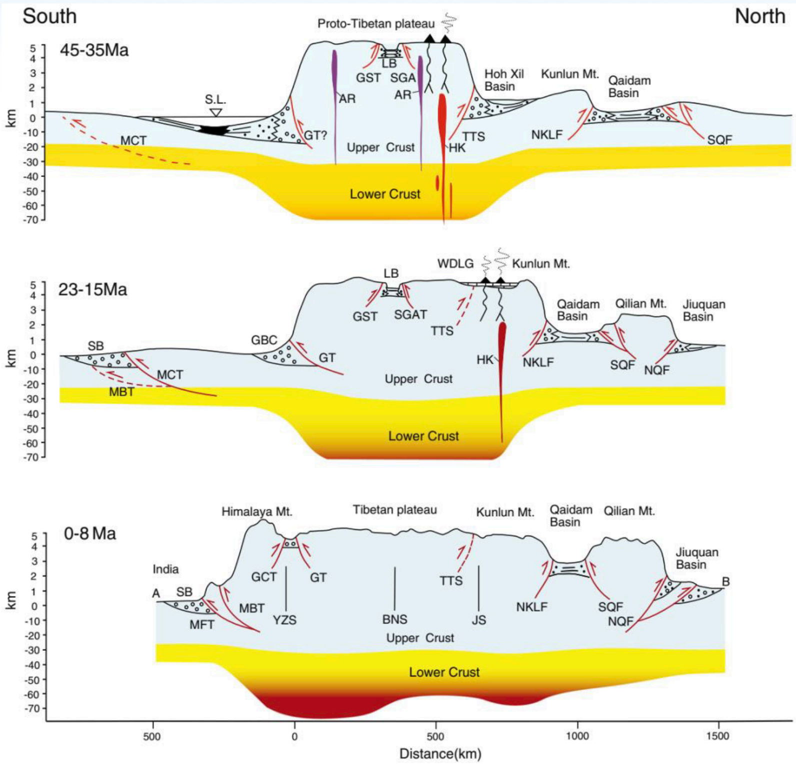

Fig. 3-3.

Schematic geological evolution of the Himalayas and the Tibetan Plateau showing uplift and crustal history of the Tibetan Plateau. The plateau grew outward from an elevated proto-Tibetan Plateau (Lhasa and Qiangtang Terranes) starting in the Late Paleogene. MBT = Main Boundary Thrust; GCT = Great Counter Thrust; TTS = Tanggula Thrust system; NKLF = North Kunlun Fault; NQF = North QilianMountain Fault; GBC = Gangrinboche conglomerates; YZS = Yarlung Tsangpo suture zone; BNS = Bangong-Nujiang suture zone; JS = Jinsha River suture zone; MCT = Main Central Thrust; SL = sea level; GT = Gangdese Thrust; GST = Gaize Siling Tso Thrust; LB = Lunpola basin; SGAT = Shiquanhe Gaize Amdo Thrust; SQF = the South Qilian Mountain Fault; SB = Siwalik foreland basin; MFT = Main Frontal Thrust; HK = high-K calc-alkaline volcanics; AR = adakite volcanics; WDLG = continental Wudaoliang Group. The depth of Moho is after Gao et al. (2009). Source: Wang et al., 2014; Wang et al., 2008.

Generally, tectonics and climate together control the evolution of topography, the development of drainage systems, and the production and deposition of clastic sediments. The rise of source areas and subsidence of sedimentary basins during the Tibetan Plateau uplift have been widely documented in interior lacustrine and marginal marine basins, e.g., the rapid unroofing of the northern Tanggula Mountains and the initiation of deposition in the Hoh Xil Basin at 60–50 Ma (*Wang et al., 2008*). Rapid sediment accumulation in South and East Asian marginal marine basins also corresponds with the uplift of the Himalayas during the Early–Middle Miocene (*Clift, 2006*). By comparison, the Pliocene–Recent fast erosion revealed by sedimentation elsewhere was primarily facilitated by rapid glacial-interglacial changes (*Zhang et al., 2001*). Over longer geological periods, tectonics and climate together controlled plateau uplift and erosion, and they alternated as the dominant control (*Wang et al., 2014*). It is challenging to precisely distinguish between the contribution of climate and tectonics in controlling erosion of source areas. Future studies should focus on the influence of the Tibetan uplift on source-to-sink systems, including spatial-temporal uplift and the interaction with regional and global climate (change).

4.2 Evolution of large rivers: Yangtze River and Yellow River

Large rivers in Asia act as conduits of sediment transport from the Tibetan Plateau to the marginal seas and significantly shape the Asian landscape. The Yangtze River (Changjiang) and the Yellow River (Huanghe) are the largest rivers in East and Southeast Asia in terms of sediment load. Their suspended sediment plumes in the East China Sea and the Bohai Sea can be seen from space as being directed southward (Fig. 3-4).

Is the Yangtze River a geologically young feature?

The modern Yangtze River has long been considered to be relatively young, formed in the Late Pliocene to Early Pleistocene (ca. 3–1.2 Ma). Important evidence comes from observations of river capture events of the upper paleo-Jinshajiang and of river terraces in the Three Gorges and from core records in the Jianghan Basin and the present-day Yangtze delta plain (*Li et al., 2001; Yang et al., 2006; Gu et al., 2014; Fig. 3-2*). The key scientific questions about the birth of Yangtze River include: (1) the time of river capture and formation of the First Bend in the upper paleo-Jinshajiang; (2) the timing of incision of the Three Gorges; and (3) when the eastern Tibet-derived sediments initially reached the East Asian marginal seas. Also, it has been debated for a long time whether the upper Yangtze River (paleo-Jinshajiang) once flowed southward as a major tributary of the Red River. Most studies focused on geomorphological observations and proposed different dates of river capture. Recently, *Zheng et al. (2013)* suggested the birth of Yangtze River took place prior to 23 Ma, in response to the rapid Tibetan uplift and monsoon strengthening around the end of the Oligocene. Based on various lines of evidence, from observation of the whole catchment to detrital zircon geochronology for provenance discrimination, they proposed a south-flowing paleo-Jinshajiang during the Paleogene, and that the present Yangtze River system formed due to the tectonic and monsoon climate evolution during the Neogene. However, recent sedimentological studies on Cenozoic stratigraphy and borehole records reveal persistent lacustrine sedimentation in the upper Jinshajiang Basin during the early to middle Miocene, which suggests that the upper Yangtze River had not been established until the late Miocene (*Wei et al., 2016*).

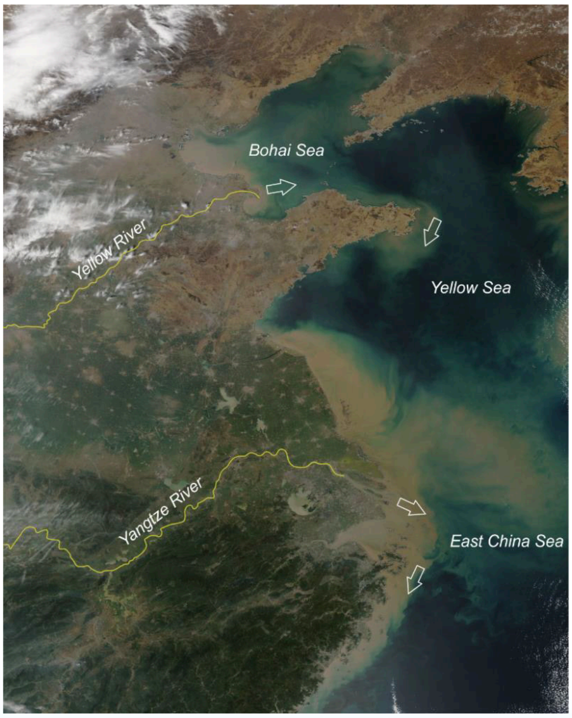

◂

Fig. 3-4.

Satellite image of East Asia and adjacent marginal seas taken on 7 April 2013, showing the lower reaches of the Yellow and Yangtze rivers and lateral transport of suspended sediments in the Bohai Sea, the Yellow Sea, and the East China Sea. Source: NASA EOSDIS (available at https://worldview.earthdata.nasa.gov/)

When and how the Three Gorges were incised are other questions related to the birth of the modern Yangtze River. Based on apatite fission-track measurements and U-Th/He low-temperature thermochronology, *Richardson et al. (2010)* suggested the incision of the Three Gorges began in the Eocene (ca. 40−45 Ma). On the contrary, facies analysis of Paleogene sediments in the Jianghan Basin, just downstream of the gorges, precludes a large river similar to the modern Yangtze flowing through the gorges before 36 Ma (*Zheng et al., 2011*). A paleomagnetic study of the late Cenozoic sediments from the Jianghan Basin, on the other hand, constrains the time of incision of the Three Gorges to the Early Pleistocene (ca. 1.17−1.12 Ma; *Zhang et al., 2008*).

Is the Yellow River older than the Quaternary?

Being China's mother river and the cradle of China's ancient civilization, there is a great research interest in the evolution of the course of the Yellow River, especially in its lower reaches. Although the Yellow River shares the headwaters in the Tibetan Plateau with the Yangtze River, it has shaped the landscape of the North China Craton and flows through the Loess Plateau before emptying into the Bohai Sea. Similar to the evolution of the Yangtze River, the formation of Square Bend in the middle reaches and the incision of Sanmen Gorge are regarded as key issues for understanding the birth of the Yellow River because they initiated the connection between its upper-middle and lower reaches (Fig. 3-2). The formation of the Yellow River is thus closely associated with the topographic evolution in response to tectonic and climatic forcing, with an estimated age commonly ranging from Late Pleistocene (ca. 120−150 ka) to Late Pliocene-Early Pleistocene (ca. 3.6–1.2 Ma) (*Lin et al., 2001; Pan et al., 2012; Hu et al., 2017*).

It is noteworthy that, based on the fluvial sedimentary record in the North China plain and in marginal seas, there is a general consensus that eastward drainage of the Yellow River was established in the middle-late Pleistocene. This suggests that the Yellow River is perhaps not as old as previously suggested by some. These data, however, are based on fluvial records and may not always be reliable because it is difficult, if not impossible, to define and trace the earliest major sink of Yellow River-derived sediments along the continental margin. Recent work on detrital zircon geochronology implies that Miocene-Pleistocene strata in the Western Foothills of Taiwan were primarily sourced from the Yangtze Block and the North China Block, which suggests that the tectonic and sedimentary evolution of Taiwan may provide important constraints on the drainage reorganization in East China (*Deng et al., 2017*).

More robust evidence comes from the age of river terraces. Magnetostratigraphic records from aeolian deposits, accumulated on the five river terraces along the Yellow River course, suggest that the formation of the Sanmen Gorge and the initiation of the through-flowing eastward drainage of the Yellow River occurred between 3.63 and 1.24 Ma (*Pan et al., 2012; Hu et al., 2017*). The dramatic increase in sediment accumulation in the Bohai Sea at ca. 1.0 Ma (*Yao et al., 2012*) resulted from the initiation of an enlarged Yellow River catchment through the Sanmen Gorge. Probably since the middle Pleistocene, the Yellow River started to dominate deposition in the North China plain and the Bohai and Yellow seas. Obviously, the sediment source-to-sink transport pathways of the Yellow River in the East Asian continental margin need more research.

In summary, the time of formation of the Yangtze and Yellow rivers has been a subject of debate for more than a century, with estimates ranging from the Late Quaternary (ca. 120–150 ka), Early Pleistocene (ca. 2 Ma), to pre-Miocene (>23 Ma). The evolution of the two large rivers still remains a mystery. Previous studies on the evolution of the Yangtze and Yellow rivers mostly focused on river capture in the upper highland catchments, incision of gorges in the middle reaches, and the sedimentary record in the lowland basins and marginal seas. Integrated and multi-disciplinary investigations of the whole source-to-sink system are required. Although tectonics is widely accepted as the first-order control on the evolution of these large rivers, the climate factor has long been underestimated and its interplay with tectonics and river system development deserves more attention. Because this climate factor may change in the coming decades and centuries, understanding the effects of climate change can be of great societal importance.

4.3 Depositional system in the South China Sea

The South China Sea, the largest East Asian marginal sea, receives more than 700 million tons of terrigenous sediments annually, largely weathering products from the Tibetan Plateau. In addition to the Pearl, Red, and Mekong rivers, dozens of small mountainous rivers from the adjacent continents and islands discharge into the South China and adjacent seas making them the world's largest sediment sink (*Milliman and Farnsworth, 2011*).

Long-term evolution of the South China Sea Basin

The Tibetan Plateau is an important sediment provider, and also a major control on the tectonic evolution of the South China Sea. Opening of the South China Sea was driven by back-arc extension and extrusion of the Indochina Block along the Red River Fault Zone (*Tapponnier et al., 1990; Briais et al., 1993*) and/or by southward subduction of an earlier paleo-South China Sea under Borneo (*Morley, 2002*). It remains unclear when the rifting started. Based on seismic data, it was suggested that the strongest phase of extension began in the Eocene (*Clift and Lin, 2001*), but new data, based on basin analysis, indicate that the earliest extension dates back into the Mesozoic (*Shu et al., 2009*). The end of the rifting and the start of seafloor spreading in the South China Sea is dated at ~33 Ma (*Sibuet et al., 2016*). Despite arguments that spreading ceased earlier (*Barckhausen et al., 2014*), it is generally agreed that seafloor spreading in the South China Sea terminated around 15 Ma (*Li et al., 2014*), as a result of either the cessation of motion along the Red River Fault Zone (*Gilley et al., 2003)* or the collision of the Nansha Islands Block with Borneo (*Hutchison et al., 2000*). Since the end of seafloor spreading, the South China Sea Basin has been continuously affected by the eastward subduction of ocean crust under the Luzon Arc, resulting from the collision with mainland Asia in Taiwan (*Huang et al., 2006*; Fig. 3-2).

Before the Luzon Arc reached its present position during the latest Miocene, the South China Sea had a free connection to the Pacific Ocean, allowing deposition of red beds just above the oceanic basalts (*Expedition 349 Shipboard Scientists, 2014*). The causes of the start and end of the deposition of red beds remain poorly known, most likely they represent a period with enhanced ventilation at the ocean floor. Changes of the East Asian monsoon have been well documented by terrigenous sediments in the South China Sea, showing at least three profound shifts in the intensity of the East Asian monsoon, at ～15 Ma, ～8 Ma, and ～3 Ma (*Wan et al., 2007*).

Climate-related source-to-sink processes in the South China Sea

Except for regions where tectonics are still active, such as Taiwan, North Borneo, and the eastern fringe of Tibetan Plateau, the monsoon climate is presently the predominant factor affecting the weathering of source areas adjacent to the South China Sea (*Liu et al., 2016*). Upon entering the South China Sea, dispersal of fluvial sediments is controlled predominantly by marine currents (Fig. 3-5). Submarine canyons are important in delivering sediment from rivers and from the continental shelf to the deep sea, mostly by sediment gravity flows (*Liu et al., 2016*). There are extensive submarine canyons off South China and Taiwan, either connected to rivers, such as the Gaoping Canyon, or starting at the upper continental slope, such as the Formosa and Penghu canyons. The sediments delivered to the deep sea are further dispersed westward to the South China Sea deep basin by contour currents (*Zhao et al., 2015*).

The westward-propagating mesoscale eddies generated by the intrusion of the Kuroshio Current are also significant agents transporting sediments, both at the sea surface as suspended matter and solutes (*Liu et al., 2010*) and in the deep basin (*Zhang et al., 2014*). The broad South China Sea Southern Cyclonic Gyre in winter and the Southern Anticyclonic Gyre in summer are the dominant controls of the distribution of sediments from the Mekong River and rivers from the Malay Peninsula, Sumatra and Borneo. Thus, sediments in the southern South China Sea and the Sunda Shelf are well mixed (*Liu et al., 2016*). Alongshore currents and differential settling of clay minerals are essential in the transport of sediments from the Pearl and Red rivers. Issues to be solved are, for example, the quantity of sediments from different sources, the relative significance of processes affecting the dispersal of sediments, and the sediment dynamics in the deep sea.

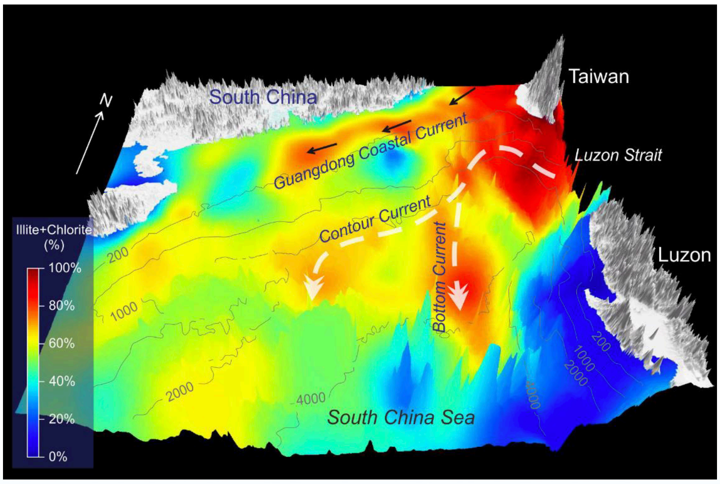

Fig. 3-5.

Spatial distribution of the percentage content of illite + chlorite in seafloor surface sediments of the northern South China Sea, showing lateral transport of clay minerals by the Guangdong Coastal Current, contour currents, and bottom currents, respectively. The map is created using the three-dimensional topography with overlays of illite + chlorite distribution (%). Isobath curves of 200, 1000, 2000, and 4000 m are indicated to show the seafloor configuration. Scale bar indicates total amount of illite and chlorite in percentage. Source: Liu et al., 2016.

Variations of fluvial sediment input into the South China Sea during the Late Quaternary glacial-interglacial cycles were controlled by changes in the weathering of source rocks, fluvial runoff, marine circulation, and, of course, the cyclic rise and fall of global sea level. The cold and arid climate in the sediment source areas favored physical denudation (*Liu et al., 2007*). The cyclic rise and fall of sea level in the late Quaternary greatly changed the land-sea configuration of the South China Sea, leading to the exposure of the wide northern South China Shelf and the Sunda Shelf during the lowstands. At the last glacial maximum, sea level in the area fell to ~125 m below the present level (*Hanebuth et al., 2000*) and the continental shelf of the South China Sea was almost fully exposed, allowing extensive drainage systems and even rainforest vegetation to develop (*Sun et al., 2003; Wang et al., 2009*). The continental shelf also became an active sediment source because

(1) most sediments were directly brought to the deep basin due to the seaward extension of river mouths, and

(2) the exposure of the shelf and the incision of river valleys led to its erosion. Changes in the land-sea configuration also had a great impact on the surface circulation pattern in the South China Sea: a basin-wide anticyclonic gyre in summer and a cyclonic gyre in winter (*Wang et al., 1995*). Obviously, the semi-enclosed South China Sea is an ideal area to study sediment source-to-sink transport processes during the climate and sea-level changes in the late Cenozoic. Understanding these will help to predict future changes.

References

An, Z., Wu, G., Li, J., Sun, Y., Liu, Y., Zhou, W., Cai, Y., Duan, A., Li, L., Mao, J., Cheng, H., Shi, Z., Tan, L., Yan, H., Ao, H., Chang, H., Feng, J., 2015. Global monsoon dynamics and climate change. Annual Review of Earth and Planetary Sciences 43, 29–77.

Barckhausen, U., Engels, M., Franke, D., Ladage, S., Pubellier, M., 2014. Evolution of the South China Sea: revised ages for breakup and seafloor spreading. Marine and Petroleum Geology 58, 599–611.

Briais, A., Patriat, P., Tapponnier, P., 1993. Updated interpretation of magnetic anomalies and seafloor spreading stages in South China Sea: implications for the Tertiary tectonics of Southeast Asia. Journal of Geophysical Research 98, 6299–6328.

Chung, S.L., Lo, C.H., Lee, T.Y., Zhang, Y., 1998. Diachronous uplift of the Tibetian plateau starting 40 Myr ago. Nature 394, 769–773.

Clift, P., Lin, J., 2001. Preferential mantle lithospheric extension under the South China margin. Marine and Petroleum Geology 18, 929–945.

Clift, P.D., 2006. Controls on the erosion of Cenozoic Asia and the flux of clastic sediment to the ocean. Earth and Planetary Science Letters 241, 571–580.

Dadson, S.J., Hovius, N., Chen, H., Dade, W.B., Hsieh, M.L., Willett, S.D., Hu, J.C., Horng, M.J., Chen, M.C., Stark, C.P., Lague, D., Lin, J.C., 2003. Links between erosion, runoff variability and seismicity in the Taiwan orogen. Nature 426, 648–651.

Deng, K., Yang, S.Y., Li, C., Su, N., Bi, L., Chang, Y.P., Chang, S.C., 2017. Detrital zircon geochronology of river sands from Taiwan: implications for sedimentary provenance of Taiwan and its source link with the east China mainland. Earth-Science Reviews 164, 31–47.

Deng, T., Ding, L., 2015. Paleoaltimetry reconstructions of the Tibetan Plateau: progress and contradictions. National Science Review 2, 417–437.

Ding, L., Qasim, M., Jadoon, I.A.K., Khan, M.A., Xu, Q., Cai, F., Wang, H., Baral, U., Yue, Y., 2016. The India–Asia collision in north Pakistan: Insight from the U-Pb detrital zircon provenance of Cenozoic foreland basin.

Earth and Planetary Science Letters 455, 49–61.

Ding, L., Spicer, R.A., Yang, J., Xu, Q., Cai, Q., Li, S., Lai, Q., Wang, H., Spicer, T.E.V., Yue, Y., Shukla, A., Srivastava, G., Ali Khan, M., Bera, S., Mehrotra, R., 2017. Quantifying the rise of the Himalaya orogen and implications for the South Asian monsoon. Geology 45, 215–218

Dupont-Nivet, G., Hoorn, C., Konert, M., 2008. Tibetan uplift prior to the Eocene-Oligocene climate transition: Evidence from pollen analysis of the Xining Basin. Geology 36, 987–990.

Durrieu de Madron, X., Wiberg, P.L., Puig, P., 2008. Sediment dynamics in the Gulf of Lions: the impact of extreme events. Continental Shelf Research 28, 1867–1876.

Expedition 349 Scientists, 2014. South China Sea tectonics: opening of the South China Sea and its implications for southeast Asian tectonics, climates, and deep mantle processes since the late Mesozoic. International Ocean Discovery Program Preliminary Report, 349. http://dx.doi.org/10.14379/iodp.pr.349.2014

Gao, R., Xiong, S.S., Li, Q.S., Lu, Z.W., 2009. The Moho depth of Qinghai Tibet plateau revealed by seismic detection. Acta Geosci. Sin. 30 (6), 761 773.

Garzione, C.N., 2008. Surface uplift of Tibet and Cenozoic global cooling. Geology 36, 1003–1004.

Gilley, L.D., Harrison, T.M., Leloup, P.H., Ryerson, F.J., Lovera, O.M., Wang, J.-H., 2003. Direct dating of left-lateral deformation along the Red River shear zone, China and Vietnam. Journal of Geophysical Research 108, 2127, doi:10.1029/2001JB001726, B2.

Gu, J.W., Chen, J., Sun, Q.L., Wang, Z.H., Wei, Z.X., Chen, Z.Y., 2014. China's Yangtze delta: Geochemical fingerprints reflecting river connection to the sea. Geomorphology 227, 166–173.

Hanebuth, T., Stattegger, K., Grootes, P.M., 2000. Rapid flooding of the Sunda Shelf: A late glacial sea-level record. Science 288, 1033–1035.

Harris, N., 2006. The elevation history of the Tibetan Plateau and its implications for the Asian monsoon. Palaeogeography, Palaeoclimatology, Palaeoecology 241, 4–15.

Hu, X., Garzanti, E., Moore, T., Raffi, I., 2015. Direct stratigraphic dating of India-Asia collision onset at the Selandian (middle Paleocene, 59 ± 1 Ma). Geology 43, 859–862.

Hu, Z.B., Pan, B. T., Bridgland, D., Vandenberghe, J., Guo, L.Y., Fan, Y.L., Westaway, R., 2017. The linking of the upper-middle and lower reaches of the Yellow River as a result of fluvial entrenchment. Quaternary Science Reviews 166, 324–338.

Huang, C.-Y., Yuan, P.B., Tsao, S.-J., 2006. Temporal and spatial records of active arc-continent collision in Taiwan: A synthesis. Geological Society of America Bulletin 118, 274–288.

Hutchison, C.S., Bergman, S.C., Swauger, D.A., Graves, J.E., 2000. A Miocene collisional belt in north Borneo: uplift mechanism and isostatic adjustment quantified by thermochronology. Journal of the Geological Society 157, 783–793.

Kuehl, S.A., Alexander, C.R., Blair, N.E., Harris, C.K., Marsaglia, K.M., Ogston, A.S., Orpin, A.R., Roering, J.J., Bever, A.J., Bilderback, E.L., Carter, L., Cerovski-Darriau, C., Childress, L.B., Corbett, D.R., Hale, R.P., Leithold, E.L., Litchfield, N., Moriarty, J.M., Page, M.J., Pierce, L.E.R., Upton, P., Walsh, J.P., 2016. A source-to-sink perspective of the Waipaoa River margin. Earth-Science Reviews 153, 301–334.

Li, C.-F., Xu, X., Lin, J., Sun, Z., Zhu, J., Yao, Y., Zhao, X., Liu, Q., Kulhanek, D.K., Wang, J., Song, T., Zhao, J., Qiu, N., Guan, Y., Zhou, Z., Williams, T., Bao, R., Briais, A., Brown, E.A., Chen, Y., Clift, P.D., Colwell, F.S., Dadd, K.A., Ding, W., Hernández Almeida, I., Huang, X.-L., Hyun, S., Jiang, T., Koppers, A.A.P., Li, Q., Liu, C., Liu, Z., Nagai, R.H.,Peleo-Alampay, A., Su, X., Tejada, M.L.G., Trinh, H.S., Yeh, Y.-C., 2014. Ages and magnetic structures of the South China Sea constrained by deep tow magnetic surveys and IODP Expedition 349. Geochemistry, Geophysics, Geosystems 15, 4958–4983.

Li, J.J., Xie, S.Y., Kuang, M.S., 2001. Geomorphic evolution of the Yangtze Gorges and the time of their formation, Geomorphology 41, 125–135.

Lin, A.M., Yang, Z.Y., Sun, Z.M., Yang, T.S., 2001. How and when did the Yellow River develop its square bend? Geology 29, 951–954.

Liu, J.T., Hsu, R.T., Hung, J.-J., Chang, Y.-P., Wang, Y.-H., Rendle-Bühring, R.H., Lee, C.-L., Huh, C.-A., Yang, R.J., 2016. From the highest to the deepest: The Geoping River–Geoping Submarine Canyon dispersal system. Earth-Science Reviews 153, 274–300.

Liu, Z., Colin, C., Huang, W., Le, K.P., Tong, S., Chen, Z., Trentesaux, A., 2007. Climatic and tectonic controls on weathering in South China and the Indochina Peninsula: clay mineralogical and geochemical investigations from the Pearl, Red, and Mekong drainage basins. Geochemistry, Geophysics, Geosystems 8, Q05005, doi:10.1029/2006GC001490.

Liu, Z., Colin, C., Li, X., Zhao, Y., Tuo, S., Chen, Z., Siringan, F.P., Liu, J.T., Huang, C.-Y., You, C.-F., Huang, K.-F., 2010. Clay mineral distribution in surface sediments of the northeastern South China Sea and surrounding fluvial drainage basins: source and transport. Marine Geology 277, 48–60.

Liu, Z., Zhao, X., Wang, C., Liu, S., Yi, H., 2003. Magnetostratigraphy of Tertiary sediments from the Hoh Xil Basin: implications for the Cenozoic tectonic history of the Tibetan Plateau. Geophysical Journal International 154, 233–252.

Liu, Z., Zhao, Y., Colin, C., Stattegger, K., Wiesner, M.G., Huh, C.-A., Zhang, Y., Li, X., Sompongchaiyakul, P., You, C.-F., Huang, C.-Y., Liu, J.T., Siringan, F.P., Le, K.P., Sathiamurthy, E., Hantoro, W.S., Liu, J., Tuo, S., Zhou, S., He, Z., Wang, Y., Bunsomboonsakul, S., Li, Y., 2016. Source-to-sink processes of fluvial sediments in the South China Sea. Earth-Science Reviews 153, 238–273.

Ma, P., Wang, C., Meng, J., Ma, C., Zhao, X., Li, Y., Wang, M., 2017. Late Oligocene-early Miocene evolution of the Lunpola Basin, central Tibetan Plateau, evidences from successive lacustrine records. Gondwana Research 48, 224–236.

MARGINS, 2004. NSF MARGINS Program Science Plans 2004. Margins Office, Lamont-Doherty Earth Observatory, 170 pp.

Milliman, J.D., Farnsworth, K.L., 2011. River Discharge to the Coastal Ocean: A Global Synthesis. Cambridge University Press, Cambridge, 384 pp.

Milliman, J.D., Syvitski, J.P.M., 1992. Geomorphic/tectonic control of sediment discharge to the ocean: the importance of small mountainous rivers. Journal of Geology 100, 525–544.

Morley, C.K., 2002. A tectonic model for the Tertiary evolution of strike-slip faults and rift basins in SE Asia. Tectonophysics 347, 189–215.

Nittrouer, C.A., Austin, J.A., Field, M.E., Kravitz, J.H., Syvitski, J.M.P., Wiberg, P.I., 2007. Writing a Rosetta Stone: Insights into Continental-Margin Sedimentary Processes and Strata, Special Publication 37 of the International Association of Sedimentologists. Blackwell Publishing Ltd., Oxford, 549 pp.

Pan, B.T., Hu, Z.B., Wang, J.P., Vandenberghe, J., Hu, X.F., Wen, Y.H., Li, Q., Cao, B., 2012. The approximate age of the planation surface and the incision of the Yellow River. Palaeogeography, Palaeoclimatology, Palaeoecology 356–357, 54–61.

Raymo, M.E., Ruddiman, W.F., 1992. Tectonic forcing of late Cenozoic climate. Nature 359, 117–122.

Richardson, N.J., Densmore, A.L., Seward, D., Wipf, M., Li, Y., 2010. Did incision of the Three Gorges begin in the Eocene? Geology 38, 551–554.

Romans, B.W., Castelltort, S., Covault, J.A., Fildani, A., Walsh, J.P., 2016. Environmental signal propagation in sedimentary systems across timescales. Earth-Science Reviews 153, 7–29.

Shu, L., Zhou, X., Deng, P., Wang, B., Jiang, S., Yu, J., Zhao, X., 2009. Mesozoic tectonic evolution of the Southeast China Block: New insights from basin analysis. Journal of Asian Earth Sciences 34, 376–391.

Sibuet, J.-C., Yeh, Y.-C., Lee, C.-S., 2016. Geodynamics of the South China Sea. Tectonophysics 692, 98–119.

Sun, X., Luo, Y., Huang, F., Tian, J., Wang, P., 2003. Deep-sea pollen from the South China Sea: Pleistocene indicators of East Asian monsoon. Marine Geology 201, 97–118.

Tapponnier, P., Lacassin, R., Leloup, P.H., Scharer, U., Zhong, D., Wu, H., Liu, X., Ji, S., Zhang, L., Zhong, J., 1990. The Ailao Shan/Red River metamorphic belt: Tertiary left-lateral shear between Indochina and South China. Nature 343, 431–437.

Tapponnier, P., Zhiqin, X., Roger, F., Meyer, B., Arnaud, N., Wittlinger, G., Jingsui, Y., 2001. Oblique stepwise rise and growth of the Tibet Plateau. Science 294, 1671–1677.

Tremblay, M.M., Fox, M., Schmidt, J.L., Tripathy-Lang, A., Wielicki, M.M., Harrison, T.M., Zeitler, P.K., Shuster, D.L., 2015. Erosion in southern Tibet shut down at ~10 Ma due to enhanced rock uplift within the Himalaya. Proceedings of the National Academy of Sciences (PNAS) 112, 12030–12035.

Walsh, J.P., Wiberg, P.L., Aalto, R., Nittrouer, C.A., Kuehl, S.A., 2016. Source-to-sink research: Economy of the Earth's surface and its strata. Earth-Science Reviews 153, 1–6.

Wan, S., Li, A., Clift, P.D., Stutt, J.-B., 2007. Development of the East Asian monsoon: mineralogical and sedimentologic records in the northern South China Sea since 20 Ma. Palaeogeography, Palaeoclimatology, Palaeoecology 254, 561–582.

Wang, C., Dai, J., Zhao, X., Li, Y., Graham, S.A., He, D., Ran, B., Meng, J., 2014. Outward-growth of the Tibetan Plateau during the Cenozoic: A review. Tectonophysics 621, 1–43.

Wang, C., Zhao, X., Liu, Z., Lippert, P.C., Graham, S.A., Coe, R.S., Yi, H., Zhu, L., Liu, S., Li, Y., 2008. Constraints on the early uplift history of the Tibetan Plateau. Proceedings of the National Academy of Sciences (PNAS) 105, 4987–4992.

Wang, P., 2004. Cenozoic deformation and the history of sea-land interactions in Asia. In: Clift, P., Kuhnt, W., Wang, P., Hayes, D. (eds.), Continent-Ocean Interactions within East Asian Marginal Seas, AGU Geophysical Monograph 149, 1–22.

Wang, P., Wang, L., Bian, Y., Jian, Z., 1995. Late Quaternary paleoceanography of the South China Sea: surface circulation and carbonate cycles. Marine Geology 127, 145–165.

Wang, X., Sun, X., Wang, P., Stattegger, K., 2009. Vegetation on the Sunda Shelf, South China Sea, during the Last Glacial Maximum. Palaeogeography, Palaeoclimatology, Palaeoecology 278, 88–97.

Wei, H.H., Wang, E.C., Wu, G. L., Meng, K., 2016. No sedimentary records indicating southerly flow of the paleo-Upper Yangtze River from the First Bend in southeastern Tibet. Gondwana Research 32, 93–104.

Yang, S.Y., Li, C.X., Yokoyama, K., 2006. Elemental compositions and monazite age patterns of core sediments in the Changjiang delta: implications for sediment provenance and development history of the Changjiang River. Earth and Planetary Science Letters 245, 762–776.

Yao, Z., Guo, Z., Xiao, G., Wang, Q., Shi, X., Wang, X., 2012. Sedimentary history of the western Bohai coastal plain since the late Pliocene: implications on tectonic, climatic and sea-level changes. Journal of Asian Earth Sciences 54–55, 192–202.

Zhang, P., Molnar, P., Downs, W.R., 2001. Increased sedimentation rates and grain sizes 2–4 Myr ago due to the influence of climate change on erosion rates. Nature 410, 891–897.

Zhang, Y., Liu, Z., Zhao, Y., Wang, W., Li, J., Xu, J., 2014. Mesoscale eddies transport deep-sea sediments. Scientific Reports 4, 5937, doi:10.1038/srep05937.

Zhang, Y.F., Li, C.A., Wang, Q.L., Chen, L., Ma, Y.F., Kang, G.C., 2008. Magnetism parameters characteristics of drilling deposits in Jianghan Plain and indication for forming of the Yangtze River Three Gorges. Chinese Science Bulletin 53, 584–590.

Zhao, Y., Liu, Z., Zhang, Y., Li, J., Wang, M., Wang, W., Xu, J., 2015. In situ observation of contour currents in the northern South China Sea: Applications for deepwater sediment transport. Earth and Planetary Science Letters 430, 477–485.

Zheng, H.B., Clift, P.D., Wang, P., Ryuji T., Jia, J.T, He, M.Y., Jourdan, F., 2013. Pre-Miocene birth of the Yangtze River. Proceedings of the National Academy of Sciences (PNAS) 110, 7556–7561.

Zheng, H.B., Jia, J.T., Chen, J., Wang, P., 2011. Forum comment: Did incision of the Three Gorges begin in the Eocene? Geology 39, 244.

Chapter 4.

Precambrian sedimentology in China: Tracking long-term co-evolution and interplay among continents, atmosphere, ocean and life

Chao Li[1], Genming Luo[1], Shihong Zhang[2], Jun Hu[1], Shucheng Xie[1], Timothy W.Lyons[3]

[1]State Key Laboratory of Biogeology and Environmental Geology, China University ofGeosciences, Wuhan 430074, China

[2]State Key Laboratory of Biogeology and Environmental Geology, China University ofGeosciences, Beijing 100083, China

[3]Department of Earth and Planetary Sciences, University of California, Riverside, CA 92521,US

Definitions:

1. Precambrian is a geological period older than 541 Ma, representing the early evolution of the Earth.
2. "Snowball Earth" Events denote the Earth's extreme cooling events in geological history, during which glaciers likely expanded to equator regions, making the Earth look like an enormous snowball.
3. Great Oxidation Events denote the rapid oxygenation events of Earths's surface in geological history during which the atmospheric O_2 levels rose substantially.

1. Overview

The Precambrian (>541 Ma) accounts for ~88% of Earth's history, representing its early evolution. A series of significant geological events occurred in the Precambrian, including assembly and dispersal of supercontinents (e.g., Nuna, Rodinia), great oxidation events (GOEs), secular changes in oceanic chemistry, global glaciations ("Snowball Earth" Events), and the origin and evolution of early life including metazoans. These events were lithologically and geochemically archived in sedimentary records and represent the center of Precambrian sedimentology studies in past decades.

Many of these events are coeval, and the interplay (cause-and-effect relationships) existed among them (Fig. 4-1). For example, the development of oxygenic photosynthesis at ~3.0 Ga is responsible for the Paleoproterozoic Great Oxidation Event (GOE1) hundreds of millions of years later, whereas a second significant O_2 rise in the Neoproterozoic (GOE2) was responsible for the emergence and diversification of metazoans through a substantial oceanic oxygenation (*Lyons et al., 2014*). In contrast, generally low atmospheric O_2 levels and widespread anoxic and euxinic ocean waters in the middle Proterozoic may have challenged the diversification of eukaryotes and emergence of metazoans (i.e., "Boring Billion"; *Planavasky et al., 2014a; Anbar and Knoll, 2002*).

Many questions remain. As illustrated in Figure 4-1C, increasing evidence indicates that the history of atmospheric oxygenation was more complex than previously thought. For example, on the basis of chromium (Cr) isotope data from a suite of Proterozoic sediments, Planavsky et al. (2014a) inferred less than 0.1% of present atmospheric level (PAL) between 1.8 and 0.8 Ga, whereas *Zhang et al. (2016)* suggested >4% PAL of atmospheric oxygen levels at ~1.4 Ga based on trace metal and biomarker data, and *Zhang et al. (2018)* found a progressive oceanic oxygenation since ~1.57 Ga. Furthermore, *Sperling et al. (2015)* inferred only a limited rise in oxygen through the Ediacaran and Cambrian periods based on a global compilation of iron speciation data, which challenges the classic idea that atmospheric O_2 had reached near-modern levels in the Cambrian (*Canfield, 2005; Chen et al., 2015*). Increasing evidence also indicates that the oceanic oxygenation was more complex than previously thought (Fig. 4-1E). For example, recent studies pointed to only pulsed or stepwise shelf oxygen for the highly stratified Precambrian oceans (*e.g., Li et al., 2017a; Jin et al., 2016; Shi et al., 2018; Sahoo et al., 2016*), in contrast to the complete oxygenation of Precambrian deep oceans proposed previously (*e.g., Canfield et al., 2007, 2008; Chen et al., 2015; Holland, 1984, 2006; Scott et al., 2008*).

Increasing research indicates that the assembly and breakup of supercontinents may have played a trigger role in the oxygenation of Precambrian world. Campbell and Allen (2008) proposed that the amalgamation of Earth's land masses into supercontinents may have finally raised atmospheric O_2 levels through mountain building, which enhanced weathering and terrestrial nutrient fluxes to oceans and thus marine productivity and organic burial. Alternatively, oxygenation of Earth's surface might have been linked to the breakup of supercontinents rather than the formation (Fig. 4-1). For example, a key driver of GOE1 (~2.4-2.05Ga) may lie with the breakup of an unnamed early Paleoproterozoic supercontinent (*Müller et al., 2005*). Dispersal of supercontinents results in the formation of extensive continental margins (Figs. 4-1A and B) with high marine productivity and rapid sedimentation enhancing burial of the produced organic matter. Indeed, modern oceanographic studies indicate that today's continental margins only, which account for ~6% of ocean area, contribute >40% of net marine production (*Ducklow and McCallister, 2004*). In addition, continental rifting could have increased terrestrial P fluxes into the oceans, which might further enhance the marine productivity in marginal regions (*Bekker and Holland, 2012; Papineau et al., 2013*). Overall, the increase in the extent of continental margins would enhance global organic production and burial and in turn release of photosynthetic O_2 to the atmosphere. Increasing atmospheric O_2 levels would further enhance oxidative weathering and riverine sulfate fluxes into oceans. These processes are suggested for the extremely positive $\delta^{13}C_{carb}$ excursion (i.e., the Lomagundi Event; Fig. 4-1B; *Kump et al., 2011*) and increased marine sulfate concentrations at that time, reflecting both increasing sulfate fluxes to the oceans and decreasing marine pyrite burial (Fig. 4-1D; *Planavsky et al., 2012*). Similarly, the Neoproterozoic oxidation event (i.e., GOE2; <0.8 Ga) can be explained by the breakup of Rodinia.

The rapid decline of atmospheric O_2 levels after 2.05 Ga can also be linked to the assembling of supercontinent "Nuna" since 2.1 Ga (*Zhao et al., 2002, 2004*) by invoking the same mechanisms outlined above but in reverse. This relationship is consistent with the rapid decline of marine sulfate concentrations suggested at the end Lomagundi

Event (Fig. 4-1D). On the other hand, some statistics for the areal extent of continental margins show instead an increase rather than a decrease after 2.1 Ga (Fig. 4-1B). Clearly, there is need for additional work.

The extremely low inferred levels of O_2 during 1.8-1.4 Ga can be linked to the full formation and stabilization of Nuna, as suggested by statistical analysis of global paleomagnetic data (*Zhang et al., 2012*), and the less extensive continental margins and associated organic production and burial implied. Such processes could be manifested in the stable δ^{13}Ccarb records observed during this period (Fig. 4-1B). Low marine oxygen levels during the mid-Proterozoic are supported by suppressed U-Mo enrichments in marine shales (*Partin et al., 2013; Scott et al., 2008; Reinhard et al., 2013*) and low marine sulfate concentrations during this period (*Kah et al., 2004; Canfield et al., 2010; Li et al., 2015a; Luo et al., 2015*). Similarly, low O_2 levels during 1.0-0.8 Ga can be explained by the full formation and stabilization of Rodinia.

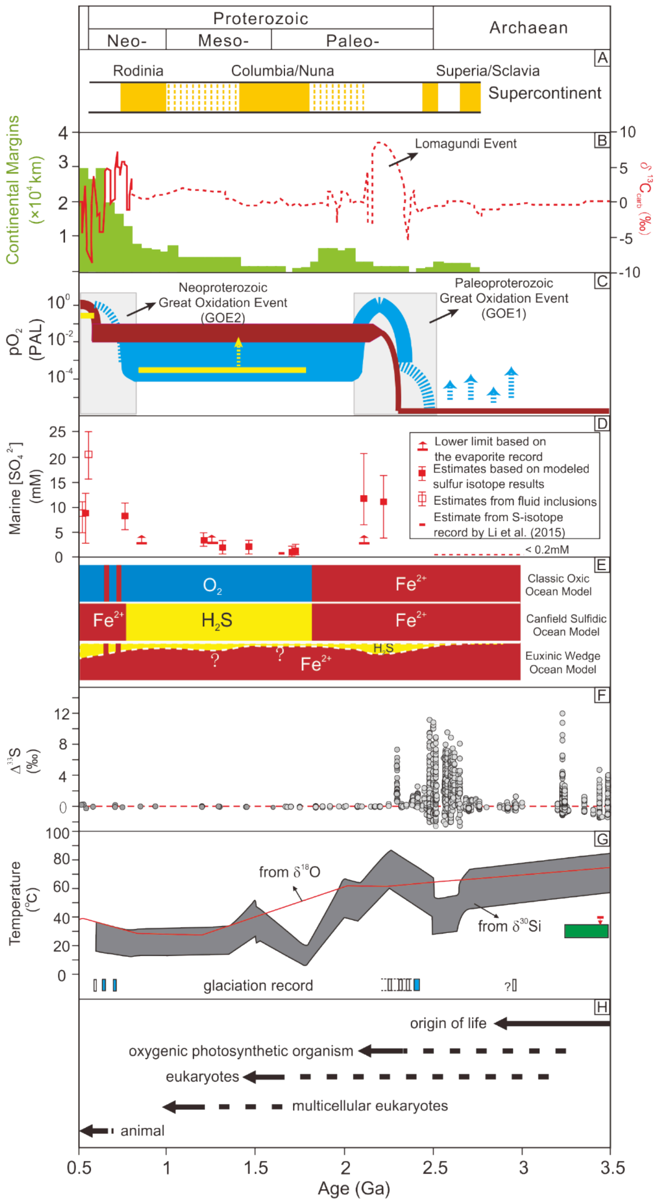

◂

Fig. 4-1.

Co-evolution of continents, atmosphere, oceans, and life in Precambrian.

(A) The assembly and dispersal of supercontinents. Data sources: Campbell and Allen (2008); Li et al. (2008); Zhao et al. (2002, 2004); Zhang et al. (2012).

(B) Variations of the areal extent of continental margins (Bradley, 2008) and inorganic carbon isotope composition (δ^{13}Ccarb; Campbell and Allen, 2008).

(C) Evolution of Earth's atmospheric oxygen content (pO_2, atmospheric partial pressure of O_2). Modified from Lyons et al. (2014). The faded red curve shows a "classical, two-step" view of atmospheric evolution (Kump, 2008), while the blue curve shows the emerging, more dynamic model presented in Lyons et al. (2014). The lateral yellow bar between 1.8 and 0.8 Ga reflects the atmospheric O_2 level (< 0.1% PAL) given in Planavsky et al., (2014a), while the yellow arrow at 1.4 Ga represents the atmospheric O_2 level (>4% PAL) given in Zhang et al. (2016). The yellow bar around 0.54 Ga represents the atmospheric O_2 level (10-40% PAL) proposed in Sperling et al. (2015).

(D) Evolution of marine sulfate concentration. Data sources: Habicht et al. (2002); Planavsky et al. (2012); Li et al. (2015a).

(E) Redox evolution of deep ocean. Modified from Li et al. (2016).

(F) Temporal variation of mass-independent fractionation of sulfur isotopes ($\Delta^{33}S$) during the Precambrian. Modified from Zhelezinskaia et al. (2014) and the most recently published data in Johnson et al. (2013) (It includes only the syngenetic pyrite sulfur data. The sulfur isotope data obtained from SIMS are averaged according to depth) and Luo et al. (2016).

(G) Precambrian temperature estimated from multiple proxies. Red line represents the estimate from the highest $\delta^{18}O$ value of chert (modified from Knauth and Lowe, 2003). The gray band represents temperatures evaluated from $\delta^{30}Si$ of chert (modified from Robert and Chaussidon, 2006). Temperatures estimated from coupled $\delta^{18}O$ and δD values from chert are indicated by the green box (Hren et al., 2009) and those estimated from the highest $\delta^{18}O$ of phosphate are represented by the red box (Blake et al., 2010). The glaciation records are modified from Hoffman et al. (1998), Gumsley et al. (2017) and Young et al. (1998). Blue boxes: 'Snow-ball Earth' glaciations; blank boxes: Continental glaciations.

(H) Evolutionary history of life on Earth. The earliest records of life on Earth are as old as 3.7 Ga (Nutman et al., 2016) or 4.1 Ga (Bell et al., 2015). Oxygenic photosynthesis must be present before the GOE, either directly before the GOE (Fischer et al., 2016) or as early as 3.0 Ga (Crowe et al., 2013; Planavsky et al., 2014b). The earliest convincing evidence for eukaryotic life is present at ~1.7 to 1.6 Ga (e.g., Butterfield, 2015), although the origin of eukaryotes could have been much earlier (Javaux et al., 2010). Records of multicellular eukaryotes appear as early as ~1.2 Ga (Butterfield, 2000) or ~1.6 Ga (Zhu et al., 2016a). The first appearance of animals, indicated by biomarker evidence for early sponges, occurs during the Cyrogenian "Snowball Earth" episode (Love et al., 2009).

In summary, although significant steps have been taken over the past decades, the first-order scientific questions about Precambrian sedimentology remain. These questions are centered on the co-evolution and interplay of the continents, atmosphere, oceans and life and will continue to be so. Based on our review above, some sub-order questions can be outlined as follow:

(1) Origins and early evolution of complex life

1.1 What were the distributions and controls on the earliest complex life (eukaryotes) in the Mesoproterozoic?

1.2 What were the patterns and controls on the transition from the Ediacaran fauna to the complex organisms and ecologies of the Cambrian?

1.3 When did organic export production and burial become dominated by eukaryotic biomass rather than prokaryotic?

(2) The environmental backdrop of evolving complex life

2.1 Were there tectonic drivers of first-order environmental change and co-evolving life? Specifically, what were the patterns of supercontinent formation/breakup and their potential biogeochemical effects?

2.2 What specifically were the oxygen, nutrient and overall chemical and physical conditions for this early evolution of complex life?

2.3 Was the "Boring Billion" really boring or more dynamic? What internal and external drivers led to the end of the "Boring Billion"?

2.4 What was the nature of Neoproterozoic oxidation event? Was there an upward baseline shift but with continued dynamic redox and extensively low oxygen conditions even in the Ediacaran and early Paleozoic oceans?

2.5 What was the nature of the transition from the Neoproterozic oxidation event to Phanerozoic-style oxygenation? And when was the 'terminal oxygenation event'?

(3) The interplay between life and environmental factors

3.1 What were the potential patterns of redox dynamics during the Ediacaran and their relationships to co-evolving metazoans?

3.2 How did N and P cycling control environmental (redox, etc.) and biological evolution? Conversely, how were nutrient cycles, through feedbacks, controlled by the co-evolution of life and the environment?

3.3 How do the abundances of bioessential trace metals (Mo, Zn etc.) track or interplay with the evolution of life and the environment?

2. Research frontiers in Precambrian sedimentology

areal extent of continental margins show instead an increase Based on the main research progress over the past decades, as reviewed above, we can identify a few research frontiers in the Precambrian sedimentology, which are key elements for us to answer the first-order scientific question, i.e., the co-evolution and interplay of continents, atmosphere, ocean and life in Precambrian.

2.1. Assembly and breakup of supercontinents

Among the three well-known supercontinents, the youngest Pangea ultimately formed and dispersed in the Phanerozoic, but Rodinia and Nuna existed in the late Precambrian (Meso- and Neoproterozoic). Important progress following publication of three pioneering papers (*Moores, 1991; Dalziel, 1991; Hoffman, 1991*) laid out the basic framework for the Neoproterozoic Rodinia supercontinent. The initial models placed Laurentia in the center of Rodinia; India, cratonic Australia and East Antarctic were juxtaposed on the southwestern side of Laurentia. Siberia and Baltica were positioned adjacent the northern-northeastern side of Laurentia, while Amazonia, Congo and Kalahari were placed along the eastern side of Laurentia. Breakup of Rodinia led to assembly of Gondwana. This transition dominated Late Neoproterozoic geological history. Major advances over the past 25 years include significant revisions of the configuration of Rodinia (*e.g., Li et al., 2008*) and tighter constraints on the timing of its assembly and breakup (*e.g. Li and Evans, 2011*). However, the most important steps lie with current research, supported through long-term international cooperation (IGCP projects, Rodinia series meetings, establishment of international research centers, such as TSRC between Australia and U.S., etc.). These studies seek to resolve the linkages among Late Neoproterozoic global events, such as supercontinent formation/breakup, superplume activity, "Snowball Earth" climate, true polar wander, and the appearance and proliferation of multicellular animal, which all lead towards a holistic view of the mechanisms of Earth evolution (*e.g., Li and Zhong, 2009; Li et al., 2013b; Evans et al, 2016*).

The concept of a pre-Rodinia supercontinent, referred to as both Nuna and Columbia, was proposed separately by multiple researchers (*Hoffman, 1997; Zhao et al., 2002; Roger and Santosh, 2002*), but models for Nuna reconstruction are still in their early stages. Many authors (*Hoffman, 1997; Zhao et al., 2002; Roger and Santosh, 2002*) agree that by ~2.1-1.8 Ga orogenic belts were distributed globally and were linked to the assembly of Nuna, but how and when Nuna dispersed is not well known.

Numerous studies have explored Nuna in recent years through synthesis of globally distributed paleomagnetic and geological data, and a consensus is emerging for its configuration. The timing of the final assembly, however, and the break-up of Nuna remain subjects of intensive debate. There are two basic opinions: The first one, based mainly on paleomagnetic evidence from Baltica, Laurentia, Australia, north China, Siberia, and Amazonia, suggests that a tectonically coherent Nuna was assembled by ~1.78 Ga and reached global-scale proportions (*e.g. Zhang et al., 2012*; see Fig. 4-2). The second opinion, however, based mainly on geological evidence, suggests that plate convergence between western Laurentia and northeastern Australia continued longer and that eventual consolidation of Nuna was not complete until ~1.60 Ga (*Pisarevsky et al., 2014; Pehrsson et al., 2015*). It is also possible that the supercontinent Nuna formed by ~1.78 Ga but experienced some subsequent breakup and reassembly. Geological records from many cratons suggest that Nuna experienced multiple extensional episodes between 1.7 and 1.2 Ga. However, high-quality paleomagnetic signals, which include those from sedimentary successions in rift basins and widely exposed dikes, are in good agreement about the existence of a tectonically coherent Nuna, suggesting that no significant dispersal occurred during these extensional events. The breakup of Nuna, marking the tectonic transition from Nuna to Rodinia, may have commenced between 1.4 and 1.3 Ga, but available paleomagnetic data are not sufficient to constrain this transition more precisely.

Prior to the assembly of Nuna, older supercontinents may have existed (*e.g., Ernst and Bleeker, 2010*), but the records have been deeply metamorphosed, strongly deformed or largely eroded away. It is possible that assembly of giant continents and large continent growth more generally during the Archean and Paleoproterozoic may have influenced oxygenation of the atmosphere and oceans (*Campbell and Allen, 2008; Lee et al., 2016*). Exploring links between supercontinent cycles and the dynamic redox evolution of the Precambrian world is another exciting research frontier.

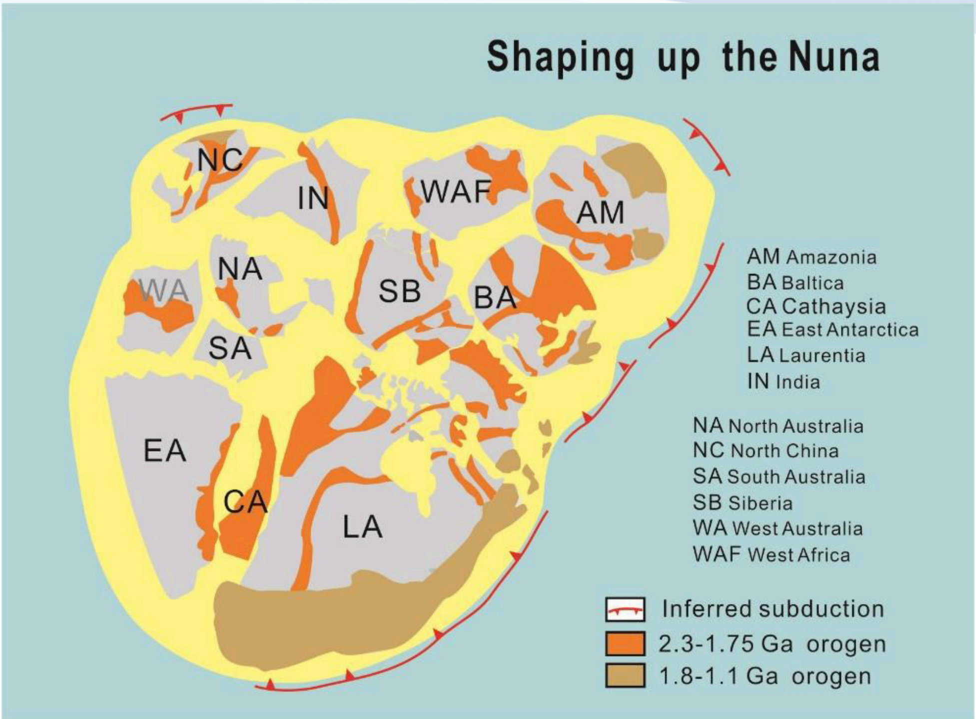

Fig. 4-2. The configuration of Nuna (modified from Zhang et al., 2012).

2.2. Evolution of atmospheric oxygen content

The modern atmosphere contains 21% (by volume) molecular oxygen (O_2), whereas numerous lines of evidence suggest that Earth's early atm osphere was far more limited in its O_2 content (*e.g., Farquhar et al., 2000; Holland, 1978; Rasmussen and Buick, 1999*). Low atmospheric O_2 levels (pO_2) have been supposed as the main factor affecting biotic evolution (e.g., Planavsky et al., 2014a; Li et al., 2017a). Thus, how/when the atmosphere firstly reached irreversibly high pO_2 has been a hot topic in both the Earth and life sciences over the past five decades. Great progress has been made over the past 15 years. First, there are multiple new proxies for the atmospheric oxygen content, particularly including mass independent fractionation of multiple sulfur isotopes (*Farquhar et al., 2000*) (Fig. 4-1F); redox-sensitive trace elemental concentration, such as Mo and U (*Anbar et al., 2007; Partin et al., 2013; Scott et al., 2008*) and non-traditional metal isotopic compositions, such as those for Cr, Mo, and Cu (*Frei et al., 2009; Fru et al., 2016; Chen et al., 2015*). Second, the evolution history of pO_2 was likely more complex than the previous two-step model for unidirectional increase with upward jumps at the beginning and end of the Proterozoic Eon (*Kump, 2008; Lyons et al., 2014*). Furthermore, transient accumulation of atmospheric O_2 may have occurred before the Great Oxidation Event (GOE), such as at ~3.0 and 2.5 Ga (*Anbar et al., 2007; Crowe et al., 2013*). Furthermore, multiple lines of evidence suggest that pO_2 decreased after the GOE, perhaps at ~2.06 Ga (*Kump et al., 2011; Lyons et al., 2014; Scott et al., 2014*). These lower values may have persisted to the Late Mesoproterozoic (*Luo et al., 2015; Planavsky et al., 2014a*). Third, the transition from an anoxic to irreversibly oxic atmosphere is now well constrained (*Luo et al., 2016*). The first emergence of significant O_2 in the atmosphere was traditionally placed in the interval between 2.5 and 2.3 Ga (*e.g., Bekker et al., 2004; Guo et al., 2009*). More recently, the transition was more precisely constrained at ~2.33 Ga based on high temporally resolved multiple sulfur isotope compositions of diagenetic pyrite in a continuous sedimentary sequence in three coeval drill cores in South Africa (*Luo et al., 2016*) (Fig. 4-3). These new data provide a robust framework for future research on the mechanism for the GOE and the co-evolution of Earth's life and the surface environment.

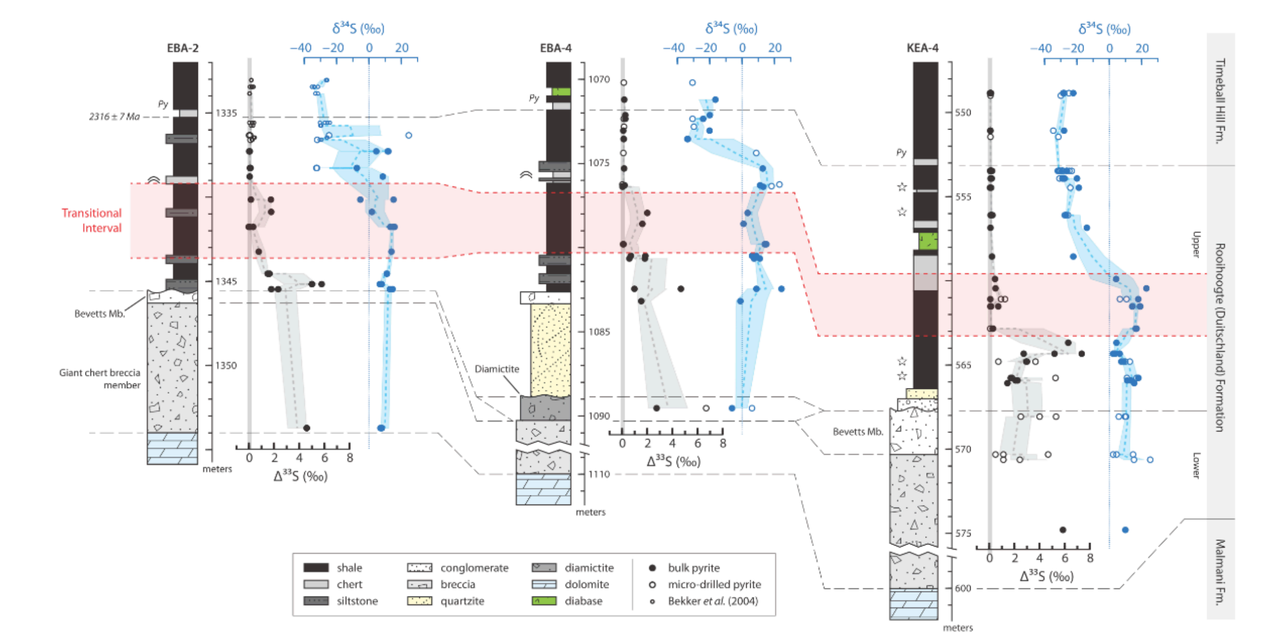

Fig. 4-3. ▲

The GOE recorded in multiple sulfur isotope compositions of diagenetic pyrite (after Luo et al., 2016; open access article). All isotope data are reported relative to VCDT. The dashed lines represent three-point moving averages, while the shaded regions represent 1 standard error of mean (SEM) on the 3 points. The transition interval highlighted in pink is defined on the basis of variation in the Δ^{33}S records. The Re-Os date of 2316 ± 7 Ma on syngenetic pyrite from the boundary between the Timeball Hill and Rooihoogte formations in core EBA-2 is from Hannah et al. (2004).

Among the critical issues to be solved is the mechanism behind the first accumulation of O_2 in the atmosphere, which depends on the balance between the sources and sinks of O_2. Oxygenic photosynthesis is the main source, while oxidation of reduced gases and other materials is the main sink. The origin of oxygenic photosynthesis may have occurred much earlier than the first accumulation of O_2 in the atmosphere, suggesting that the main mechanism for eventual atmospheric oxygenation was a decline in the fluxes of reduced gases (*e.g., Konhauser et al., 2009; Kump and Barley, 2007*) (Fig. 4-1H). This possibility is consistent with the hypothesis that transient accumulations of oxygen (whiffs) occurred before the GOE. The lines of evidence for whiffs of oxygen in the atmosphere, however, and localized accumulations in the surface ocean (oases) before the GOE have been challenged, and some researchers favor the possibility that the origin of oxygenic photosynthesis was simultaneous with the first accumulation of O_2 in the atmosphere (see the review by *Fischer et al., 2016*). Another issue to be resolved is the duration and magnitude of declining pO_2 following the GOE (*e.g., Planavsky et al., 2014a; Planavsky et al., 2016; Zhang et al., 2016*) and the extent and duration of a second oxidation event in the late Neoproterozoic, followed eventually by increases in pO_2 close to the modern value (*e.g., Lyons et al., 2014*). Further, additional exciting research lies with the impacts of increasing atmospheric oxygen content on life, including the consequences of rising pO_2 during the GOE for predominantly anaerobic communities. Related hot research topics include pO_2 variations during the Mesoproterozoic and relationships to the origin and evolution of eukaryotic organisms, as well as the second oxidation event during the Neoproterozoic-Early Cambrian and attendant rise of animals (*e.g., Li et al., 2015c, 2017a; Shi et al., 2018; Sahoo et al., 2012; Sperling et al., 2015*).

Intensive cooperation is needed between geologists and paleobiologists. Sedimentary geochemical records with higher temporal resolution are required, and the proxies for pO_2 must be refined, through theoretical calculations, experimental simulations and modern analogs. Additional high-quality genomic data are required to improve our understanding of the evolutionary tree of life. These efforts will be enhanced through further integration with fossil records and indicators of evolving microbial community structure and environmental conditions.

2.3. Ocean chemistry

It is widely acknowledged that the oxygen concentration of Earth's atmosphere approached the present level via two major steps—the Great Oxidation Event (GOE) at the beginning of the Proterozoic Eon and the Neoproterozoic Oxidation Event (NOE) at the end of the Proterozoic Eon (*Lyons et al., 2014*; Fig. 4-1C). Increasing atmospheric O_2 levels in the Proterozoic would have resulted in oxygenation of the oceans as well. However, increasing evidence suggests that history of ocean oxygenation was more complex than previously imagined (*Lyons et al., 2014; Li et al., 2016*; Fig. 4-1E). In the classic model (*Holland, 1984, 2006*), the Archean and Early Proterozoic deep oceans were ferruginous (anoxic and Fe(II)-bearing) and transitioned to oxygenated or partially oxygenated conditions by ~1.8 Ga roughly in phase with the GOE. This proposed transition was defined by the termination of global deposition of iron formations (IFs) attributed to a decline in the abundance of soluble Fe(II) in seawater. *Canfield (1998)* raised another possibility (known as the "Canfield Ocean" or "sulfidic ocean" model), i.e., the deep ocean after 1.8 Ga became euxinic (anoxic and H_2S-bearing), leading to a termination of the IF deposition owing to sequestration of soluble Fe(II) into sedimentary iron sulfide minerals, such as pyrite. A ferruginous deep ocean was subsequently hypothesized to have returned in the Neoproterozoic (*Canfield et al., 2008*). However, recent studies have yielded evidence for a highly redox-stratified structure for the early-Earth oceans (>520 Ma) in which a mid-depth euxinic water mass was maintained dynamically on continental shelves between oxic proximal-shelf waters and ferruginous deep-ocean waters (i.e., the "euxinic wedge" model; *Li et al., 2010a; Poulton et al., 2010; Poulton and Canfield, 2011; Guilbaudet al., 2015; Jin et al., 2016; Reinhard et al., 2009, 2013; Planavsky et al., 2011; Feng et al., 2014*). This oceanic structure likely did not change in nature until the Cambrian (*Jin et al., 2016; Li et al., 2017a*).

Our advancing knowledge of the redox evolution of the Precambrian oceans, as described above, also indicates future direction for our research efforts:

(1) The recognition of large spatial heterogeneity of Precambrian ocean chemistry will motivate a new generation of comprehensive biogeochemical models for the oceans. For example, *Li et al. (2015b)* proposed an idealized chemical zonation model for early oceans (>520 Ma) that includes (from shallow nearshore to deep offshore regions) oxic, nitrogenous, manganous-ferruginous, sulfidic, methanic, and ferruginous zones, which is helpful to explain the spatial heterogeneity of elemental geochemical records (e.g., C, N, S and trace metals) widely observed in the Precambrian rocks. To develop and test these comprehensive theoretical models, we need additional samples and data at higher spatial and temporal resolution, more quantitative proxies, as well as biogeochemical modeling based on large databases (*e.g., Reinhard et al., 2016*).

(2) The intimate relationship between ocean redox and biological evolution requires a more complete understanding of the co-evolution of ocean redox and early life. It is generally accepted that the buildup of oxygen in the Earth's atmosphere and oceans has fundamentally reshaped the dynamics of nearly all major biogeochemical cycles and ultimately paved the way for the diversification of complex life on Earth. The detailed mechanisms behind these relationships must be further elucidated.

2.4. Climate change

The most impressive feature of Precambrian climate is the episodic "Snowball Earth" glaciations during which glaciers extended to low latitudes (*e.g., Hoffman et al., 1998; Kirschvink et al., 2000*) (Fig. 4-1G). One example occurred in the early Paleoproterozoic as indicated by multiple (3 to 4) layers of glacial diamictite in Africa, Australia, and North America. The correlation of these diamictites among these regions is difficult, and the timing of these diamictites has been only poorly constrained to the interval between 2.45 to 2.2 Ga (*Young, 2014*). Among these glacial diamictites, only one has solid paleomagnetic data suggesting that the glaciers extended to low latitudes (*Kopp et al., 2005*). The younger Precambrian "Snowball Earth" glaciations occurred in the Neoproterozoic, about 720 and 635 million years ago (Ma), known as the Sturtian and Marinoan glaciations, respectively (*Hoffman et al., 1998; Macdonald et al., 2010; Zhou et al., 2004*). These two glaciations occurred globally with particular good sedimentary records in South China (Fig. 4-4). Strong evidence suggests that these two glaciations were well extended into low latitudes (*Hoffman et al., 1998; Kirschvink et al., 2000*).

Although the fundamental drivers of the two main episodes of "Snowball Earth" glaciation are not well understood, the rough coincidence between the glaciations and a primary increases in pO_2 suggests a causal relationship (*Lyons et al., 2014*). One possibility is that an increase in pO_2 induced a decline in atmospheric concentrations of CH_4, an important greenhouse gas, leading to global cooling (*Pavlov et al., 2003; Haqq-Misra et al., 2008*). However, to date, the evidence for this hypothesized decline in pCH_4 has been indirect, and new estimates suggest generally low atmospheric methane leading up to the onset of Neoproterozoic glaciation (Olson et al., 2016). Links between Paleoproterozoic glaciation and declining methane stability are more easily established (*e.g., Haqq-Misra et al., 2008*). Furthermore, the precise temporal sequences are not fully understood. Geological records in South Africa, for example, show that the Early Paleoproterozoic diamictites can be below the disappearance of mass independent fractionation, which raises questions about the relationship between rising oxygen, declining methane stability and global cooling.

In addition to the two major glacial episodes, two other smaller glacial intervals have also been reported at ~2.9 Ga, as indicated by a glacial tillite in Africa (*Young et al., 1998*) and at about 580 Ma known as the Gaskiers glaciation (*e.g., Bowring et al., 2003*). Except for these glaciations, the climate in the other intervals of Precambrian might have been warm, if not very warm (Fig. 4-1G). Oxygen and silicon isotope compositions of chert suggest temperatures in the Archean surface ocean from 55 to 85 ºC, which may have decreased to ~20 ºC by the end Proterozoic (*Knauth and Lowe, 2003; Robert and Chaussidon, 2006*). This conclusion lies with assumption that the geochemical signals are primary and that the oxygen isotope composition of seawater was the same as the present-day value. However, coupled δD and $\delta^{18}O$ data for chert and $\delta^{18}O$ of phosphate suggest that the Early Archean temperature was about 26 to 40 ºC, which is much lower than earlier estimates (*Blake et al., 2010; Hren et al., 2009*). Considering the less bright sun during the Precambrian, however, maintenance of warm enough temperatures to sustain mostly ice-free oceans and continents demands high levels of greenhouse gases, such as CO_2 and CH_4 (*Kasting and Howard, 2006*). Further work is needed to better constrain early ocean temperatures and the factors that maintained or destabilized those conditions.

Patterns of Precambrian climate variability remain largely unknown, particularly at high resolution. Ancient climate research requires additional proxies. For example, recently developed clumped isotope compositions of CO_2 may provide an additional paleothermometer. However, post-depositional alternation of the host carbonate lithologies offers particular challenges. Further, microbial biogeochemical cycles, as related to evolving oceanic chemical composition (e.g., dissolved sulfate levels and ocean redox) would have impacted climate (*Olson et al., 2016*).

Fig. 4-4.

Typical Nantuo diamictites (Marinoan age) and overlying cap carbonates (a featured postglacial deposit) in South China. Photo was taken by Alex Sessions (Caltech) from the Jiulongwan Section, Yangtze-gorges area, South China.

2.5. Evolution of the biogeochemical cycles of carbon, nitrogen and sulfur

The cycling of carbon, nitrogen and sulfur is intimately coupled to changes in microbial processes and redox conditions at Earth's surface. Carbon isotope compositions of Precambrian carbonate ($\delta^{13}C_{carb}$) show large transient perturbations within two key intervals (Fig. 4-1B). One interval, the Early Paleoproterozic, is characterized by generally high values (~ +10 ‰) around 2.3-2.06 Ga, known as the Lomagundi-Jatuli event (*e.g., Karhu and Holland, 1996; Melezhik et al., 2007; Martin et al., 2013*). This excursion is followed by declining values around ~2.0 Ga. Various models have been proposed to explain this trend, including organic burial (*Baker and Fallick, 1989a,b*), oceanic stratification leading to low values in deep water but strongly positive data in shallow water (*Keith, 1982; Aharon, 2005; Bekker et al., 2008*), methanogensis (*Hayes and Waldbauer, 2006*) and low rates of remineralization of primary production dominated by anoxygenic photosynthesis (*Kirschvink and Kopp, 2008*).

The subsequent negative excursion could reflect massive oxidation of organics under elevated atmospheric oxygen content (*Kump et al., 2011*).

The second interval with large negative δ^{13}Ccarb perturbations (down to -12‰) occurred in the Late Neoproterozoic (*e.g., Fike et al., 2006; Macdonald et al., 2010; Swanson-Hysell et al., 2010*). Multiple mechanisms have been proposed to explain these large fluctuations. The negative values, in particular the mid-Ediacaran Shuram-Wonoka excursion (SWE), have been attributed to a number of different sources, e.g., low primary production and resultant low organic burial (*Hoffman et al., 1998*), massive release of seafloor gas hydrate (*Jiang et al., 2003*), deposition of authigenic carbonate due to the enhanced anaerobic microbial oxidation of organic matter (*Tziperman et al., 2011; Schrag et al., 2013; Cui et al., 2017*), global diagenetic alteration (*Knauth and Kennedy, 2009; Derry, 2010; Swart and Kennedy, 2012*), oxidation of recycled continentally derived organic carbon (*Kaufman et al, 2007*), hydrocarbons from marine seeps (*Lee et al., 2015*), or a large pool of dissolved organic carbon (DOC) (100-1000 times modern values) (*Rothman et al., 2003; Fike et al., 2006; McFadden et al., 2008*). Recent investigation of the Shuram-Wonoka excursion in South China revealed high spatial heterogeneity consistent with spatially heterogeneous oxidation (i.e., partial oxidation) of subsurface reduced carbon in shelf areas (*Li et al., 2017b*). This model minimizes the likelihood of inadequate oxidant supplies imagined in previous studies that assumed whole-ocean oxygenation and corresponding shifts in δ^{13}C on the same scale (*Bristow and Kennedy, 2008*), while also explaining the spatial heterogeneity of the SWE.

In contrast, δ^{13}Ccarb is unusually stable (-2‰ to +1‰; *Kah et al., 2012; Li et al., 2003*) during the Mesoproterozoic, which has contributed to its reputation as the "Boring Billion". It is notable, however, that the long-term δ^{13}Ccarb record of marine carbonates clusters around 0‰, despite development of diverse pathways of carbon fixation by microbes and more complex organisms and the parallel evolutionary and ecological history of microbial recycling of organic matter. The implied stable, relatively low levels of organic burial are consistent with estimates for low atmospheric O_2 and demand further research about coupled nutrient cycling/availability.

Sulfur isotope compositions during the Precambrian provide temporal constraints on the evolution of key microbial metabolism processes that are also coupled to evolving atmospheric O_2 content. Isotopic offsets between oxidized (sulfate) and reduced (pyrite) sulfur fingerprint the origins of microbial sulfate reduction, with current estimates extending back to at least 3.5 Ga (*Shen et al. 2001*). These records of microbial sulfur cycling also carry suggestions of vanishingly low sulfate availability in the early oceans (*e.g., Crowe et al. 2014*), which further points to trace levels of oxygen in the Archean atmosphere and oceans. Additional opportunities for tracking ancient microbial activities and their consequences lie with studies measuring all four sulfur isotopes (^{32}S, ^{33}S, ^{34}S, ^{36}S). Furthermore, on time scales of >100 My, δ^{13}C and δ^{34}S records are negatively correlated, suggesting a still poorly understood negative feedback mechanism, i.e., one that may work to stabilize environmental oxygen availability (*Lyons et al., 2015*).

Similarly, δ^{15}N values from Precambrian samples are used to determine the relative timing of the evolution of nitrogen metabolisms during the progressive oxygenation of Earth's surface. Two key biological innovations in the nitrogen cycle during Precambrian were the evolution of N2 fixation and proliferation of the aerobic nitrogen cycle (*Lyons et al., 2015; Stüeken et al., 2015, 2016*). The regular occurrence of very negative δ^{15}N values in sediments deposited before ~2.5 Ga are thought to reflect an anaerobic nitrogen cycle dominated by N_2 fixation and/or the uptake of a large pool of bioavailable ammonium in anoxic oceans (*Stüeken et al., 2015*). An increase in δ^{15}N values between ~2.5 and 2.0 Ga, coincident roughly with the GOE, is generally interpreted to reflect the transition to a modern-type aerobic nitrogen cycle dominated by nitrate-dependent processes of nitrogen loss, although this interpretation might be complicated by recent indications of anaerobic pathways for ammonium oxidation in marine sediments using Fe(III) or Mn(IV) oxides instead of O_2 (*Lyons et al., 2015; Busigny et al.,* *2013*). A shift toward positive $\delta^{15}N$ values, similar to modern ones, was observed to occur in sediments younger than ~2.0 Ga (*Lyons et al., 2015; Stüeken et al., 2016*).

Recent advances in our understanding of elemental cycles during the Precambrian also highlight inevitable gaps in our knowledge. These research opportunities include:

(1) Connections among diverse cycles, in particular between the nitrogen cycle and other biogeochemical processes, constraints on the evolution of nitrogen metabolisms, and advanced frontiers in sulfur geochemistry studied at both micro- and macroscales.

(2) The integration of organic/microbial data with a robust context of other complementary proxies, including sophisticated petrographic, paleontological, sedimentological, and diagenetic approaches along with quantitative estimates on trace metal, phosphorus, and macronutrient availability in the early oceans.

(3) Exploring the linkages between modern and ancient perspectives, including a new generation of "omic" data with independent constraints on evolving background environments and geochemical fingerprints of microbial activity.

Fig. 4-5.▲

Microbially-induced large carbonate concretions in the upper Ediacaran Doushantuo Formation, South China. Please refer to Dong et al (2013) for the microbially mediated formation of these carbonate concretions. Photo was taken by Xuelei Chu (Chinese Academy of Sciences) from the Jiulongwan Section, Yangtze-gorges area, South China.

2.6. Microbial sediments

Microbial sediments reflect microbially mediated processes that range from precipitation of minerals to sediment binding, trapping, and baffling. Microbial sediments include stromatolites, oncolites, and thrombolites and microbially induced sedimentary structures (MISS) (Fig. 4-5). Studies of MISS (*e.g., Noffke et al., 2001; Gerdes et al., 2000; Schieber, 2004; Eriksson et al., 2007; Porada et al., 2007*) have identified sedimentary structures related to microbial metabolism, including microbial growth, decay and the microbial rupture. The global diversity and abundance of microbial mats and the related MISS show a sharp increase at 1.8 Ga. This shift might be related to the coincident variations in oceanic chemistry linked to patterns of biospheric oxygenation (*Arnold et al., 2004; Rouxel et al., 2005; Holland, 2006*). Furthermore, microbial mats played an important role in the evolution of animals through substrate modification (*Bottjer et al., 2000*).

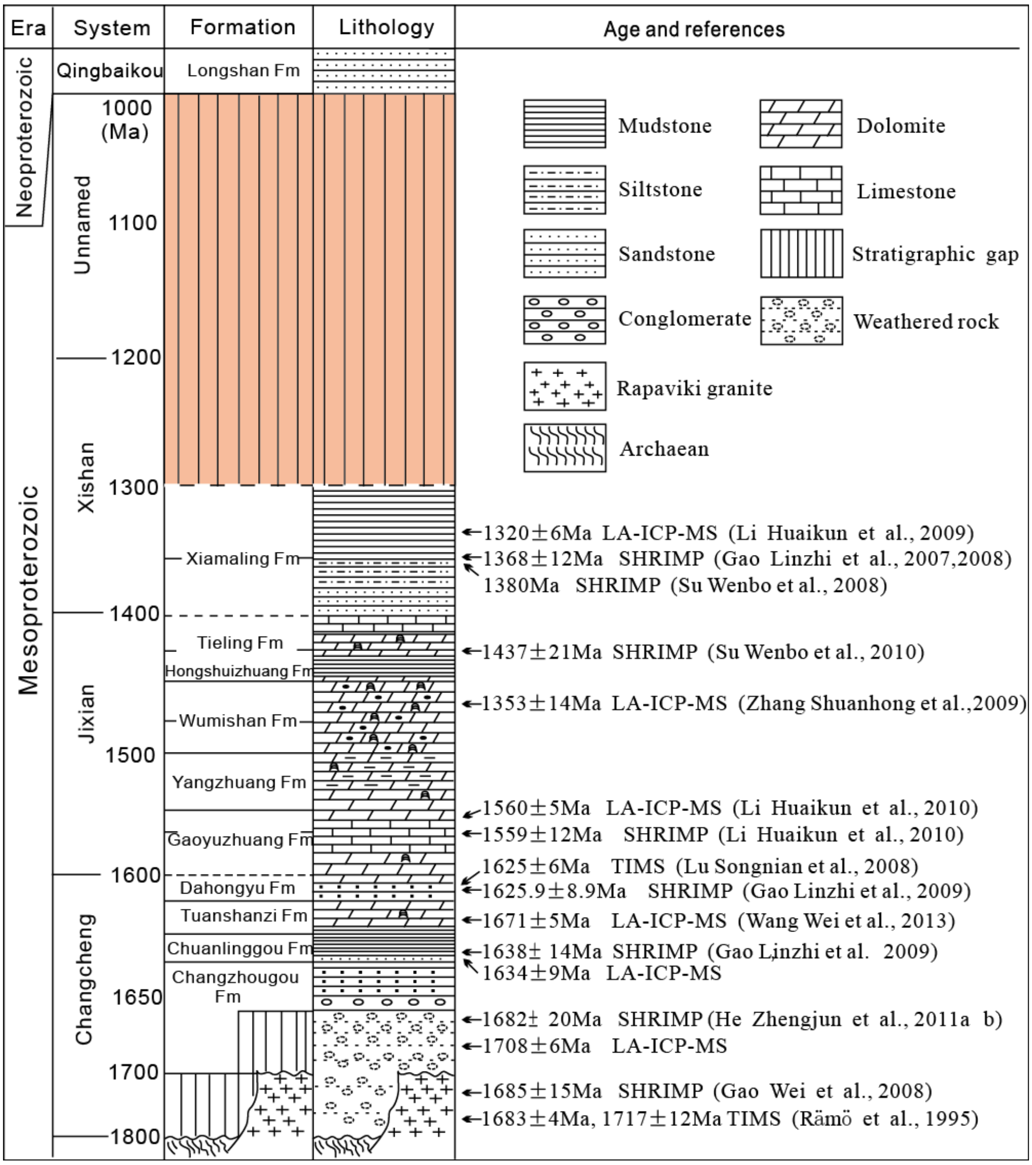

Fig. 4-6.▲

Mesoproterozoic chronostratigraphic framework and key zircon U-Pb ages reported for Yan-Liao Aulacogen, North China Craton. Modified from Qiao et al (2014).

Dolostone often dominates carbonate rocks from the Precambrian. An important area of current research is exploring the relationship between dolomite and microbes, such as sulfate reduction bacteria (SRB) and halophiles, which may be critical in inducing dolomite precipitation under Earth surface conditions (*Sánchez-Román et al., 2008; Vasconcelos et al., 1995; Zhang et al., 2015; Zhang etal., 2012*). Recently, for example, *Rodriguez-Blanco et al. (2015)* suggested that dolomite forms in three stages: (1) rapid formation of Mg-containing amorphous calcium carbonate (Mg-ACC) in dolomite-oversaturated solution, (2) transformation from Mg-ACC to non-stoichiometric -dolomite through a spherical growth mechanism, and (3) dissolution and recrystallization of non-stoichiometric to form the ordered stoichiometric dolomite. Microbes can participate in all three stages.

Iron formations (IFs) are marine sedimentary rocks unique to the Precambrian often featuring alternating layers of chert and iron-rich minerals (e.g. magnetite, hematite) (*Klein, 2005*). These voluminous deposits are limited primarily to the Late Archean and the Early Prototerozoic, with a later recurrence in the Neoproterzoic likely linked to “Snowball Earth” glaciation and related controls on ocean chemistry (*Kopp et al., 2005*). IFs are commonly categorized as Algoma or Superior type, with the Fe largely attributed to volcanic/hydrothermal sources (Bekker et al., 2010). Iron concentrations presumably built up in the generally oxygen- and sulfate-lean deep oceans (*e.g., Canfield et al., 2008; Lyons et al., 2014*). Three genetic models have emerged: (1) UV photo-oxidation of Fe^{2+}, (2) microbial photoferrotrophy involving electrons from Fe^{2+} to fix CO_2, and (3) abiotic oxidation with the O_2 from oxygenic photosynthesis (see reviews by *Posth et al., 2011 and Bekker et al, 2010*). It is likely that all three processes contributed to the essential Fe oxidation, with photoferrotrophy perhaps dominant (*Konhauser et al., 2007*). Many issues about the IFs remain to be solved in future. Further research is needed to fully expose the relationship among microbial activity, oceanic chemistry and precipitation of IFs.

3. Precambrian sedimentology in China: advantages, opportunities and future strategy

It is clear that Precambrian sedimentology in China has contributed significantly to our understanding of the top scientific question, i.e., the co-evolution and interplay of life and environments on the early Earth and its many sub-directions. There are two major advantages to conducting research on Precambrian sedimentology in China. First, China has vast, high-quality exposures of Paleoproterozoic to early Cambrian strata (~2.3-0.5 Ga) in North China, South China and the Tarim region (northwestern China). Second, extensive works have already been conducted on the basic geology of these strata (e.g., paleogeography, stratigraphy, paleontology, geochronology, etc.) in recent decades (*see representative reviews by Wang and Li, 2003; Wang et al., 2015; Zhu et al., 2007; Zhu, 2010; Shu et al., 2014; Xiao et al., 2014; and references therein*). Two areas of research are particularly significant among these extensive works. Firstly, a series of paleontological discoveries in the Neoproterozoic-Cambrian strata of South China have reshaped our understanding of the early evolution of morphologically complex multicellular eukaryotes, including macroscopic algae and animals (*e.g., Yin et al., 2007; Yuan et al., 2011; Shu et al., 2014; Xiao et al., 2014; Yin et al., 2015; Han et al., 2017*), and fostered many national and international research projects exploring the relationship between early metazoans and their environments (*e.g., McFadden et al., 2008; Li et al., 2010a, 2015c, 2017a; Sahoo et al., 2012; Zhang and Cui, 2016*). Secondly, a series of zircon U-Pb ages provides the basis for a high-resolution chronostratigraphic framework of Proterozoic strata in the Yan-Liao Aulacogen, North China Craton (Fig. 4-6), which suggests a middle Mesoproterozoic age (~1.7-1.3 Ga) for Proterozoic strata in North China [*see reviews of Qiao et al. (2014) and Su (2016)*] in contrast to a Neoproterozoic age (<0.9) Ga for Proterozoic strata in South China [*see review by Zhu et al. (2016b)*]. These works provide a solid base for our broader understanding of the evolving oceans, atmosphere, and life during the mid-to-late Precambrian and will continue to do so for decades to come.

As indicated above, however, there is a stratigraphic gap between South China and North China Proterozoic strata (~1.3 to ~0.9 Ga). Recent geochronological and paleontological studies have shown that this age gap can be filled by the ~1.4-1.1 Ga Shengnongjia and Macaoyun Groups in the Shengnongjia area (western Hubei Province; Fig. 4-7; *Li et al., 2013a*) in combination with the ~1.0-0.9 Ga Huainan and Feishui Groups in the Huainan area (Anhui Province; *Tang et al., 2013*). These newly identified Proterozoic strata thus enhance the opportunity for studies in China of the long-term continuous coevolution and interplay of the continents, oceans, atmosphere, and life throughout the Proterozoic. We note that new opportunities for future development of Precambrian sedimentology in China also come from the increasing funding supplied recently by the Chinese government, which has allowed launching of larger, more comprehensive projects such as the Deep Earth and Deep Time Detection Projects.

In terms of future strategy, we propose the following critical targets for future research of Precambrian sedimentology in China based on the advantages and opportunities in China, as well as on the progress made in Precambrian sedimentology during the past decades:

(1) Assembly and breakup of supercontinents and formation and evolution of sedimentary basins

1.1 Assembly and breakup of supercontinents Nuna (Columbia) and Rodinia.

1.2 Formation and evolution of Chinese sedimentary basins in the context of assembly and breakup of supercontinents.

1.3 Environmental (atmosphere, ocean, biogeochemical elemental cycles, etc.) and biological effects of supercontinent assembly and breakup.

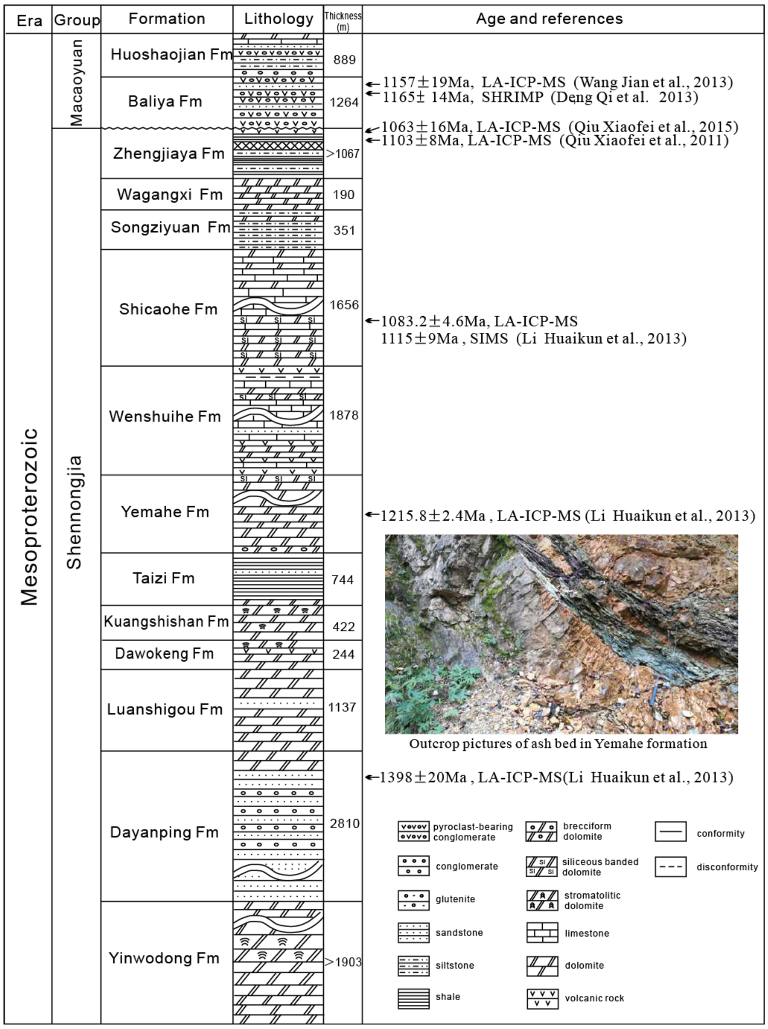

Fig. 4-7. ▲
Mesoproterozoic chronostratigraphic framework and key zircon U-Pb ages reported for Shengnongjia area, South China Craton. Modified from Li et al. (2013a).

(2) Coevolution and interplay between life and environments

2.1 The origin of life and its atmospheric and oceanic backdrops.

2.2 Origin, evolution and interplay of eukaryotes with atmospheric and oceanic environments in Mesoproterozoic.

2.3 Origin, evolution and interplay of animals with atmospheric and oceanic environments in Neoproterozoic.

2.4 Microbial roles in the formation of critical sedimentary rock types (e.g., iron formations, dolomites, etc.).

(3) Formation of mineral and energy resources in Precambrian

3.1 Neoproterozoic black shale system and shale gas in South China.

3.2 Mesoproterozoic oil-gas resources and reservoir evaluation in North China.

3.3 Proterozoic oil-gas resources and reservoir evaluation in Tarim region of northwestern China.

3.4 Geomicrobial roles in Precambrian oil-gas systems.

3.5 Formation of key mineral resources in Precambrian

4. Requirements to make progress

To make substantial progress or breakthroughs toward these targets, requirements include but are not limited to: (1) new ideas and bold innovations (new scientific questions, new models, new hypotheses, new theories etc.); (2) new proxies and methods (e.g., better age dating techniques such as Re/Os dating of organic-rich shales for high-resolution geochronology) and quantitative modeling methods (e.g., biogeochemical modeling of pO_2, modern simulations, etc.); and (3) increased openness and inclusiveness of the Precambrian sedimentological research community. Needed in the future is a new generation of extensive, collaborative, integrated research within and beyond China that involves sedimentology, stratigraphy, biogeochemistry, paleontology, geomicrobiology, geochronology, paleogeography, and tectonics. Additionally, international collaboration will remain a vital part of this mix. These studies will continue to benefit from decades of fundamental geologic research in key regions chosen for their well-preserved strata spanning essential intervals of Earth history. Through it all, the integrated perspective of Precambrian history captured in Chinese Precambrian sedimentary rocks, as revealed by world-class scientific teams, will remain among the most important windows to Earth's remarkable early history.

References

An, Z., Wu, G., Li, J., Sun, Y., Liu, Y., Zhou, W., Cai, Y., Aharon, P., 2005. Redox stratification and anoxia of the early Precambrian oceans: Implications for carbon isotope excursions and oxidation events. Precambrian Research 137, 207-222.

Anbar, A.D., Duan, Y., Lyons, T.W., Arnold, G.L., Kendall, B., Creaser, R.A., Kaufman, A.J., Gordon, G.W., Scott, C., Garvin, J., 2007. A whiff of oxygen before the great oxidation event? Science 317, 1903-1906.

Anbar, A.D., Knoll, A.H., 2002. Proterozoic ocean chemistry and evolution: a bioinorganic bridge? Science 297, 1137-1142.

Arnold, G.L., Anbar, A.D., Barling, J., Lyons, T.W., 2004. Molybdenum isotope evidence for widespread anoxia in mid-Proterozoic oceans. Science 304, 87-90.

Baker, A.J. and Fallick, A. E., 1989a. Evidence from Lewisian limestone for isotopically heavy carbon in two-thousand-million-year-old sea water. Nature, 337, 352-354.

Baker, A.J. and Fallick, A. E., 1989b. Heavy carbon in two-thousand-million-year-old marbles from Lofoten-Vesteralen, Norway: Implications for the Precambrian carbon cycle. Geochimica et Cosmochimica Acta, 53, 1111-1115.

Bekker, A., Holland, H.D., 2012. Oxygen overshoot and recovery during the early Paleoproterozoic. Earth and Planetary Science Letters 317-318, 295-304.

Bekker, A., Holland, H.,D., Wang, P.L., Rumble, D., Stein, H.J., Hannah, J.L., Coetzee L. L., Beukes N. J., 2004. Dating the rise of atmospheric oxygen. Nature, 427, 117-120.

Bekker A., Holmden C., Beukes N. J., Kenig F., Eglinton B., Patterson W. P., 2008. Fractionation between inorganic and organic carbon during the Lomagundi (2.22-2.1 Ga) carbon isotope excursion. Earth and Planetary Science Letters, 271, 278-291.

Bekker A., Slack J. F., Planavsky N., Krapež B., Hofmann A., Konhauser K. O., Rouxel, O. J., 2010. Iron formation: the sedimentary product of a complex interplay among mantle, tectonic, oceanic, and biospheric processes. Economic Geology, 105, 467-508.

Bell E. A., Boehnke P., Harrison T. M., Mao W. L., 2015. Potentially biogenic carbon preserved in a 4.1 billion-year-old zircon. Proceedings of the National Academy of Sciences, 112, 14518-14521.

Blake R. E., Chang S. J., Lepland A., 2010. Phosphate oxygen isotopic evidence for a temperate and biologically active Archaean ocean. Nature, 464, 1029-1033.

Bottjer D. J., Hagadorn J. W., Dornbos S. Q., 2000. The Cambrian substrate revolution. GSA Today, 10, 1-7.

Bowring S., Maow P., Landing E., Ramezani J., Grotzinger J., 2003. Geochronological constraints on terminal Neoproterozoic events and the rise of metazoan. Regulat Toxicol Pharmacol, 25: 60-67.

Bradley D. C., 2008. Passive margins through earth history. Earth-Science Reviews, 91, 1-26.

Bristow, T., Kennedy, M. J., 2008. Carbon isotope excursions and the oxidant budget of the Ediacaran atmosphere and ocean. Geology, 36, 863-866.

Busigny, V., Lebeau, O., Ader, M., Krapež, B., Bekker, A., 2013. Nitrogen cycle in the Late Archean ferruginous ocean. Chemical Geology 362, 115-130.

Butterfield N. J., 2000. Bangiomorpha pubescens n. gen., n.sp.: Implications for the evolution of sex, multicellularity, and the Mesoproterozoic-Neoproterozoic radiation of eukaryotes. Paleobiology, 26, 386-404.

Butterfield N. J., 2015. Early evolution of the Eukaryota. Palaeontology 58, 5-17.

Campbell I. H., Allen C. M., 2008. Formation of supercontinents linked to increases in atmospheric oxygen. Nature Geoscience, 1, 554-558.

Canfield D. E., 1998. A new model for Proterozoic ocean chemistry. Nature, 396, 450-453.

Canfield D. E., Poulton S. W., Knoll A. H., Narbonne G. M., Ross G., Goldberg T., Strauss H., 2008. Ferruginous conditions dominated later Neoproterozoic deep-water chemistry. Science, 321, 949-952.

Canfield D. E., Poulton S. W., Narbonne G. M., 2007. Late-Neoproterozoic deep-ocean oxygenation and the rise of animal life. Science, 315(5808), 92-95.

Canfield D.E., 2005. The early history of atmospheric oxygen. Annual Review Earth Planetary Science, 33, 1-36.

Canfield D.E., Farquhar J., Zerkle A.L., 2010. High isotope fractionations during sulfate reduction in a low-sulfate euxinic ocean analog. Geology, 38, 415-418.

Chen X., Ling H. F., Vance D., Shields-Zhou G. A., Zhu M., Poulton S. W., Och L. M., Jiang S., Li D., Cremonese L. Archer C., 2015. Rise to modern levels of ocean oxygenation coincided with the Cambrian radiation of animals. Nature Communications, 6, Article number: 7142.

Crowe S. A., Døssing L. N., Beukes N. J., Bau M., Kruger S. J., Frei R., Canfield D. E., 2013. Atmospheric oxygenation three billion years ago. Nature, 501, 535-539.

Crowe S. A., Paris G., Katsev S., Jones C., Kim S.-T., Zerkle A. L., Nomosatryo S., Fowle D. A., Adkins J. F., Sessions A. L., Farquhar J., Canfield D. E., 2014. Sulfate was a trace constituent of Archean seawater. Science, 346, 735-739.

Cui H., Kaufman A. J., Xiao S., Zhou C., Liu X. M., 2017. Was the Ediacaran Shuram Excursion a globally synchronized early diagenetic event? Insights from methane-derived authigenic carbonates in the uppermost Doushantuo Formation, South China. Chemical Geology, 450, 59-80.

Dalziel I. W. D., 1991. Pacific margins of Laurentia and East Antarctica-Australia as a conjugate rift pair: Evidence and implications for an Eocambrian supercontinent. Geology, 19, 598-601.

Deng Q., Wang J., Wang Z J., Qiu Y S., Yang W. X., Jiang X. S., Du Q. S., 2013. New evidence for the age of the Macaoyuan Group on the northern margin of the Yangtze block, South China- implications for stratigraphic correlation and palaeogeographic framework. Geological Bulletin of China, 2, 631-638.

Derry L. A., 2010. A burial diagenesis origin for the Ediacaran Shuram–Wonoka carbon isotope anomaly. Earth and Planetary Science Letters, 294, 152-162.

Dong J., Zhang S., Jiang G., Li H., Gao R., 2013. Greigite from carbonate concretions of the Ediacaran Doushantuo Formation in South China and its environmental implications. Precambrian Research, 225, 77-85.

Ducklow H., McCallister S. L., 2004. The biogeochemistry of carbon dioxide in the coastal oceans. In: Robinson, A.R., Brink, K. (Eds.), The Global Coastal Ocean-Multiscale Interdisciplinary Processes: The Sea. Harvard University Press, Cambridge, Massachusetts, pp. 269-315.

Eriksson P. G., Schieber J., Bouougri E., 2007. Classification of structures left by microbial mats in their host sediments, in: Schieber, J., Bose, P.K., Eriksson, P.G. (Eds.), Atlas of microbial mat features preserved within the clastic rock records. Elsevier, Amsterdam, pp. 39-52.

Ernst R., Bleeker W., 2010. Large igneous provinces (LIPs), giant dyke swarms, and mantle plumes: Significance for breakup events within Canada and adjacent regions from 2.5 Ga to the Present. Canadian Journal of Earth Sciences, 47, 695–739.

Evans D. A. D., Li Z.-X., Murphy J. B., 2016. Four-dimensional context of Earth's supercontinents. In: Li, Z. X., Evans, D. A. D. & Murphy, J. B. (eds) Supercontinent Cycles Through Earth History. Geological Society, London, Special Publications, 424, http://doi.org/10.1144/SP424.12.

Farquhar J., Bao H. M., Thiemens M., 2000. Atmospheric influence of earth's earliest sulfur cycle. Science, 289, 756-758.

Feng L. J., Li C., Huang J., Chang H. J., Chu X. L., 2014. A sulfate control on marine mid-depth euxinia on the early Cambrian (ca. 529–521 Ma) Yangtze platform, South China. Precambrian Research, 246, 123-133.

Fike D. A., Grotzinger J. P., Pratt L. M., Summons R. E., 2006. Oxidation of the Ediacaran Ocean. Nature, 444, 744-747.

Fischer W. W., Hemp J., Johnson J. E., 2016. Evolution of Oxygenic Photosynthesis. Annual Review of Earth and Planetary Sciences, 44, 647-683.

Frei R., Gaucher C., Poulton S. W., Canfield D. E., 2009. Fluctuations in Precambrian atmospheric oxygenation recorded by chromium isotopes. Nature, 461, 250-253.

Fru E. C., Rodriguez N. P., Partin C. A., Lalonde S. V., Anderson P., Weiss D. J., EI Albani A.,Rodushkin I., Konhauser K. O., 2016. Cu isotopes in marine black shales record the Great Oxidation Event. Proceedings of the National Academy of Sciences, 113(18), 4941-4946.

Gao L. Z., Zhang C. H., Liu P. J., Ding X. Z., Wang Z. Q., Zhang Y. J., 2009. Recognition of Meso- and Neoproterozoic stratigraphie framework in North and South China. Acta Geoscientica Sinica, 30, 433-446.

Gao L. Z., Zhang C. H., Shi X. Y., Song B., Wang Z. Q., Liu Y. M., 2008. Mesoproterozoic age for Xiamaling Formation in North China Plate indicated by zircon SHRIMP dating. Chinese Science Bulletin, 2008, 53, 2617-2623.

Gao L. Z., Zhang C. H., Shi X. Y., Zhou H. R., Wang Z. Q., 2007. Zircon SHRIMP U-Pb dating of the tuff bed in the Xiamaling Formation of the Qingbaikouan System in North China. Geological Bulletin of China, 26, 249-255.

Gao W., Zhang C. H., Gao L. Z., Shi X. Y., Liu Y. M., Song B., 2008. Zircon SHRIMP U- Pb age of rapakivi granite in Miyun, Beijing, China, and its tectono- stratigraphic implications. Geological Bulletin of China, 27, 793-798

Gerdes G., Klenke T., Noffke N., 2000. Microbial signatures in peritidal siliciclastic sediments: a catalogue. Sedimentology, 47, 279-308.

Guilbaudet R., Poulton S. W., Butterfield N. J., Zhu M., Shields-Zhou G. A., 2015. A global transition to ferruginous conditions in the early Neoproterozoic oceans. Nature Geoscience, 8, 466-470.

Gumsley A. P., Chamberlain K. R., Bleeker W., Soderlund U., De Kock M. O., Larsson E. R., Bekker A., 2017. Timing and tempo of the Great Oxidation Event. Proc. Natl. Acad. Sci. USA, 114, 1811-1816.

Guo Q. J., Strauss H., Kaufman A. J., Schroder S., Gutzmer J., Wing B., Baker M. A., Bekker A., Jin Q. S., Kim S. T., Farquhar J., 2009. Reconstructing earth's surface oxidation across the Archean-Proterozoic transition. Geology, 37, 399-402.

Habicht K. S., Gade M., Thamdrup B., Berg P., Canfield D. E., 2002, Calibration of sulfate levels in the Archean Ocean. Science, 298, 2372–2374.

Han J., Morris S. C., Ou Q., Shu D., Huang, H., 2017. Meiofaunal deuterostomes from the basal Cambrian of Shaanxi (China). Nature, 542(7640), 228-231.

Hannah J. L., Bekker A., Stein H. J., Markey R. J., Holland H. D., 2004. Primitive Os and 2316 Ma age for marine shale: implications for Paleoproterozoic glacial events and the rise of atmospheric oxygen. Earth and Planetary Science Letters, 225, 43-52.

Haqq-Misra J. D., Domagal-Goldman S. D., Kasting P. J., Kasting J. F., 2008. A revised, hazy methane greenhouse for the Archean Earth. Astrobiology, 8, 1127-1141.

Hayes J. M., Waldbauer J. R., 2006. The carbon cycle and associated redox processes through time. Phil. Trans. R. Soc. B, 361, 931-950.

He Z. J., Niu B. G., Zhang X. Y., Zhao L., Liu R. Y., 2011a. Discovery of the paleo-weathered mantle of the rapakivi granite covered by the Proterozoic Changzhougou Formation in the Miyun area, Beijing and their detrital zircon dating. Geological Bulletin of China, 30, 798-802

He Z. J., Zhang X. Y., Niu B. G., Liu R. Y., 2011b. The paleo-weathering mantle of the Proterozoic rapakivi granite in Miyun County, Beijing and the relationship with the Changzhougou Formation of Changchengian System. Earth Science Frontiers, 18, 123-130

Hoffman P. F., Kaufman A. J., Halverson G. P., Schrag D. P., 1998. A Neoproterozoic snowball earth. Science, 281, 1342-1346.

Hoffman, P. F., 1991. Did the breakout of Laurentia turn Gondwanaland inside-out? Science, 252, 1409-1412.

Hoffman, P. F., 1997. Tectonic genealogy of North America. In: Van der Pluijm, B.A. & Marshak, S. (eds) Earth Structure: An Introduction to Structural Geology and Tectonics, McGraw-Hill, New York, 459-464.

Holland H. D., 1978. The chemistry of the atmosphere and oceans. Wiley-Interscience, New York.

Holland H. D., 1984. The chemical evolution of the atmosphere and oceans. Princeton, NJ: Princeton University Press, p. 582.

Holland H. D., 2006. The oxygenation of the atmosphere and oceans. Philosophical Transactions of the Royal Society B: Biological Sciences, 361(1470), 903 - 915.

Hren M. T., Tice M. M., Chamberlain C. P., 2009. Oxygen and hydrogen isotope evidence for a temperate climate 3.42 billion years ago. Nature, 462, 205-208.

Javaux E. J., Marshall C. P., Bekker A., 2010. Organic-walled microfossils in 3.2-billion-year-old shallow-marine siliciclastic deposits. Nature, 463, 934-939.

Jiang G. Q., Kennedy M. J., Christie-Blick N., 2003. Stable isotopic evidence for methane seeps in Neoproterozoic postglacial cap carbonates. Nature, 426, 822-826.

Jin C., Li C., Algeo T. J., Planavsky N. J., Cui H., Yang X., Zhao Y., Zhang X., Xie S., 2016. A highly redox-heterogeneous ocean in South China during the early Cambrian (~529-514 Ma): Implications for biota-environment co-evolution. Earth and Planetary Science Letters, 441, 38-51.

Johnson J. E., Webb S. M., Thomas K., Ono S., Kirschvink J. L., Fischer W. W., 2013. Manganese-oxidizing photosynthesis before the rise of cyanobacteria. Proceedings of the National Academy of Sciences, 110, 11238-11243.

Kah L. C., Bartley J. K., Teal D. A., 2012. Chemostratigraphy of the Late Mesoproterozoic Atar Group, Taoudeni Basin, Mauritania: Muted isotopic variability, facies correlation, and global isotopic trends. Precambrian Research, 200-203, 82-103.

Kah L.C., Lyons T.W., Frank T.D., 2004. Low marine sulphate and protracted oxy-genation of the proterozoic biosphere. Nature 431, 834-838.

Karhu J. A., Holland H. D., 1996. Carbon isotopes and the rise of atmospheric oxygen. Geology, 24, 867-870.

Kasting J. F., Howard M. T., 2006. Atmospheric composition and climate on the early Earth. Philosophical Transactions of the Royal Society B: Biological Sciences, 361, 1733-1742.

Kaufman A. J., Corsetti F. A., Varni M. A., 2007. The effect of rising atmospheric oxygen on carbon and sulfur isotope anomalies in the Neoproterozoic Johnnie Formation, Death Valley, USA. Chemical Geology, 237, 47-63.

Keith M. L., 1982. Violent volcanism, stagnanat oceans and some inferences regarding petroleum, strata-bound ores and mass extinctions. Geochemica et Cosmochimica Acta, 46, 2621-2637.

Kirschvink J. L., Gaidos E. J., Bertani L. E., Beukes N. J., Gutzmer J., Maepa L. N., Steinberger R. E., 2000. Paleoproterozoic snowball earth: Extreme climatic and geochemical global change and its biological consequences. Proc. Natl. Acad. Sci. USA, 97, 1400-1405.

Kirschvink J. L., Kopp R. E., 2008. Palaeoproterozoic ice houses and the evolution of oxygen-mediating enzymes: the case for a late origin of photosystem II. Philosophical Transactions of the Royal Society B: Biological Sciences, 363(1504), 2755-2765.

Klein C., 2005. Some Precambrian banded iron-formations (BIFs) from around the world: Their age, geologic setting, mineralogy, metamorphism, geochemistry, and origins. American Mineralogist, 90, 1473-1499.

Knauth L. P., Kennedy M. J., 2009. The late Precambrian greening of the Earth. Nature, 460, 728-732.

Knauth L. P., Lowe D. R., 2003. High Archean climatic temperature inferred from oxygen isotope geochemistry of cherts in the 3.5 Ga Swaziland Supergroup, South Africa. Geological Society of America Bulletin, 115, 566-580.

Konhauser K. O., Amskold L., Lalonde S. V., Posth N. R., Kappler A., Anbar A. 2007. Decoupling photochemical Fe (II) oxidation from shallow-water BIF deposition. Earth and Planetary Science Letters, 258, 87-100.

Konhauser K. O., Pecoits E., Lalonde S. V., Papineau D., Nisbet E. G., Barley M. E., Arndt N. T., Zahnle K., Kamber B. S., 2009. Oceanic nickel depletion and a methanogen famine before the Great Oxidation Event. Nature, 458, 750-754.

Kopp R. E., Kirschvink J. L., Hiburn I. A., Nash C. Z., 2005. The Paleoproterozoic snowball earth: A climate disaster triggered by the evolution of oxygenic photosynthesis. Proc. Natl. Acad. Sci. USA, 102, 11131-11136.

Kump L. R., 2008. The rise of atmospheric oxygen. Nature, 451, 277-278.

Kump L. R., Barley M. E., 2007. Increased subaerial volcanism and the rise of atmospheric oxygen 2.5 billion years ago. Nature, 448, 1033-1036.

Kump L. R., Junium C., Arthur M.A., Brasier A., Fallick A., Melezhik V., Lepland A., Črne A. E., Luo G., 2011. Isotopic evidence for massive oxidation of organic matter following the great oxidation event. Science, 334, 1694-1696.

Lee C., Love G. D., Fischer W. W., Grotzinger J. P., Halverson G. P., 2015. Marine organic matter cycling during the Ediacaran Shuram excursion. Geology, 43, 1103-1106.

Lee Cin-Ty A., Yeung L. Y., McKenzie N. R., Yokoyama Y., Ozaki K., Lenardic A., 2016. Two-step rise of atmospheric oxygen linked to the growth of continents. Nature Geoscience, 9, 417-424.

Li C., Cheng M., Algeo T.J., Xie S., 2015b. A theoretical prediction of chemical zonation in early oceans (>520 Ma). Science China Earth Sciences, 58, 1901-1909.

Li C., Hardisty D., Luo G., Huang J., Algeo T. J., Cheng M., Shi W., An Z., Tong J., Xie S., Jiao N., Lyons T. W., 2017b. Uncovering the spatial heterogeneity of Ediacaran carbon cycling. Geobiology, 15:211-224.

Li C., Jin C., Planavsky N. J., Algeo T. J., Cheng M., Yang X., Zhao Y., Xie S. 2017a. Coupled oceanic oxygenation and metazoan diversification during the early–middle Cambrian? Geology, 2017a, 45: 743-746.

Li C., Love G. D., Lyons T. W., Fike D. A., Sessions A. L., Chu X., 2010a. A stratified redox model for the ediacaran ocean. Science, 328 (5974), 80-83.

Li C., Peng P., Sheng G., Fu J., Yan Y., 2003. A molecular and isotopic geochemical study of Meso- to Neoproterozoic (1.73-0.85 Ga) sediments from the Jixian section, Yanshan Basin, North China. Precambrian Research, 125, 337-356.

Li C., Planavsky N. J., Love G. D., Reinhard C. T., Hardisty D., Feng L., Bate S. M., Huang J., Zhang Q., Chu X., Lyons T. W., 2015a. Marine redox conditions in the middle Proterozoic ocean and isotopic constraints on authigenic carbonate formation: Insights from the Chuanlinggou Formation, Yanshan Basin, North China. Geochimica et Cosmochimica Acta, 2015a, 150, 90-105.

Li C., Planavsky N. J., Shi W., Zhang Z., Zhou C., Cheng M., Tarhan L. G., Luo G., Xie S.,2015c. Ediacaran Marine Redox Heterogeneity and Early Animal Ecosystems. Scientific Reports, 5, Article number: 17097.

Li C., Zhu M., Chu X., 2016. Atmospheric and Oceanic Oxygenation and evolution of early life on Earth: New contributions from China. Journal of Earth Science, 2016, 27, 167-169.

Li H. K., Lu S. N., Li H. M., Sun L. X., Xiang Z. Q., Geng J. Z., Zhou H. Y., 2009. Zircon and beddeleyite U-Pb precision dating of basic rock sills intruding Xiamaling Formation, North China. Geological Bulletin of China, 28,1396-1404.

Li H. K., Zhang C. L., Xiang Z. Q., Lu S. N., Zhang J., Geng J. Z., Qu L. S., Wang Z. X., 2013a. Zircon and baddeleyite U-Pb geochronology of the Shennongjia Group in the Yangtze Craton and its tectonic significance. Acta Petrologica Sinica, 29, 673-697.

Li H. K., Zhu S. X., Xiang Z. Q., Su W. B., Lu S. N., Zhou H. Y., Geng J. Z., Li S., Yang F. J., 2010. Zircon U-Pb dating on tuff bed from Gaoyuzhuang Formation in Yanqing, Beijing: Further constraints on the new subdivision of the Mesoproterozoic stratigraphy in the northern North China Craton. Acta Petrologica Sinica, 26, 2131-2140.

Li Z. X., Bogdanova S. V., Collins A. S., Davidson A., De Waele B., Ernst R. E., Fitzsimons I. C. W., Fuck R. A., Gladkochub D. P., Jacobs J., Karlstrom K. E., Lu S., Natapov L. M., Pease V., Pisarevsky S. A., Thrane K., Vernikovsky V., 2008. Assembly, configuration, and break-up history of Rodinia: a synthesis. Precambrian Research, 160, 179-210.

Li Z. X., Evans D. A. D., 2011. Late Neoproterozoic 40° intraplate rotation within Australia allows for a tighter-fitting and longer-lasting Rodinia. Geology, 39, 39-42.

Li Z. X., Evans D. A. D., Halverson G. P., 2013b. Neoproterozoic glaciations in a revised global palaeogeography from the breakup of Rodinia to the assembly of Gondwanaland: Sedimentary Geology, 294, 219-232.

Li Z. X., Zhong S. 2009. Supercontinent-superplume coupling, true polar wander and plume mobility: plate dominance in whole-mantle tectonics. Physics of Earth and Planetary Interiors, 176, 143-156.

Love G. D., Grosjean E., Stalvies C., Fike D. A., Grotzinger J. P., Brandley A. S., Kelly A. E., Bhatia M., Meredith W., Snape C. E., Bowring S. A., Condon D. J., Summons R. E., 2009.Fossil steroids record the appearance of Demospongiae during the Cryogenian period. Nature, 457, 718-721.

Lu S., Zhao G., Wang H., Hao G., 2008. Precambrian metamorphic basement and sedimentary cover of the North China Craton: A review. Precambrian Research, 160:77-93.

Luo G. M., Ono S., Beukes N., Wang D. T., Xie S. C., Summons R. E., 2016. Rapid oxygenation of Earth's atmosphere 2.33 billion years ago. Science Advances, 2, e1600134.

Luo G. M., Ono S., Huang J., Algeo T. J., Li C., Zhou L., Robinson A., Lyons T. W., Xie S., 2015. Decline in oceanic sulfate levels during the early Mesoproterozoic. Precambrian Research, 258, 36-47.

Lyons T. W., Fike D. A., Zerkle A., 2015. Emerging Biogeochemical Views of Earth9s Ancient Microbial Worlds. Elements, 11, 415-421.

Lyons T. W., Reinhard C. T., Planavsky N. J., 2014. The rise of oxygen in Earth’s early ocean and atmosphere. Nature, 506(7488), 307-315.

Macdonald F. A., Schmitz M. D., Crowley J. W., Roots C. F., Jones D. S., Maloof A. C., Strauss J. V., Cohen P. A., Johnston D. T., Schrag D. P., 2010. Calibrating the Cryogenian. Science, 327, 1241-1243.

Martin A. P., Condon D. J., Prave A. R., Lepland A., 2013. A review of temporal constraints for the Palaeoproterozoic large, positive carbonate carbon isotope excursion (the Lomagundi-Jatuli Event). Earth-Science Reviews, 127, 242-261.

McFadden, K. A., Huang, J., Chu, X. L., Jiang, G. Q., Kaufman, A. J., Zhou, C. M., Yuan, X. L., Xiao, S. H., 2008. Pulsed oxidation and biological evolution in the Ediacaran Doushantuo Formation. Proceedings of the National Academy of Sciences of the United States of America, 105, 3197-3202.

Melezhik V. A., Huhma H., Condon D. J., Fallick A. E., Whitehouse M. J., 2007. Temporal constraints on the Paleoproterozoic Lomagundi-Jatuli carbon isotopic event. Geology, 35, 655-658.

Moores E. M., 1991. Southwest US–East Antarctic (SWEAT) connection: A hypothesis, Geology, 19, 425-428.

Müller S. G., Krapež B., Barley M. E., Fletcher I. R., 2005. Giant iron-ore deposits of the Hamersley province related to the breakup of Paleoproterozoic Australia: New insights from in situ SHRIMP dating of baddeleyite from mafic intrusions. Geology, 33, 577-580.

Noffke N., Gerdes G., Klenke T., Krumbein W. E., 2001. Microbially Induced Sedimentary Structures--A

New Category within the Classification of Primary Sedimentary Structures: Perspectives. Journal of Sedimentary Research, Section A: Sedimentary Petrology and Processes, 71, 649-656.

Nutman A. P., Bennett V. C., Friend C. R. L., Van Kranendonk M. J., Chivas A. R., 2016. Rapid emergence of life shown by discovery of 3,700-million-year-old microbial structures. Nature, 537, 535-538.

Olson, S.L., Reinhard, C.T., Lyons, T.W., 2016. Limited role for methane in the mid-Proterozoic greenhouse. Proceedings of the National Academy of Sciences 113, 11447-11452.

Papineau D., Purohit R., Fogel M.L., Shields-Zhou G. A., 2013. High phosphate availability as a possible cause for massive cyanobacterial production of oxygen in the Paleoproterozoic atmosphere. Earth and Planetary Science Letters, 362, 225-236.

Partin C. A., Bekker A., Planavsky N. J., Scott C. T., Gill B. C., Li C., Podkovyrov V., Maslov A. V., Konhauser K. O., Lalonde S. V., Love G. D., Poulton S. W., Lyons T. W., 2013. Large-scale fluctuations in Precambrian atmospheric and oceanic oxygen levels from the record of U in shales. Earth and Planetary Science Letters, 369-370, 284-293.

Pavlov, A.A., Hurtgen, M., Kasting, J.F., Arthur, M.A., 2003. Methane-rich Proterozoic atmosphere? Geology 31, 87-90.

Pehrsson S. J., Eglington B. M., Evans D. A. D., Huston D., Reddy S. M., 2015. Metallogeny and its link to orogenic style during the Nuna supercontinent cycle. In: Li Z. X., Evans D. A. D., Murphy J. B. (eds) Supercontinent Cycles through Earth History. Geological Society, London, Special Publications, 424. First published online July 1, 2015, http://doi.org/10.1144/SP424.5.

Pisarevsky S. A., Elming S. A., Pesonen L. J., Li Z. X., 2014. Mesoproterozoic paleogeography: supercontinent and beyond. Precambrian Research, 244, 207-225.

Planavsky N. J., Asael D., Hofmann A., Reinhard C. T., Lalonde S. V., Knudsen A., Wang X., Ossa Ossa F., Pecoits E., Smith A. J. B., Beukes N. J., Bekker A., Johnson T. M., Konhauser K. O., Lyons T. W., Rouxel O. J., 2014b. Evidence for oxygenic photosynthesis half a billion years before the Great Oxidation Event. Nature Geoscience, 7, 283-286.

Planavsky N. J., Bekker A., Hofmann A., Owens J. D., Lyons T. W., 2012. Sulfur record of rising and falling marine oxygen and sulfate levels during the Lomagundi event. Proceedings of the National Academy of Sciences of the United States of America, 109, 18300-18305.

Planavsky N. J., Cole D. B., Reinhard C. T., Diamond C., Love G. D., Luo G., Zhang S., Konhauser K. O., Lyons T. W., 2016. No evidence for high atmospheric oxygen levels 1,400 million years ago. Proceedings of the National Academy of Sciences, 113, E2550-E2551.

Planavsky N. J., McGoldrick P., Scott C. T., Li C., Reinhard C. T., Kelly A. E., Chu X., Bekker A., Love G. D., Lyons, T. W., 2011. Widespread iron-rich conditions in the mid-Proterozoic ocean. Nature, 477(7365), 448-451.

Planavsky N. J., Reinhard C.T., Wang X., Thomson D., McGoldrick P., Rainbird R. H., Johnson T., Fischer W. W., Lyons T. W., 2014a. Low Mid-Proterozoic atmospheric oxygen levels and the delayed rise of animals. Science, 346(6209), 635-638.

Porada H., Bouougri E. H., 2007. Wrinkle structures—a critical review. Earth-Science Reviews, 81, 199-215.

Posth N. R., Konhauser K. O., Kappler A., 2011. Banded Iron Formations, in: Rietner, J., Thiel, V. (Eds.), Encyclopedia of Geobiology. Springer, Dordrecht, pp. 92-103.

Poulton S. W., Canfield D. E., 2011. Ferruginous conditions: a dominant feature of the ocean through Earth's history. Elements, 7, 107-112.

Poulton S. W., Fralick P. W., Canfield D. E., 2010. Spatial variability in oceanic redox structure 1.8 billion years ago. Nature Geoscience, 3(7), 486-490.

Qiao X. F., Wang Y. B., 2014. Discussions on the lower boundary age of the Mesoproterozoic and basin tectonic evolution of the Mesoproterozoic in North China Craton. Acta Geologica Sinica, 88, 1623-1637.

Qiu X. F., Ling W. L., Liu X. M., Kusky T., Berkana W., Zhang Y. H., Gao Y. J., Lu S. S., Kuang H., Liu C. X., 2011. Recognition of Grenvillian volcanic suite in the Shennongjia region and its tectonic significance for the South China Craton. Precambrian Research, 191, 101-119.

Qiu X. F., Yang H. M., Lu S. S., Ling W. L., Zhang L. G., Tan J. J., Wang Z. X., 2015. Geochronology and geochemistry of Grenville-aged (1063 ± 16 Ma) metabasalts in the Shennongjia district, Yangtze block: implications for tectonic evolution of the South China Craton. International Geology Review, 57, 76-96.

Rämö O. T., Haapala I., Vaasjoki M., Yu J. H., Fu H. Q., 1995. 1700 Ma Shachang complex, northeast China: Proterozoic rapakivi granite not associated with Paleoproterozoic orogenic crust. Geology, 23, 815-818.

Rasmussen B., Buick R., 1999. Redox state of the Archean atmosphere: Evidence from detrital heavy minerals in ca. 3250-2750 Ma sandstones from the Pilbara Craton, Australia. Geology, 27, 115-118.

Reinhard C. T., Planavsky N. J., Olson S. L., Lyons T. W., Erwin D. H., 2016. Earth's oxygen cycle and the evolution of animal life. Proceedings of the National Academy of Sciences of the United States of America 113, 8933-8938.

Reinhard C. T., Planavsky N. J., Robbins L. J., Partin C. A., Gill B. C., Lalonde S. V., Bekker A., Konhauser K. O., Lyons, T. W., 2013. Proterozoic ocean redox and biogeochemical stasis. Proceedings of the National Academy of Sciences, 110, 5357-5362.

Reinhard C. T., Raiswell R., Scott C., Anbar A. D., Lyons T. W., 2009. A late Archean sulfidic sea stimulated by early oxidative weathering of the continents. Science, 326(5953), 713-716.

Robert F., Chaussidon M., 2006. A palaeotemperature curve for the Precambrian oceans based on silicon isotopes in cherts. Nature, 443, 969-972.

Rodriguez-Blanco J. D., Shaw, S., Benning, L. G., 2015. A route for the direct crystallization of dolomite, American Mineralogist, 100, 1172-1181.

Rogers J. J. W., Santosh M., 2002. Configuration of Columbia, a Mesoproterozoic supercontinent. Gondwana Research, 5, 5-22.

Rothman D. H., Hayes J. M., Summons R. E., 2003. Dynamics of the Neoproterozoic carbon cycle. Proceedings of the National Academy of Sciences of the United States of America, 100, 8124-8129.

Rouxel, O.J., Bekker, A., Edwards, K. J., 2005. Iron Isotope Constraints on the Archean and Paleoproterozoic Ocean Redox State. Science, 307, 1088-1091.

Sahoo S. K., Planavsky N. J., Jiang G., Kendall B., Owens J. D., Wang X., Shi X., Anbar, A. D., Lyons T. W., 2016. Oceanic oxygenation events in the anoxic Ediacaran ocean. Geobiology, 14, 457-468.

Sahoo S. K., Planavsky N. J., Kendall B., Wang X., Shi X., Scott C., Anbar A. D., Lyons T. W., Jiang G., 2012. Ocean oxygenation in the wake of the Marinoan glaciation. Nature, 489, 546-549.

Sánchez-Román, M., Vasconcelos, C., Schmid, T., Dittrich, M., McKenzie, J. A., Zenobi, R., Rivadeneyra, M. A., 2008. Aerobic microbial dolomite at the nanometer scale: Implications for the geologic record. Geology, 36, 879-882.

Schieber, J., 2004. Microbial mats in the silisiclastic rock record: a summary of the diagnostic features, in: Eriksson, P.G., Altermann, W., Nelson, D.R. (Eds.), The Precambrian Earth: Tempos and Events. Elsevier, Amsterdam, pp. 663-673.

Schrag D. P., Higgins J. A., Macdonald F. A., Johnston D. T., 2013. Authigenic carbonate and the history of the global carbon cycle. Science, 339, 540-543.

Scott C., Lyons T. W., Bekker A., Shen Y., Poulton S. W., Chu X., Anbar A. D., 2008. Tracing the stepwise oxygenation of the Proterozoic ocean. Nature 452, 456-459.

Scott C., Wing B. A., Bekker A., Planavsky N. J., Medvedev P., Bates S. M., Yun M., Lyons T. W., 2014. Pyrite multiple-sulfur isotope evidence for rapid expansion and contraction of the early Paleoproterozoic seawater sulfate reservoir. Earth and Planetary Science Letters, 389, 95-104.

Shen Y. A., Buick R., Canfield D. E., 2001. Isotopic evidence for microbial sulphate reduction in the early Archaean era. Nature, 410, 77-81.

Shi W., Li C., Luo G., Huang J., Algeo T. J., Jin C., Zhang Z., Cheng M. 2018. Sulfur isotope evidence for transient marine-shelf oxidation during the Ediacaran Shuram Excursion. Geology, in press. DOI:10.1130/G39663.1.

Shu D., Isozaki Y., Zhang X., Han J., Maruyama S., 2014. Birth and early evolution of metazoans. Gondwana Research, 25, 884-895.

Sperling E. A., Wolock C. J., Morgan A. S., Gill B. C., Kunzmann M., Halverson G. P., Macdonald F. A., Knoll A. H., Johnston D. T., 2015. Statistical analysis of iron geochemical data suggests limited Late Proterozoic oxygenation. Nature, 523, 451-454.

Stüeken E. E., Kipp M. A., Koehler M. C., Buick R., 2016. The evolution of Earth's biogeochemical nitrogen cycle. Earth-Science Reviews, 160, 220-239.

Stüeken, E.E., Buick, R., Guy, B.M., Koehler, M.C., 2015. Isotopic evidence for biological nitrogen fixation by molybdenum-nitrogenase from 3.2 Gyr. Nature 520, 666-669.

Su W. B., Li H. K., Huff W. D., Ettensohn F. R., Zhang S. H., Zhou H. Y., 2010. SHRIMP U-Pb dating for a k-bentonite bed in the Tieling Formation, North China. Science Bulletin, 55, 3312-3323.

Su W. B., Revision of the Mesoproteroozic chronostratigraphic subdivision both of North China and Yangtze Cratons and the relevant issues. Earth Science Frontiers, 2016, 23, 156-185.

Su W. B., Zhang S. H., Huff W. D., Li H. K., Ettensohn F. R., Chen X. Y., Yang H. M., Han Y. G., Song B., Santosh M., 2008. SHRIMP U–Pb ages of K-bentonite beds in the Xiamaling Formation: Implications for revised subdivision of the Meso- to Neoproterozoic history of the North China Craton. Gondwana Research, 14, 543-553.

Swanson-Hysell N., Rose C. V., Calmet C. C., Halverson G. P., Hurtgen M. T., Maloof A. C., 2010. Cryogenian glaciation and the onset of carbon isotope decoupling. Science, 328, 608-611.

Swart P. K., Kennedy M. J., 2012. Does the global stratigraphic reproducibility of $\delta^{13}C$ in Neoproterozoic carbonates require a marine origin? A Pliocene–Pleistocene comparison. Geology, 40, 87-90.

Tang Q., Pang K., Xiao S., Yuan X., Ou Z., Wan B., 2013. Organic-walled microfossils from the early Neoproterozoic Liulaobei Formation in the Huainan region of North China and their biostratigraphic significance. Precambrian Research, 236, 157-181.

Tziperman E., Halevy I., Johnston D. T., Knoll A. H., Schrag D. P., 2011. Biologically induced initiation of Neoproterozoic snowball-Earth events. Proceedings of the National Academy of Sciences USA, 108, 15091-15096.

Vasconcelos C., McKenzie J. A., Bernasconi S., Grujic D., Tiens A. J., 1995. Microbial mediation as a possible mechanism for natural dolomite formation at low temperatures. Nature, 377, 220.

Wang J., Deng Q., Wang Z J., Qiu Y. S., Duan T. Z., Jiang X. S., Yang Q. X., 2013. New evidences for sedimentary attributes and timing of the “Macaoyuan conglomerates” on the northern margin of the Yangtze block in southern China. Precambrian Research, 235, 58-70.

Wang J., Li Z. X., 2003. History of Neoproterozoic rift basins in South China: Implications for Rodinia break-up. Precambrian Research, 122, 141-158.

Wang W., Liu S., Santosh M., Deng Z., Guo B., Zhao Y., Zhang S., Yang P., Bai X., Guo, R., 2013. Late Paleoproterozoic geodynamics of the North China Craton: Geochemical and zircon U–Pb–Hf records from a volcanic suite in the Yanliao rift. Gondwana Research, 27, 300-325.

Xiao S. H., Muscente A. D., Chen L., Zhou C. M., Schiffbauer J. D., Wood A. D., Polys N. F., Yuan X. L., 2014. The Weng’an biota and the Ediacaran radiation of multicellular eukaryotes. National Science Review, 1, 498-520.

Yin L., Zhu M., Knoll A. H., Yuan X., Zhang J., Hu J., 2007. Doushantuo embryos preserved inside diapause egg cysts. Nature, 446, 661-663.

Yin Z., Zhu M., Davidson E. H., Bottjer D. J., Zhao F., Tafforeau P., 2015. Sponge grade body fossil with cellular resolution dating 60 Myr before the Cambrian.

Proceedings of the National Academy of Sciences, 112, E1453-E1460.

Young G. M., 2014. Contradictory correlations of Paleoproterozoic glacial deposits: Local,regional or global controls? Precambrian Research, 247, 33-44.

Young G. M., Brunn V. V., Gold D. J. C., Minter W. E. L., 1998. Earth's oldest reported glaciation: Physical and chemical evidence from the Archean Mozaan Group (~2.9 Ga) of South Africa. The Journal of Geology, 106, 523-538.

Yuan X., Chen Z., Xiao S., Zhou C., Hua H., 2011. An early Ediacaran assemblage of macroscopic and morphologically differentiated eukaryotes. Nature, 470, 390393.

Zhang F., Xu H., Shelobolina E. S., Konishi H., Converse B., Shen Z., Roden E. E., 2015. The catalytic effect of bound extracellular polymeric substances excreted by anaerobic microorganisms on Ca-Mg carbonate precipitation: Implications for the “dolomite problem”, American Mineralogist, 100, 483-494.

Zhang K., Zhu X., Wood R. A., Shi Y., Gao Z., Poulton S. W., 2018. Oxygenation of the Mesoproterozoic ocean and the evolution of complex eukaryotes, Nature Geoscience, 11, 345-350.

Zhang S. C., Wang X., Wang H., Bjerrum C. J., Hammarlund E. U., Costa M. M., Connelly J. N., Zhang B., Su J., Canfield D. E., 2016. Sufficient oxygen for animal respiration 1400 million years ago. Proceedings of the National Academy of Sciences of the United States of America. 113, 1731-1736.

Zhang S. H., Li Z. X., Evan D. A. D., Wu H., Li, H., Dong J., 2012. Pre-Rodinia supercontinent Nuna shaping up: a global synthesis with new paleomagnetic results from North China. Earth and Planetary Science Letters, 353-354, 145-155.

Zhang S., Zhao Y., Yang Z., He Z., Wu H., 2009. The 1.35 Ga diabase sills from the northern North China Craton: implications for breakup of the Columbia (Nuna) supercontinent. Earth and Planetary Science Letters, 288, 588- 600.

Zhang X., Cui L., 2016. Oxygen requirements for the Cambrian explosion. Journal of Earth Science, 27, 187-195.

Zhao G., Cawood P. A., Wilde S. A., Sun M., 2002. Review of global 2.1–1.8 Ga orogens: Implications for a pre-Rodinia supercontinent. Earth-Science Reviews, 59, 125-162.

Zhao G., Sun M., Wilde S.A., Li S., 2004. A Paleo-Mesoproterozoic supercontinent: assembly,growth and breakup. Earth-Science Review, 67, 91-123.

Zhelezinskaia I., Kaufman A. J., Farquhar J., Cliff J., 2014. Large sulfur isotope fractionations associated with Neoarchean microbial sulfate reduction. Science, 346, 742-744.

Zhou C. M., Tucker R., Xiao S. H., Peng Z. X., Yuan X. L., Chen Z., 2004. New constraints on the ages of Neoproterozoic glaciations in South China. Geology, 32, 437-440.

Zhu M. Y., 2010. The origin and Cambrian explosion of animals: fossil evidence from China. Acta Palaeontologica Sinica, 49(3), 269-287 (in Chinese with English abstract).

Zhu M., Zhang J., Yang A., Li G., Zhao F., Lu M., Yin Z., 2016b. Stratigraphic and depositional frameworks of the Neoproterozoic source-reservior-cap rock associations in South China. In: Sun S. and Wang T. (Eds.), Geology and Hydrocarbon resources of the middle-upper Proterozoic in East China. Science Press, Beijing, pp.107-135.

Zhu M., Zhang J., Yang, A., 2007. Integrated Ediacaran (Sinian) chronostratigraphy of South China. Palaeogeography, Palaeoclimatology, Palaeoecology, 254, 7-61.

Zhu S., Zhu M., Knoll A. H., Yin Z., Zhao F., Sun S., Qu Y., Shi M., Liu H., 2016a. Decimetre-scale multicellular eukaryotes from the 1.56-billion-year-old Gaoyuzhuang Formation in North China. Nature Communications, 7, 11500.

Chapter 5.

Facilities and labs

Yanan Shen[1], Zhifei Liu[2], Cheng Quan[3], Yuan Gao[4], Tiantian Wang[4], Laiming Zhang[4]

[1] **University of Science and Technology of China, Hefei 230026, China**

[2] **Tongji University, Shanghai 200092, China**

[3] **Chang'an University, Xi'an 710064, China**

[4] **China University of Geosciences (Beijing), 100083 Beijing, China**

Paleoenvironmental change in space and time has been, and will be, one of the frontier topics in Earth Sciences (*Stanley and Luczaj, 2014*). The geochemical record of sedimentary rocks reveals important information about biogeochemical processes and evolution of the paleoenvironment. Recent technological or methodological innovations offer exciting opportunities for significant advances in the analysis and interpretation of geochemical records in sedimentary rocks, enabling a better understanding of paleoenvironmental changes (*Eiler et al., 2014*). In particular, sediment cores, acquired by continental drilling, document the most continuous and complete geological and geochemical records. With such long and continuous sedimentary records recovered in well-preserved drill cores, a high-resolution chronostratigraphic framework can be established, and multiple paleoenvironmental proxies can be used to reconstruct climate change throughout Earth's history.

Geochronology provides a temporal framework for geological events, which is critical to constrain the timing of paleoenvironmental changes. Carbonate clumped isotope thermometry is a relatively new paleotemperature proxy (*Eiler, 2011*), which has several properties that supplement existing methods of paleoclimate reconstruction. Multiple-S isotopes in sedimentary sulfate and pyrite provide important constraints on the biogeochemical sulfur cycle and offer new insights into mass extinctions in the geological past (cf. *Shen et al., 2011*). In addition to multiple isotope measurements, numerical modelling provides a vital tool for quantitative interpretations and predictions of geological events. Therefore, the integration of these research methods and techniques will open up new directions for studying paleoenvironmental changes in space and time.

1.Continental drilling

Continental drilling to acquire long and continuous sediment cores is essential to document regional atmospheric, hydrologic, and climatic changes at different spatial and temporal scales in geologic time, providing a record that is important to resolve climate dynamics relevant to both climate modeling and the societal impact of climate change. Promoted by the International Continental Scientific Drilling Program (ICDP) (*Harms et al., 2007*) and other scientific continental drilling initiatives, cores covering the time span from 3.5 billion years ago to Present have been obtained in lakes and terrestrial sedimentary basins across the world (Fig. 5-1). Taking advantage of these continuous records, sedimentologists and paleoclimatologists establish high-resolution chronostratigraphic frameworks and apply multiple paleoclimate proxies to decipher the processes and mechanisms of climate change in the Quaternary and in 'deep time' (cf. *An et al., 2006; Olsen et al., 2010; Wang et al., 2013; Clyde et al., 2013*). Scientific progress has been achieved in paleoclimate reconstructions on different timescales, with detailed studies on rapid climate change, and precise correlations between marine and terrestrial paleoclimate records.

In-depth scientific assessment of natural climate variability based on continental drilling will allow us to close gaps in our knowledge of the impact of climate change on the terrestrial landscape and its ecosystems, vegetation, and other biota, and, ultimately, the human environment. Scientific continental drilling will continue to play an important role in future sedimentologic and (paleo)climatic studies.

2.Geochronology: Radioisotope Geochronology and Astrochronology

Geochronology is of fundamental importance for understanding and deciphering the Earth history by placing geologic records into a robust temporal framework, with which we can test and assess the causal links between tectonic, climatic and biotic changes and extinction events, and calibrate their rates in deep time (cf. *Schmitz and Kuiper, 2013*). The precision and accuracy of the geologic timescale constrains our understanding of many geological, evolutionary and paleoecological processes (*Erwin, 2006*). Recent advances in geochronology techniques with their increased resolving power facilitate the production of a high-resolution temporal framework in deep time.

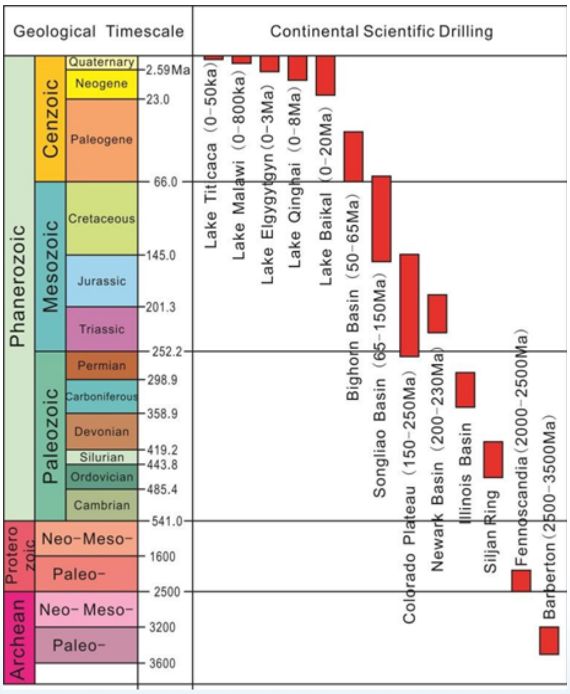

Fig. 5-1

Geologic age distribution of continuous sedimentary records obtained by continental scientific drilling in the last two decades (from Gao et al., 2017).

Radiogenic isotope geochronology, based on the radioactive decay of unstable elements, allows for the calibration of geologic events with absolute time. Uranium-lead (U-Pb) geochronology and Argon-Argon ($^{40}Ar/^{39}Ar$) geochronology are the most commonly used absolute dating methods, with the former using principally zircon and the latter mainly relying on sanidine feldspar (*Schmitz, 2012*). The major state-of-the-art U-Pb geochronology techniques are isotope dilution thermal ionization mass spectrometry (ID-TIMS) and in situ microbeam analysis by secondary ion mass spectrometry (SIMS) and laser-ablation inductive coupled plasma mass spectrometer (LA-ICP-MS) (*Mattinson, 2013*). ID-TIMS is the benchmark and preferable method for high-precision geochronology in deep time, analyzing the entire single grain or a grain fragment. Major improvements of this method include: (1) reductions in analytical blank levels, which allows the analysis of increasingly younger, lower U, and smaller crystal fragments, (2) a switch from physical to chemical abrasion that selectively and effectively eliminates the Pb-loss effect, and (3) the scrutiny and recalibration of tracer solutions and decay constants (*Mattinson, 2013*). With all of this progress, modern ID-TIMS has a relative precision of ± 0.1% and ± 0.03% for individual crystal fragments and weighted mean isotope ratios, respectively (*Schmitz and Kuiper, 2013*).

Microbeam techniques can determine U-Pb dates on tiny spots within individual zircon grains, which has the advantage of high-spatial resolution and rapid analysis. However, the relative precision of SIMS and LA-ICP-MS are 1% and 3-5%, which limits their use for high-precision time scales. Future microbeam techniques will allow for the analysis of even smaller domains, offering higher spatial resolution. Now, many labs use ID-TIMS and in situ microbeam techniques in combination to complement each other. The $^{40}Ar/^{39}Ar$ method uses the decay of ^{40}K to ^{40}Ar via electron capture, and the state-of-the-art techniques yield a precision of ≤0.1%. The inter-calibration of the $^{40}Ar/^{39}Ar$ chronometer with astronomical time has refined the calibration of the reference mineral, giving an absolute age of 28.201 ± 0.046 Ma for the Fish Canyon Tuff (FCT) sanidine standard (*Kuiper et al., 2008*). By using pairs of high-precision U–Pb and $^{40}Ar/^{39}Ar$ ages for selected rocks, *Renne et al. (2010)* obtained a joint determination of the 40K decay constants and the radiogenic argon-to-potassium ratio ($^{40}Ar^*/^{40}K$) of the FCT sanidine. A common traveling Ar pipette system is planned to isolate the source of inter-laboratory $^{40}Ar/^{39}Ar$ bias, and the application of the new generation of multi-collector mass spectrometers will improve the accuracy of the $^{40}Ar/^{39}Ar$ method.

Astrochronology is another important tool in high-precision geochronology. It relies on the correlation or tuning of cyclic sedimentary successions (cyclostratigraphy) to astronomical target curves (*Hinnov and Hilgen, 2012*). This astronomical target curve was computed based on astronomical solutions for the Solar System and has led to high quality data for the Cenozoic Era. Because of the chaotic behavior of the Solar System, the accuracy of orbital models is expected to decrease sharply beyond 60 Ma (*Laskar et al., 2011*). However, we can establish “floating” astrochronologies for the geologic past. By using radioisotope geochronology or radioisotopically calibrated magnetostratigraphy as anchor points, we may assign ’absolute’” ages to the ‘floating’ timescale. Moreover, by inter-calibration of astrochronology with high-precision geochronology, we will be able to refine the astronomical target curves and select the better astronomical solutions (*Ma et al., 2017; Hinnov and Hilgen, 2012*).

With increasing precision achieved in radioisotope geochronology, differences in published ages for the same samples and events using different radioisotope methods or the same method in different laboratories have spurred the start of the EARTHTIME Initiative (*www.earth-time.org*) in 2003. The EARTHTIME Initiative has promoted the unprecedented cooperation among geochronologists to resolve inter-laboratory and inter-chronometer calibration, sample handling, data-analysis issues and the robust integration of geochronology, palaeontology and stratigraphy. EARTHTIME has achieved many improvements, such as new reference materials, improved best practices, common software platforms for data reduction and analysis, etc. Most importantly, these developments have promoted geochronologists to cooperate on exploring issues related to accuracy of the different chronometers, inter-laboratory calibration, and to share ideas within and between disciplines.

China has abundant excellent sedimentary sequences for geochronological studies. However, the high-precision geochronology facilities are somewhat outdated. There are no labs for high-precision U-Pb ID-TIMS geochronology on single zircon grains. Fortunately, inspired by the success of the EARTHTIME initiative, EARTHTIME-CN (China) was launched in 2013, with the goal of advancing collaborative geochronological research in China. EARTHTIME-CN is a national, multi-institutional initiative that aims at forming a Chinese platform for the integration of radioisotopic geochronology with magneto-/chemo-/bio-stratigraphy and astrochronology. The purpose is to refine calibrations of the geologic history so that high-resolution records of paleobiological and paleoenvironmental change can be constructed on a local to global scale. EARTHTIME-CN fosters nation-wide collaboration between geochronologists and users of their data, as well as networking with the broader international EARTHTIME community. Presently, six Ar-Ar, one SIMS and four ID-TIMS facilities in China participate in this initiative. Continued improvements under the EARTHTIME-CN initiative promise a bright future for high-precision geochronology in China and the further development of the associated disciplines.

3.Clumped Isotope Studies

Recent advances in isotope mass spectrometry have led to a new field of isotope studies, clumped isotope geochemistry, which analyses natural doubly-substituted isotopologues in low natural abundances (*Eiler, 2011*). Most recently, technical breakthroughs in high-resolution gas source multi-collector mass spectrometer have extended the field of clumped isotope geochemistry from simple compounds like CO_2 and O_2 to a wide range of compounds (e.g. methane). This range can be extended to a variety of more complex organic compounds (*Eiler et al., 2014; Stolper et al., 2014*).

The most notable tool to emerge from this young field is carbonate clumped isotope thermometry, a technique for reconstructing the growth temperatures of carbonate minerals by evaluating the extent to which ^{13}C and ^{18}O together occur within the same $^{13}C^{18}O^{16}O_2^{-2}$ ion group (*Eiler, 2011*). It can be applied to all (Ca, Mg, Fe) CO_3 carbonates (Bonifacie et al., 2017), and a universal carbonate clumped isotope thermometer calibration has been validated for inorganic carbonates, biosynthetic carbonates and carbonate-apatites (*Eiler, 2011; Kelson et al., 2017*). The technique is based on a homogeneous isotope exchange equilibrium and it thus constrains, independent of temperature, the isotopic composition of water from which carbonate grew (*Ghosh et al., 2006*). These developments have yielded progress in quantitative paleothermometry and paleoaltimetry in deep time, which is a continuing unresolved problem, but central to many aspects of sedimentology. Therefore, it is highly necessary to provide more support for the development and application of this technique.

In North America, Europe, and Australia, there are many clumped isotope labs but only a few in China, which can measure clumped isotopes. To measure carbonate clumped isotopes, the liberated CO_2 is purified in an acid bath by repeated cryogenic separation, chromatography, and removal of contaminants (water, non-condensable gases, isobaric interference), and then introduced into a mass spectrometer (*Passey et al., 2010*). At present, most measurements have been conducted using a 10 kV MAT 253 (plus) dual-inlet isotope ratio mass spectrometer (*Spencer and Kim, 2015*). To date, average analysis time is ~2.5 - 3 h per sample and average sample requirements are ~2-8 mg carbonate equivalent for most mass spectrometer setups (*Huntington and Lechler, 2015*). Future demands for faster analysis time and smaller sample size will require improvements in both facilities and laboratory skills.

4.Multiple S-isotope Studies

The biogeochemical cycle of sulfur plays a significant role in atmospheric and ocean chemistry. The measurement of all four stable sulfur isotopes (^{32}S, ^{33}S, ^{34}S, and ^{36}S) has yielded a new approach to understand sulfur cycling in the oceans and the atmosphere. In particular, the multiple S isotope composition of oceanic sulfate and sedimentary pyrite have been increasingly instrumental to understand paleoenvironmental changes of the Earth's atmosphere and oceans in the geological past (e.g. *Farquhar et al., 2000; Johnston et al., 2005*), as well as in the modern world (e.g. *Tostevin et al., 2014*).

The seminal discovery of mass-independent S-isotope compositions in Archean and Paleoproterozoic sulfate and pyrite has provided unequivocal evidence for the timing and early evolution of atmospheric oxygen (*Farquhar et al., 2000*). The numerous following up studies of $\Delta^{33}S$, $\delta^{34}S$, and $\Delta^{36}S$ from sulfides and sulfates in Archean and Paleoproterozoic rocks have demonstrated that the surface sulfur cycle in the Archean-Paleoproterozoic was markedly different from today (Fig. 5-2). In particular, Earth's multiple-S isotopes record preserves only mass-dependent fractionations since ~2300 Ma. The disappearance of mass-independent isotopic signatures indicates that an increase in atmospheric oxygen partial pressures occurred ~2300 Ma ago, during the Great Oxygenation Event (GOE). The near zero $\Delta^{33}S$ data (blue circles in Fig. 2) for the past ~2300 Ma were considered to be a typical feature of biological processes (*Farquhar etal., 2003; Johnston, 2011*). Mass-dependent fractionations for the isotopes of S are normally quite small and at the level of analytical precision. Along with improved analytical techniques, recent advances in sulfate-reducing bacteria culture experiments and the establishment of accurate sulfate reduction models allow for a better understanding of multiple-S isotope behavior during metabolic sulfate reduction. Additionally, minor $\Delta^{33}S$ values from different metabolic sulfate reduction processes (e.g., bacterial sulfate reduction, microbial sulfur disproportion) can be distinguished because each metabolism produces a distinctive relationship between $\Delta^{33}S$ and $\delta^{34}S$. Therefore, multiple-S isotope records preserved in sedimentary rocks have been used to reconstruct biogeochemical metabolism, as well as environmental evolution and their probable links to mass extinctions in the past 540 million years (*Johnston, 2011; Shen et al., 2011; Sim et al., 2015; Zhang et al., 2015, 2017*).

For multiple-S isotope analysis, pyrite and sulfate in rock samples were converted to Ag_2S through routine wet chemical methods (*Goldberg et al., 2011; Zhang et al., 2015*). To measure S isotopic composition, Ag2S is reacted with excess F2 at 250 ◦C in a nickel reaction tube for more than 8 h and converted to sulfur hexafluoride (SF6), which then was transferred to the sample bellows of the mass spectrometer. At present, very high-precision multiple-S isotope analyses are conducted in China using the ThermoFinnigan MAT253 mass spectrometer facilities at the University of Science and Technology of China. These facilities can not accommodate the enormous need for analyses because the current average analysis time is 2 - 3 h per sample and the amount of sample needed is ~1 - 20 g depending on rock type. Therefore, there is an urgent need to update analytical techniques and train highly skilled researchers to meet future demands for higher analysis efficiency, smaller sample size and better precision.

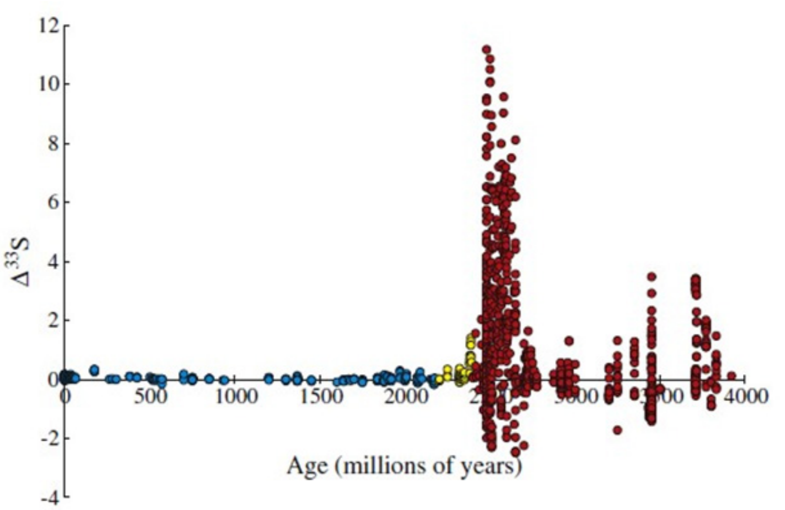

Fig. 5-2
Plot of $\Delta^{33}S$ versus geological age (in millions of years). A remarkable massindependent signal existed prior to 2450 Ma, while mass-dependent fractionations dominated the remaining record (from Farquhar et al., 2000; Johnston, 2011).

5.Monitoring modern marine and oceanic processes

Understanding modern sedimentary processes is undoubtedly helpful for deciphering the past geological record, although the environment and magnitude of variations may have varied significantly. Indeed, understanding modern processes is essential for understanding the past. Diverse monitoring systems and devices are required. The two ways of monitoring marine systems are the Eulerian way of measuring ocean currents and related parameters at a fixed location, such as mooring systems in the water column and bottom landers on the seafloor (*Tengberg et al., 1995*), and the Lagrangian way of measuring the motion of an oceanographic vehicle, such as vehicle-towed devices and underwater gliders (*Davis et al., 2008*).

5.1. Subsurface mooring system

Subsurface mooring is accompolished with a collection of instruments, connected to a wire anchored at the seafloor. The attached instrumentation is wide-ranging and dependent on various monitoring purposes. For the observation of sedimentary processes in the coastal ocean, the instruments commonly include a sediment trap, an acoustic Doppler current profiler

(ADCP), a current meter (RCM), a conductivity-temperature-depth turbidity system (CTD) and deepwater laser in-situ scattering and transmissometry (LISST-DEEP) for current velocity, temperature, salinity, and particle concentration measurements (*Zhang et al., 2014; Zhao et al., 2015*). The sediment trap is the key device for recording sediment dynamics and related geochemical and biological observations (Fig. 5-3), while a time series of suspended sediment particles are collected for multi-disciplinary analysis (*Schroeder et al., 2015*).

Fig. 5-3.
Time-series sediment trap (McLane MARK 78H-21) of Tongji University deployed in the South China Sea. The sediment trap was deployed for one full year and retrieved 21 bottles of suspended sediment samples with about 18-days duration for each sample (photograph by Zhifei Liu/ Tongji University).

5.2. Bottom tripod

Tripods are self-contained, fully submerged structures resting stably on the seafloor, on which various instruments, such as data logger, power supply, and recovery system, are attached (*Cacchione et al., 2006*). The tripod offers high stability without significant flow interference near the seafloor so that current and suspended particle measurements of the Bottom Boundary Layer (BBL) are representative of open flow conditions (Fig. 5-4). Tripods can be assembled onboard ships close to research areas. This mobility allows such systems to be deployed worldwide. The bottom measurement system has made significant contributions to our understanding of BBL dynamics and sediment transport in the coastal ocean.

Fig. 5-4. ▲

Free Ascent Tripod (FAT) of Tongji University deployed in the South China Sea. The FAT is a self-contained, three-legged structure that rests stably on the seafloor. The FAT consists of three major components: frames, a flotation and release system. Various hydrological, sediment dynamic and imaging instruments are mounted on the frames, including: acoustic Doppler current profiler (ADCP), Aquadopp current profiler, Vector current-meter probe, conductivity-temperature-depth turbidity systems (CTD, RBR-Virtuoso and RBR-Duo), transmissometer, deepwater Laser In Situ Scattering and Transmissometry (LISST-DEEP), and camera system (photograph by Yanwei Zhang/Tongji University).

5.3. Underwater glider

The underwater glider is a type of autonomous underwater vehicle (AUV) that uses small changes in its buoyancy to move up and down in the ocean. While not as fast as conventional AUVs, gliders using buoyancy-based propulsion represent a significant increase in range and duration as compared to vehicles propelled by electric motor-driven propellers. Thus, ocean sampling missions are extended from hours to weeks or months, and to thousands of kilometers. Gliders typically measure temperature, conductivity (to calculate salinity), bottom depth, currents, chlorophyll fluorescence, optical backscatter, and acoustic backscatter (*Davis et al.,2008*). Both optical and acoustic backscatter imaging can be calibrated to obtain suspended sediment concentration and fluxes used for monitoring temporal and spatial sediment transport in the water column.

6. Numerical Modelling for Next Generation Sedimentology

In the past decades, a huge amount of sedimentary data has been collected in various basins throughout China. It is projected that the amount of data will grow exponentially. The growth and development of sedimentology not only builds upon the continuously accumulation of data through research, but it calls for an integrated analysis of these "Big Data" by state-of-the-art and upcoming numerical technologies. The former aspect provides more insights into sedimentary processes, while the latter aims to mine and refine sedimentary data on 'extinct climates'.

6.1. Sedimentological Data Mining: identifying the unknown mechanisms

Present-day basin modelling uses 3D visualization of basin evolution, depending on data of sedimentation, subsidence and thermal history, tectonics, paleohydrology, and others. In general, these factors have linear relationships, although sometimes they are in terrelated with complex data structures, as found in GIS analyses. Therefore, in the next generation of sedimentological studies, comprehensive numerical modelling is urgently needed to reveal the nonlinear mechanisms by data mining, especially for those still inaccessible or recognizable in field observations and controlled experiments.

The overall goal of sedimentological data mining is to extract new information from compiled databases and transform this into new insights. New hypotheses can be subjected to cross validation or falsification. This is essential for understanding the surface history because what we know already from observations and experiments is only the tip of the iceberg. There must be unknown systematic mechanisms lurking in the deep.

As in the present generation, the next generation of sedimentological modelling by means of data mining requires data accumulation and abstraction, mainly based on observations, known interactivities, and hypotheses. These raw data are critically needed to feed data mining techniques. The data mining, at a minimum, involves anomaly detection, dependency modelling, clustering, classification, regression, and summarization, with diverse methods such as artificial neural network, genetic algorithms, agent mining, and ensemble learning.

6.2. Big Data Protocol for the Next Generation Sedimentology: exploring the 'extinct climates'

The study of the interaction among sediment deposition, diagenesis, and environments has a high priority. Exploring surface processes will shed new light on the Earth (near-)surface system dynamics. State-of-the art models employed for studying paleoenvironments consistently fail to reproduce climate patterns from a wide variety of physical data, including geochemistry, paleontological and sedimentological proxies. This must be due to our lack of understanding of 'extinct climates'. Big Data thinking opens up new horizons to creatively address this issue.

Big Data thinking is profoundly suitable for the study of 'extinct climates' because it focuses on multi-dimension correlations rather than a linear causal relationship among a few factors that can be directly observed. In other words, Big Data analysis is designed to 'predict' the potential of any unknown or poorly understood process or mechanism that might bridge the gap between physical and other proxies and paleoclimate. Such mechanism may not be active (or not recognized) in the modern Earth, but have played a critical role in 'extinct climates'.

A practical and forward thinking Sedimentological Big Data Protocol is desired for the next generation of sedimentological studies. The pursuit of this goal first and foremost depends on basic sedimentological data accumulation, including sedimentary processes, paleogeography, geochronology and geochemistry. The analysis of these data should be rooted in the latest Big Data technology, and international data interfaces should be opened to encourage the building of a world-wide database. This is vital for analyzing the interaction between (palaeo) environments and sedimentary basin fills in all dimensions.

References

An, Z.S., Ai, L., Song, Y.G., et al. 2006. Lake Qinghai Scientific Drilling Project. Scientific Drilling 1, 20-22.

Bonifacie, M., Calmels, D., Eiler, J.M., Horita, J., Chaduteau, C., Vasconcelos, C., Agrinier, P., Katz, A., Passey, B.H., Ferry, J.M., Bourrand, J.J., 2017. Calibration of the dolomite clumped isotope thermometer from 25 to 350°C, and implications for a universal calibration for all (Ca, Mg, Fe)CO3 carbonates. Geochimica et Cosmochimica Acta 200, 255-279.

Cacchione, D.A., Sternberg, R.W., Ogston, A.S., 2006. Bottom instrumented tripods: History, applications, and impacts. Continental Shelf Research 26, 2319–2334.

Clyde, W.C., Gingerich, P.D., Wing, S.L., Röhl, U., Westerhold, T., Bowen, G., Johnson, K., Baczynski, A.A., Diefendorf, A., McInerney, F., Schnurrenberger, D., Noren, A., Brady, K., 2013. Bighorn Basin Coring Project (BBCP): a continental perspective on early Paleogene hyperthermals. Scientific Drilling 16, 21-31.

Davis, R.E., Ohman, M.D., Rudnick, D.L., Sherman, J.T., 2008. Glider surveillance of physics and biology in the southern California Current System. Limnology and Oceanography 53, 2151–2168.

Eiler, J.M., 2011. Paleoclimate reconstruction using carbonate clumped isotope thermometry. Quaternary Science Reviews 30, 3575-3588.

Eiler, J.M., Bergquist, B., Bourg, I., Cartigny, P., Farquhar, J., Gagnon, A., Guo, W., Halevy, I., Hofmann, A., Larson, T.E., Levin, N., Schauble, E.A., Stolper, D., 2014. Frontiers of stable isotope geoscience. Chemical Geology 372, 119-143.

Erwin, D.H., 2006. DATES AND RATES: Temporal resolution in the deep time stratigraphic record. Annual Review of Earth and Planetary Sciences 34, 569-590.

Farquhar, J., Bao, H., Thiemens, M., 2000. Atmospheric influence of Earth’s earliest sulfur cycle. Science 289, 756-758.

Farquhar, J., Johnston, D.T., Wing, B.A., Habicht, K.S., Canfield, D.E., Airieau, S., Thiemens, M.H., 2003. Multiple sulphur isotopic interpretations of biosynthetic pathways: implications for biological signatures in the sulphur isotope record. Geobiology 1, 27-36.

Gao, Y., Wang, C., Huang, Y., Hu, B., 2017. Progress in the study of paleoclimate change in continental scientific drilling projects. Earth Science Frontiers 24, 229-241 (in Chinese with English abstract).

Ghosh, P., Adkins, J., Affek, H., Balta, B., Guo, W., Schauble, E.A., Schrag, D., Eiler, J.M., 2006. 13C-18O bonds in carbonate minerals: A new kind of paleothermometer. Geochimica et Cosmochimica Acta 70, 1439-1456.

Goldberg, T., Shields, G., Newton, R., 2011. Analytical constraints on the measurement of the sulfur isotopic composition and concentration of trace sulfate in phosphorites: Implications for sulfur isotope studies of carbonate and phosphate rocks. Geostandards and Geoanalytical Research 35, 161-174.

Harms, U., Koeberl, C., Zoback, M.D., 2007. Continental Scientific Drilling. Berlin, Springer.

Hinnov, L.A., Hilgen, F.J., 2012, Cyclostratigraphy and astrochronology, in Gradstein, F. M., Ogg, J.G., Schmitz, M.D., Ogg, G.M., The geologic time scale, Elsevier 63-83.

Huntington, K.W., Lechler, A.R., 2015. Carbonate clumped isotope thermometry in continental tectonics. Tectonophysics 647-648, 1-20.

Johnston, D.T., 2011. Multiple sulfur isotopes and the evolution of Earth's surface sulfur cycle. Earth-Science Reviews 106, 161-183.

Johnston, D.T., Wing, B.A., Farquhar, J., Kaufman, A.J., Strauss, H., Lyons, T.W., Kah, L.C., Donald, E., Canfield, D.E., 2005. Active microbial sulfur disproportionation in the Mesoproterozoic. Science 310, 1477-1479.

Kelson, J.R., Huntington, K.W., Schauer, A.J., Saenger, C., Lechler, A.R., 2017. Toward a universal carbonate clumped isotope calibration: Diverse synthesis and preparatory methods suggest a single temperature relationship. Geochimica et Cosmochimica Acta 197, 104-131.

Kuiper, K.F., Deino, A., Hilgen, F.J., Krijgsman, W., Renne, P.R., Wijbrans, J.R., 2008. Synchronizing rock clocks of Earth history. Science 320, 500-504.

Laskar, J., Fienga, A., Gastineau, M., Manche, H., 2011. La2010: A new orbital solution for the long-term motion of the Earth. Astronomy and Astrophysics 532, A89.

Ma, C., Meyers, S.R., Sageman, B.B., 2017. Theory of chaotic orbital variations confirmed by Cretaceous geological evidence. Nature 542(7642), 468-470.

Mattinson, J.M., 2013. Revolution and evolution: 100 Years of U-Pb geochronology. Elements 9, 53-57.

Olsen, P.E., Kent, D.V., Geissman, J.W., Blakey, R.C., Gehrels, G., Irmis, R.B., Kuerschner, W., Molina-Garza, R., Mundil, R., 2010. The Colorado Plateau Coring Project (CPCP): 100 million years of Earth system history. Earth Science Frontiers 17, 55-63.

Passey, B.H., Levin, N.E., Cerling, T.E., Brown, F.H., Eiler, J.M., 2010. High-temperature environments of human evolution in East Africa based on bond ordering in paleosolcarbonates. Proceedings of the National Academy of Sciences 107, 11245-11249.

Renne, P.R., Mundil, R., Balco, G., Min, K., Ludwig, K.R., 2010. Joint determination of 40K decay constants and 40Ar*/ 40K for the Fish Canyon sanidine standard, and improved accuracy for 40Ar/ 39Ar geochronology. Geochimica et Cosmochimica Acta 74, 5349-5367.

Schmitz, M.D., 2012. Radiogenic Isotope Geochronology, in Gradstein, F. M., Ogg, J. G., Schmitz, M. D., and Ogg, G. M., The Geologic Time Scale 2012, Elsevier, 115-126.

Schmitz, M.D., Kuiper, K.F., 2013. High-precision geochronology. Elements 9, 25-30.

Schroeder, A., Wiesner, M.G., Liu, Z., 2015. Fluxes of clay minerals in the South China Sea. Earth and Planetary Science Letters 430, 30-42.

Shen, Y., Farquhar, J., Zhang, H., Masterson, A., Zhang, T., Wing, B.A., 2011. Multiple S-isotopic evidence for episodic shoaling of anoxic water during Late Permian mass extinction. Nature Communications 2(210).

Sim, M.S., Ono, S., Hurtgen, M.T., 2015. Sulfur isotope evidence for low and fluctuating sulfate levels in the Late Devonian ocean and the potential link with the mass extinction event. Earth Planet Science Letters 419, 52-62.

Spencer, C., Kim, S.T., 2015. Carbonate clumped isotope paleothermometry: a review of recent advances in CO_2 gas evolution, purification, measurement and standardization techniques. Geosciences Journal 19, 357-374.

Stanley, S.M., Luczaj, J.A., 2005. Earth System History (4th Edition), W.H. Freeman and Company, New York, 1-569.

Stolper, D.A., Lawson, M., Davis, C.L., Ferreira, A.A., Neto, E.V.S., Ellis, G.S., Lewan, M.D., Martini, A.M., Tang, Y., Schoell, M., Sessions, A.L., Eiler, J.M., 2014. Formation temperatures of thermogenic and biogenic methane. Science 344, 1500-1503.

Tengberg, A., De Bovee, F., Hall, P., Berelson, W., Chadwick, D., Ciceri, G., Crassous, P., Devol, A., Emerson, S., Gage, J., Glud, R., Graziottini, F., Gundersen, J., Hammond, D., Helder, W., Hinga, K., Holby, O., Jahnke, R., Khripounoff, A., Lieberman, S., Nuppenau, V., Pfannkuche, O., Reimers, C., Rowe, G., Sahamir, A., Sayles, F., Schurter, M., Smallman, D., Wehrli, B., De Wilde, P., 1995. Benthic chamber and profiling landers in oceanography: A review of design, technical solutions and functioning. Progress in Oceanography 35, 253-294.

Tostevin, R., Turchyn, A.V., Farquhar, J., Johnston, D.T., Eldridge, D.L., Bishop, J.K.B., McIlvin, M., 2014. Multiple sulfur isotope constraints on the modern sulfur cycle. Earth and Planetary Science Letters 396, 14-21.

Wang, C., Scott, R.W., Wan, X., Graham, S.A., Huang, Y.J., Wang, P.J., Wu, H.C., Dean, W.E., Zhang, L.M., 2013. Late Cretaceous climate changes recorded in Eastern Asian lacustrine deposits and North American Epieric sea strata. Earth-Science Reviews 126, 275-299.

Zhang, G., Zhang, X., Hu, D., Li, D., Algeo, T.J., Farquhar, J., Henderson, C.M., Qin, L., Shen, M., Shen, D., Schoepfer, S.D., Chen, K., Shen, Y., 2017. Redox chemistry changes in the Panthalassic Ocean linked to the end-Permian mass extinction and delayed Early Triassic biotic recovery. Proceedings of the National Academy of Sciences 114, 1806-1810.

Zhang, G., Zhang, X., Li, D., Farquhar, J., Shen, S., Chen, X., Shen, Y., 2015. Widespread shoaling of sulfidic waters linked to the end-Guadalupian (Permian) mass Extinction. Geology 43(12), 1091-1094.

Zhang, Y., Liu, Z., Zhao, Y., Wang, W., Li, J., Xu, J., 2014. Mesoscale eddies transport deep-sea sediments. Scientific Reports 4, 5937, doi:10.1038/srep05937.

Zhao, Y., Liu, Z., Zhang, Y., Li, J., Wang, M., Wang, W., Xu, J., 2015. In situ observation of contour currents in the northern South China Sea: Applications for deepwater sediment transport. Earth and Planetary Science Letters 430, 477-485.

Chapter 6.

Sedimentology Education Status and Recommendations

Xi Chen[1] , Youfeng Gao [2] , Pujun Wang [2] , James Ogg [3]

[1] **China University of Geosciences (Beijing), Beijing 100083 , China**

[2] **Jilin University, Changchun 130012 , China**

[3] **Purdue University, West Lafayette, IN 47907, USA**

Approximately one-third of all geology graduate students in China completed their Masters or PhD dissertations in a sedimentology-related field during 2000-2014 (*Gao et al., 2017*). The majority (70%) of these students graduated with degrees in petroleum geology, followed by stratigraphy/geohistory, marine geology/geomorphology, and paleogeography/ paleoclimatology (*Gao et al., 2017*). Although the undergraduate education in geoscience is generally deficient in providing a basic background in sedimentology-related concepts, the graduate programs at the 16 Chinese universities, which offer degrees in sedimentology-related fields, are very strong.

Data from sedimentology-related graduate programs presented herein were compiled mainly from these 16 Chinese universities, i.e., Peking University, China University of Geosciences (Beijing), China University of Geosciences (Wuhan), Chengdu University of Technology, China University of Petroleum (Beijing), China University of Petroleum (east China), China University of Mining and Technology (Beijing), China University of Mining and Technology (Xuzhou), Jilin University, Nanjing University, Northwestern University, Tongji University, Chang 'an University, Yangtze University, Southwest Petroleum University and Northeast Petroleum University (*Gao et al., 2017*). These institutions have various sedimentology-related curricula, which commonly include courses in sedimentary petrography, depositional environments and facies, petroleum geology, experimental sedimentology, paleontology and stratigraphy, sequence stratigraphy, stratigraphy of orogenic belts, and historical geology. There are other institutions in China, which have relevant programs in geosciences and marine geology including aspects of sedimentology, but they were not included in this compilation.

1. Undergraduate Education Recommendations

Although there are many postgraduates conducting research related to sedimentology in China, there is not a specific major in sedimentology for undergraduate students in any Chinese universities. In Earth science departments, undergraduates have the option to study sedimentary petrography and sequence stratigraphy, but sedimentology is generally a branch of paleontology-stratigraphy or mineralogy-petrology and mineral deposit formation ("gitology"). Other aspects of sedimentology, such as carbonate rocks, basin analysis and paleoclimate, are not taught to undergraduates.

We propose that undergraduate sedimentology courses taught at Chinese universities should require students to: (1) understand terminology and concepts of sedimentology, especially terms that have different translations in Chinese-language papers, (2) be able to use basic tools in sedimentary research, such as a microscope, (3) observe, record, log and interpret field and laboratory data, such as sedimentary textures, and (4) interpret microfacies, depositional environments and diagenetic processes using conventional thin section analysis but also more advanced tools.

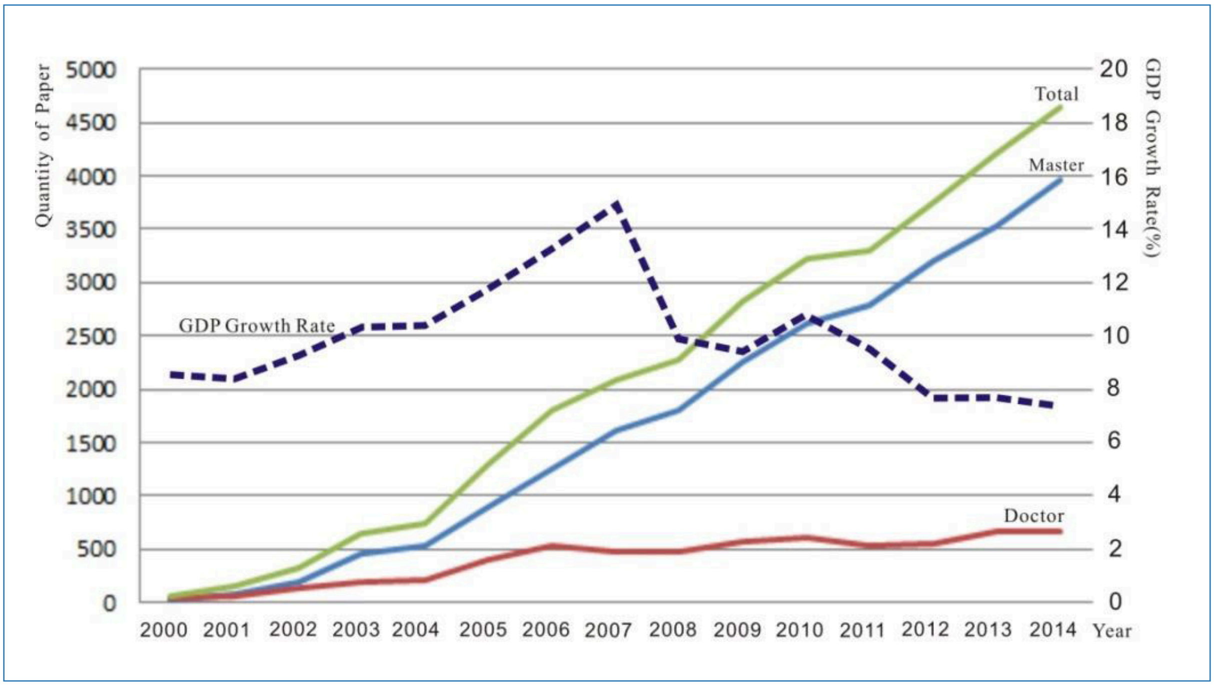

Fig. 6-1. ▲

The trend of postgraduate published dissertations in geology during 2000-2014, according to the CNK1 database. Statistics for 2015 and 2016 are still being updated, and, thus, these data, as well as unpublished theses, are not included. Source: Gao et al., 2017.

2. Graduate Education Recommendations

During the past 15 years, there has been a phenomenal surge in the total number of completed geoscience graduate degrees (Fig. 6-1) (*Gao et al., 2017*). From only 24 postgraduate geology dissertations completed in 2000, the number has surged rapidly to exceed 4500 in the year 2014, of which Master's theses represent nearly 4000 of the total. After a progressive rise between 2001 and 2005, the number of doctoral theses has remained fairly stable at 500-600 per year since 2006.

Table 1. The number of postgraduate dissertations in sedimentology and related disciplines in 2000-2014 (Gao et al., 2017)

Year	Marine Geology & Geomorphology	Sedimentary Petrology	Paleogeography & Paleoclimatology	Geohistory & Stratigraphy	Coal Geology	Petroleum Geology
2000	7	0	1	3	1	4
2001	8	3	5	4	2	21
2002	14	0	7	4	3	54
2003	18	1	8	36	0	89
2004	23	3	16	31	12	136
2005	39	6	24	57	13	226
2006	37	13	32	104	16	320
2007	50	23	37	60	16	413
2008	53	3	47	45	22	545
2009	33	4	47	25	46	807
2010	42	8	47	41	59	973
2011	71	2	49	59	48	979
2012	73	4	65	61	24	1095
2013	100	32	85	158	47	992
2014	116	24	72	130	44	1123
Total	684	126	542	818	353	7777

Approximately 30% of these postgraduate dissertations in geology pertain to topics in sedimentology (Tab. 1). During the 15 years from 2000 through 2014, there were 10,094 dissertations associated with sedimentology themes (8,126 masters; 1,968 doctoral).Definitely, the expansion of sedimentology is a key feature in the current developments in geology education in China. More than 70% of the sedimentology dissertations focused on petroleum geology (Table 1). Indeed, petroleum geology is one of the most important fields, which directly benefits the economy. In contrast, basic research areas, such as paleoclimatology, paleogeography and bio-sedimentation, are less popular topics.

Beyond basic courses in sedimentology and stratigraphy, which include facies models and sequence stratigraphy, graduate training should include a background in a subset of additional topics, such as basin analysis, provenance analysis, paleoclimatology, numerical modeling of Earth systems, geochemical and physical proxies to interpret paleoenvironment, diagenesis, and methods of regional and global correlation to geologic time.

We propose that courses and training of postgraduates should require students to obtain the following important abilities:

(1) Be able to interpret and reconstruct a basin's depositional history, subsidence and thermal history based on the field observations, the study of petrographic and diagenetic features, and experiments.

(2) Work with integration of different methods and tools to predict outcomes and understand dynamic relationships of complex systems, for instance the relationships among tectonics, climate, sedimentation, diagenetic pathways, and hydrocarbon source/reservoir/ caprocks.

(3) Quantitatively reconstruct paleo-environmental changes using multiple proxies and/or numerical modeling. Proxy data must be critically assessed against diagenetic features and noise separated from signal.

3. Status of Field Areas for Teaching and Practice

It is essential that geology students, especially those in sediment-related fields, have extensive experience in a variety of geologic settings throughout their training. The main geological institutes in China provide their own field teaching courses, including the use of established field training areas (*Gao et al., 2017*). There are six main areas for teaching field methods in China:

1) Zhoukoudian, Beijing, located in central North China Craton at the border zone of Yanshan Mountains, Taihang Mountains and the North China Plain. The outcrops span Archean to Cenozoic strata with diverse lithologies and contain unconformities resulting from tectonic events, such as Qin Yu, Jixian and Taikang movements. Structures include thrust nappes, detachment faults, and folds. This is the field mapping teaching area for junior undergraduates at the China University of Geosciences.

2) Beidaihe, Qinhuangdao, located in the eastern part of Yanshan fold belt containing the typical stratum succession of the North China Craton and typical structural features. It is the freshman class cognitive practice field area of China University of Geosciences and China University of Petroleum, providing students with a preliminary recognition of sedimentary stratigraphy.

3) Zigui (Three Gorges), located in the Huangling anticline of the Yangtze Craton, which has Proterozoic to Triassic strata overlying the Paleoproterozoic basement. The continuous stratigraphic sections includes the famous "GSSP of Sinian". This area meets the requirements for the teaching of the field practical courses required for multiple majors.

4) Liaoning Province, located in the eastern segment of Yanshan orogenic belt on the northern margin of North China Craton. This is the field area of Jilin University (Xingcheng). The region has well-exposed strata, the world's largest molybdenum deposit of skarn type, and a complex geological history that includes the world-famous dinosaur species, Sinosauropteryx, Confuciusornis, and the early Mesozoic "The first flower in the world" of ancient angiosperm fruits. In addition to Jilin University, the field area attracts students from Beijing University, Nanjing University, and Northwestern University to visit and study various sedimentologic features, including sedimentary rhythms, cycles, paleoclimate and paleoenvironment.

5) Chaohu, located on the northern margin of the Yangtze Craton. This field area comprises different lithological units with marker beds for regional correlation and is rich in fossils, mineral resources, and geomorphic features. It is the field area of Nanjing University, Northwestern University, and China University of Petroleum.

6) Qinling, located close to the Shangdan suture zone between the north and south Qinling tectonic belts. This field area contains typical North China and Yangtze strata, which

are well exposed, and is a good area to study the geological phenomena of an orogenic belt (Qinling orogenic belt) and the Ordos typical sedimentary basin.

Sedimentary geology and sedimentology are important components of field courses required for the education of geology students in China. However, field teaching is mainly provided for undergraduates and focuses only on recognition of basic rock types and practice mapping.

We propose that systematic field courses in sedimentology and sedimentary geology for senior students and postgraduates are a fundamental component of their geologic curriculum. Field excursions should not be limited to using only one of the above-mentioned established field areas of a particular university, but they should encompass different geologic settings, including orogenic belts, oil- and gas-bearing basins and extensional regions. This field training is essential for students to assist them in pursuing careers in both research and applied sedimentology and to have a solid background in techniques from interpreting lithofacies to basin analysis.

References

Gao, Y. F., Zhang, L. B., Chen, T., Wang, P. J., 2017. The future of sedimentology in China: A review and look forward to education of sedimentology. Acta Sedimentologica Sinica 35, 1078-1085. In Chinese with English abstract.